General Disclaimer

One or more of the Following Statements may affect this Document

- This document has been reproduced from the best copy furnished by the organizational source. It is being released in the interest of making available as much information as possible.

- This document may contain data, which exceeds the sheet parameters. It was furnished in this condition by the organizational source and is the best copy available.

- This document may contain tone-on-tone or color graphs, charts and/or pictures, which have been reproduced in black and white.

- This document is paginated as submitted by the original source.

- Portions of this document are not fully legible due to the historical nature of some of the material. However, it is the best reproduction available from the original submission.

SPACE DIVISION

NASA CR-144803

NASA REPORT NO.
GE-SD REPORT NO. 76SDS4203

(NASA-CR-144803) ADAPTIVE MULTIBEAM ANTENNAS FOR SPACELAB. PHASE A: FEASIBILITY STUDY Final Report, 16 Jun. 1975 - 16 Feb. 1976 (General Electric Co.) 156 p HC $6.75 CSCL 09C G3/33

N76-30447

Unclas
49591

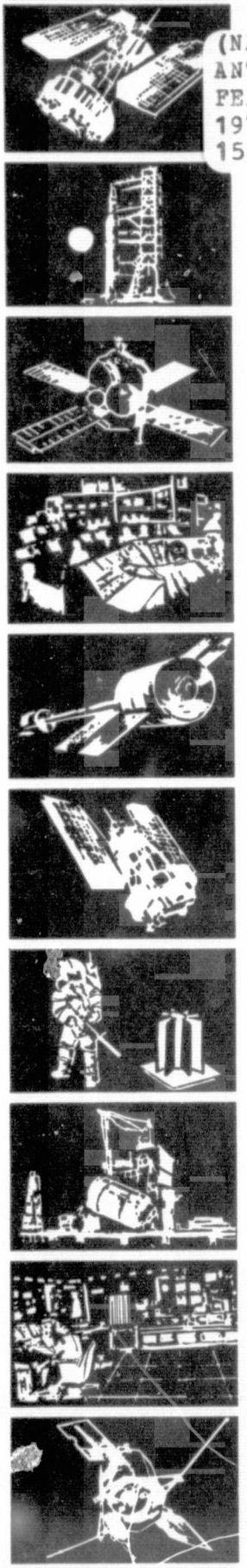

ADAPTIVE MULTIBEAM ANTENNAS FOR SPACELAB
PHASE A FEASIBILITY STUDY

C.C. ALLEN, S.P. APPLEBAUM, W.J. POPOWSKY, G. WOUCH
GENERAL ELECTRIC COMPANY
VALLEY FORGE SPACE CENTER
BOX 8555
PHILADELPHIA, PENNSYLVANIA 19101

FEBRUARY 1976

FINAL REPORT FOR PERIOD JUNE 1975 TO FEBRUARY 1976

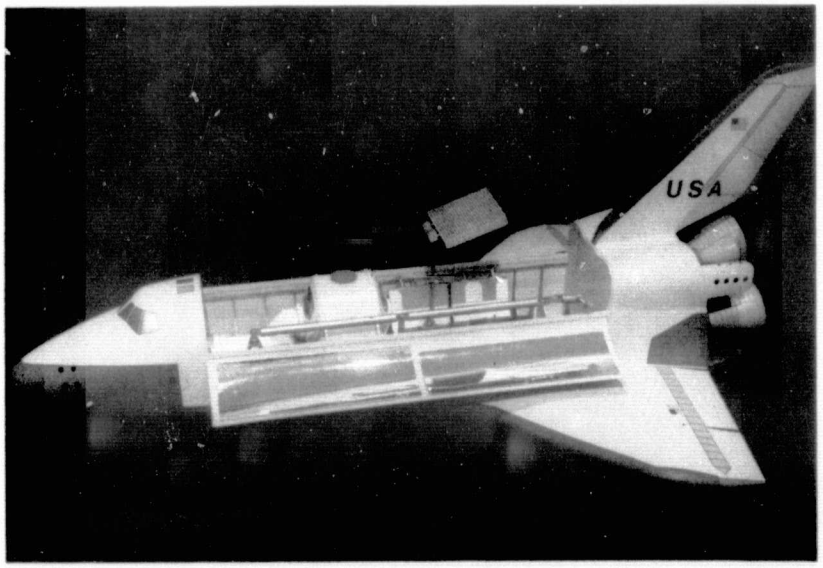

PREPARED FOR

GODDARD SPACE FLIGHT CENTER
NATIONAL AERONAUTICS AND SPACE ADMINISTRATION
GREENBELT, MARYLAND 20771

GENERAL ELECTRIC

TECHNICAL REPORT STANDARD TITLE PAGE

1. Report No.	2. Government Accession No.	3. Recipient's Catalog No.

4. Title and Subtitle	5. Report Date
Adaptive Multibeam Antennas for Spacelab Phase A Feasibility Study	February 1976
	6. Performing Organization Code
7. Author(s) C. C. Allen, S. P. Applebaum, W. J. Popowsky, G. Wouch	8. Performing Organization Report No. 76SDS4203
9. Performing Organization Name and Address General Electric Company Valley Forge Space Center, P. O. Box 8555 Philadelphia, Pennsylvania 19101	10. Work Unit No.
	11. Contract or Grant No. NAS 5-22425
	13. Type of Report and Period Covered Final Report 6/16/75 to 2/16/76
12. Sponsoring Agency Name and Address National Aeronautics and Space Administration Goddard Space Flight Center Greenbelt, Maryland 20771	14. Sponsoring Agency Code 953 (S. Durrani)

15. Supplementary Notes

16. Abstract

A Phase A Study was conducted for NASA by General Electric to determine the feasibility of using adaptive multibeam multi-frequency antennas on the Spacelab, and to define the experiment configuration and program plan needed for a demonstration to prove the concept. General Electric concluded that an adaptive multibeam antenna system is indeed feasible for conducting meaningful experiments from Spacelab and offers many advantages. Three applications missions were selected, and requirements were defined for an L-band Communications Experiment, an L-band Radiometer Experiment, and a Ku-band Communications Experiment. Reflector, passive lens, active lens, and phased array antenna systems were considered, and the Adaptive Multibeam Phased Array (AMPA) was chosen. Array configuration and beamforming network tradeoffs resulted in a single 3m x 3m L-band array with 576 elements for high radiometer beam efficiency. For communications only, the array could be thinned. Separate 0.4m x 0.4m arrays are used for transmit and receive at Ku-band with either 576 elements or thinned apertures. Each array has two independently steerable 5^{o} beams, which are adaptively controlled. The AMPA antenna system can be used alone effectively for conducting multiple experiments, or it can be integrated readily with other microwave experiments for greater commonality of equipment. Man has a vital role to play in the Spacelab/AMPA experiments, which could be implemented by the early 1980's.

17. Key Words (Selected by Author(s))	18. Distribution Statement
Antennas Communications Phased array Radiometry Adaptive processing Shuttle/Spacelab	

19. Security Classif. (of this report)	20. Security Classif. (of this page)	21. No. of Pages	22. Price*
Unclassified	Unclassified	156	

*For sale by the Clearinghouse for Federal Scientific and Technical Information, Springfield, Virginia 22151.

PREFACE

Many applications missions are under consideration by the National Aeronautics and Space Administration for the Space Shuttle era of the 1980's. A large group of experiments related to such applications missions would be conducted on Shuttle/Spacelab flights. Many of these experiments use microwaves in such fields as radiometry, communications, radar, oceanography, and earth resources and environment observation. These microwave experiments are known collectively as the Microwave Multi-Applications Payload (MMAP).

An Adaptive Multibeam Antenna (AMBA) experiment for Spacelab offers great operational versatility for a number of diverse applications, either alone or as part of MMAP. With the ability of Space Shuttle to accommodate payloads of several thousand kilograms and several hundred cubic meters, many sophisticated antenna systems formerly used only for ground, sea, and airborne applications can now be realistically considered for use in space. The most versatile of these antenna systems is the adaptive multibeam phased array.

A Phase A Feasibility Study was conducted by the General Electric Space Division for the NASA Goddard Space Flight Center to determine the feasibility of using adaptive multibeam multi-frequency antennas on the Spacelab, and to define the experiment configuration and program plan needed for a demonstration to prove the concept. It was concluded that an adaptive multibeam antenna system is indeed feasible for performing experiments on Spacelab and offers many advantages. Three applications missions for conducting adaptive multibeam antenna experiments were selected in consultation with the NASA/GSFC Technical Officer, and the Adaptive Multibeam Phased Array (AMPA) was chosen as the preferred antenna system. This report presents the various considerations, tradeoffs, analyses, results, and conclusions of the study.

TABLE OF CONTENTS

TABLE OF CONTENTS (Continued)

LIST OF ILLUSTRATIONS

LIST OF ILLUSTRATIONS (Continued)

LIST OF TABLES

SECTION 1
INTRODUCTION

The advent of Shuttle/Spacelab opens the door to many unique worthwhile experiments that are being considered by the National Aeronautics and Space Administration. One of these is the Adaptive Multibeam Antenna (AMBA) experiment, which offers great operational versatility for a number of diverse applications. With the ability of Space Shuttle to accommodate payloads of several thousand kilograms and several hundred cubic meters, many sophisticated antenna systems formerly used only for ground, sea, and airborne applications can now be realistically considered for use in space. The most versatile of these antenna systems is the adaptive multibeam phased array.

The NASA Goddard Space Flight Center awarded a Phase A Feasibility Study contract to the General Electric Space Division in June 1975 to determine the feasibility of using adaptive multibeam multi-frequency antennas on the Spacelab, and to define the experiment configuration and program plan needed for a demonstration to prove the concept. General Electric concluded during the Phase A Study that an adaptive multibeam antenna system is indeed feasible for conducting meaningful experiments from Spacelab and offers advantages not otherwise attainable. Three applications missions suitable for conducting adaptive multibeam antenna experiments on Spacelab were selected in close consultation with the NASA-GSFC Technical Officer, and the Adaptive Multibeam Phased Array (AMPA) was chosen as the preferred antenna system for those experiments. The overall results and conclusions of the study are summarized in Section 2 of this report.

The AMBA Feasibility Study consisted of five tasks. The purpose of Task 1 was to identify the requirements for services during the 1980's relevant to the study and to identify the corresponding spaceborne equipment requirements and general system level parameters. The applications for adaptive multibeam antennas considered while performing this task and the corresponding systems requirements are presented in Section 3 of this report, which concludes with the antenna system performance requirements for the three selected experiments.

In Task 2, the characteristics of several antenna types were examined and tradeoffs were made with respect to the specified antenna system performance requirements. It became evident early in this task that a phased-array antenna system offered the greatest versatility for performing the desired experiments and was actually the most practical means of achieving the desired capability. These considerations are discussed in Section 4 of the report, and design concepts for an AMPA antenna system are presented in Section 5.

The experiment configuration was developed in Task 3. This was already done for the basic experiment configuration during Tasks 1 and 2, and the effort in Task 3 concentrated on developing more detailed equipment integration and functional requirements. The overall experiment configuration and the detailed requirements are described in Section 6.

A determination of the role of man in the Spacelab/AMPA experiment was made in Task 4 of the study. Various functions that could be performed by a crew member to enhance the capability or reduce the cost of the experiment were examined along with more obvious and/or essential crew functions during both normal and contingency operations. These man-involved activities are presented in Section 7 of the report.

An overall program plan for implementing the AMBA experiment on Spacelab was developed as Task 5 of the Phase A Feasibility Study. This is presented in Section 8 with an estimated schedule for the system definition, development, manufacture, test, and integration of the AMPA based on a Level 4 Work Breakdown Structure.

A new adaptive processing technique for signal acquisition, beamforming, and tracking is reported as new technology in Section 9. With this technique, a fully-adaptive subarray of the phased array is used to adaptively control the much larger full array and also provides adaptive interference rejection.

Recommendations for specific tasks that should logically follow the Phase A Study of Adaptive Multibeam Antennas for Spacelab are given in Section 10.

SECTION 2

SUMMARY OF RESULTS AND CONCLUSIONS

The results and conclusions of the Phase A Feasibility Study of Adaptive Multibeam Antennas (AMBA) for Spacelab are summarized in this Section. The three selected AMBA experiments are described, and a block diagram of the overall experiment configuration is presented. Typical system parameters for the three selected experiments are included. Selection of the Adaptive Multibeam Phased Array (AMPA) as the preferred antenna system is discussed, and the overall AMPA antenna system is described using a system block diagram. Several photographs are shown of a preferred design concept for the AMPA antenna system on a model of Shuttle/Spacelab. Most of the material in this section is covered in greater detail in the rest of the report, together with detailed discussions of the analyses and considerations which led to these results. Conclusions reached during the study are given at the end of this section.

2.1 AMBA EXPERIMENT CONFIGURATION

Three AMBA experiments were selected for conducting meaningful experiments on Spacelab from a large number of applications missions considered in the fields of communications, radar, and radiometry. The three selected experiments are the L-band Communications Experiment, the L-band Radiometer Experiment, and the Ku-band Communications Experiment. The purpose of these experiments is the flight demonstration of an Adaptive Multibeam Phased Array (AMPA) antenna system having high operational potential.

The L-band Communications Experiment is intended to demonstrate the feasibility of low power, point-to-point communications via low orbiting spacecraft using narrow beams. Low power cooperating shipboard terminals having near hemispheric overhead coverage and operating at the maritime L-band communications frequencies are assumed for the experiment. The key measurement parameters are acquisition time, track accuracy, S/N at Spacelab, doppler compensation, received signal quality, and interference cancellation ratio.

The L-band Radiometer Experiment is intended to demonstrate the feasibility of radiometric soil moisture measurement from low orbiting spacecraft using multiple narrow beams. The

key measurement parameters are beam control versus sequence, optimum beam stepping and dwell time, temperature reading and calibration, temperature resolution, and determination of the optimum combination of beams and receivers.

The Ku-band Communications Experiment is intended to demonstrate the feasibility of low power, wideband, point-to-point communications via low orbiting spacecraft using narrow beams and to demonstrate the feasibility of frequency re-use by means of adaptive dual polarization. Moderate power cooperating ground terminals of moderate gain (40 to 50 dB) that will track Spacelab are assumed for the experiment. The key measurement parameters are acquisition time, track accuracy, S/N at Spacelab, doppler compensation, received signal quality, interference cancellation ratio, and dual polarization isolation.

A block diagram of the overall AMPA experiment configuration is shown in Figure 2-1. The AMPA antenna system on Spacelab is integrated for the greatest commonality of equipment consistent with the objectives of the three selected experiments. A single L-band phased array is used for both the L-band Communications Experiment at 1.5/1.6 GHz and the L-band Radiometer Experiment at 1.4 GHz, with much of the RF circuitry shared by both experiments. Separate phased arrays are used on transmit and receive for the Ku-band Communications Experiment at 12/14 GHz because of the greater frequency separation and bandwidth. The adaptive processing and beam control equipment is shared by all three experiments, as is the on-board data processing equipment. A data link between the Shuttle/Spacelab and ground via the Tracking and Data Relay Satellite (TDRS) system is assumed for experiment coordination.

The users for the L-band Communications Experiment would be small shipboard terminals, or possibly buoys specially instrumented for an adaptive multibeam data collection experiment at L-band. The users for the Ku-band Communications Experiment would be medium size ground terminals. For the soil moisture measurements in the L-band Radiometer Experiment, gross water sheds would be observed in mountainous regions as well as the water content of valleys and plains.

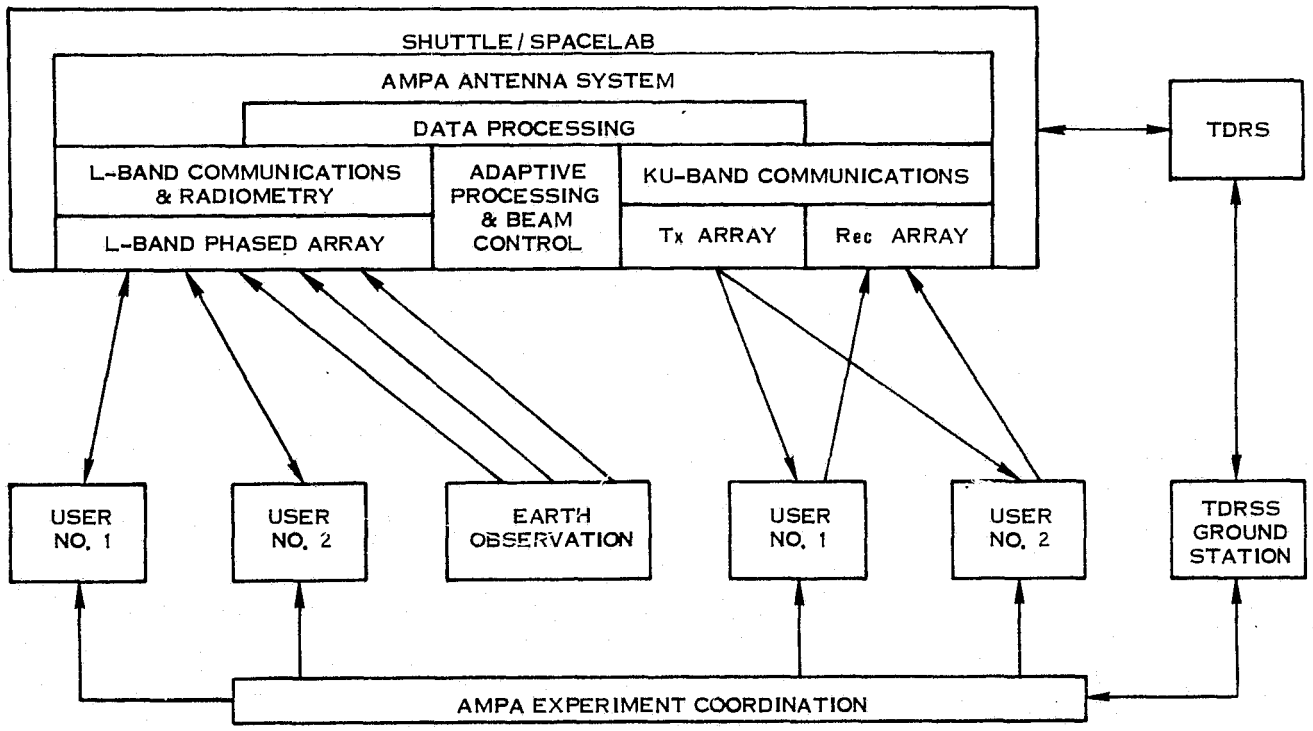

Figure 2-1. Block Diagram of AMPA Experiment Configuration

An examination of the L-band Communications Experiment resulted in a required ground transmitted power of 275 mw with a 3-dB-gain ground antenna in order to achieve 3 KBps data transmission over a PCM/PSK-PM data link for a 47.7 second contact time. The corresponding Spacelab/AMPA transmitted power required was established at 138 mw, which leaves 18.6 dB of signal margin with 10 watts of Spacelab transmitted power.

The Ku-band Communications Experiment planned will result in two fully duplex communications links of 50 MHz bandwidth. A ground transmitter power of only 6.18 watts and a ground antenna gain of 54.7 dB (15-foot reflector) are required for a reference AMPA configuration, which has a worst-case noise figure of 15 dB. The downlink transmitted power required from Spacelab is only 0.618 watts. An alternative AMPA configuration with more hardware has a best-case noise figure of 8 dB.

For the L-band Radiometer Experiment, analysis for a Shuttle orbit altitude of 400 km gives an available dwell time per spot of 1.2 seconds for four radiometer beams, or 0.6 seconds

for two radiometer beams. The corresponding temperature resolution attainable is ΔT = 0.33° K or 0.46° K, respectively, with a 5 dB noise figure for the radiometer receiver.

2.2 AMPA ANTENNA SYSTEM

The Adaptive Multibeam Phased Array (AMPA) was chosen as the preferred antenna system for conducting the selected L-band Communications, L-band Radiometer, and Ku-band Communications Experiments. It was chosen over multibeam reflector and lens antenna systems because of its greater versatility and its ability to better meet the antenna performance requirements for the selected experiments. In addition, the wide coverage angle required for conducting experiments at low orbit altitudes cannot be met satisfactorily with reflector and lens systems. Other features that favor the phased array antenna system are its suitability for full adaptive control, the commonality of equipment achievable, its adaptability to other experiment configurations, and its greater growth potential.

A block diagram of the selected design concept for the AMPA antenna system is shown in Figure 2-2. A single L-band phased array is used for both the L-band Communications Experiment and the L-band Radiometer Experiment, as mentioned in Subsection 2.1. A reference phased-array configuration was selected having 576 crossed-dipole radiating elements in a 3 meter x 3 meter aperture, which produces a nominally 5° beam. The dipoles are arranged in a 24 x 24-element array with a 3-bit phase shifter per element. The radiating elements are broadband dipoles similar to those used in the GE TPS-59 radar, and the diode phase shifters are also GE developed strip transmission line units. While thinning of the L-band array to reduce hardware is desirable and the reduced gain would be acceptable for the communications experiment, a filled array is required for the radiometer experiment to obtain good beam efficiency. The array could be thinned 50 to 80%, however, (or a smaller array used) for preliminary experiments in L-band communications only.

For the L-band Communications Experiment, the selected reference array uses a 4-dB noise figure amplifier per radiating element on receive to achieve an overall 5-dB noise figure. A single transmit amplifier per beam is used, and the transmit power is divided with strip transmission line circuits. Diplexing is achieved with 5-pole interdigital filters. Adaptive

TYPICAL MMAP EXPERIMENTS

1. ELECTROMAGNETIC ENVIRONMENT EXPERIMENT (EEE)
2. ADAPTIVE MULTI-BEAM ANTENNA (AMBA) EXPERIMENT
3. MILLIMETER WAVE COMMUNICATIONS (MMWC) EXPERIMENT
4. METEOROLOGICAL RADAR (METRAD) EXPERIMENT
5. SURFACE SPECTRUM RADAR (SSR) EXPERIMENT
6. ANTENNA RANGE EXPERIMENT (ARE)
7. COOPERATIVE SURVEILLANCE SPACELAB RADAR (CSSR) EXPERIMENT
8. DATA COLLECTION WITH MULTIBEAM (DCMB) EXPERIMENT
9. SOIL MOISTURE AND SALINITY RADIOMETER (SMS R/M) EXPERIMENT
10. ATMOSPHERIC AND OCEANOGRAPHIC IMAGING RADIOMETER (A&O R/M) EXPERIMENT
11. MW IMAGING SPECTROMETER EXPERIMENT (MWISE)
12. NAVSTAR GPS EXPERIMENT (GPS)
13. SYNTHESIZER L.O. SOURCE

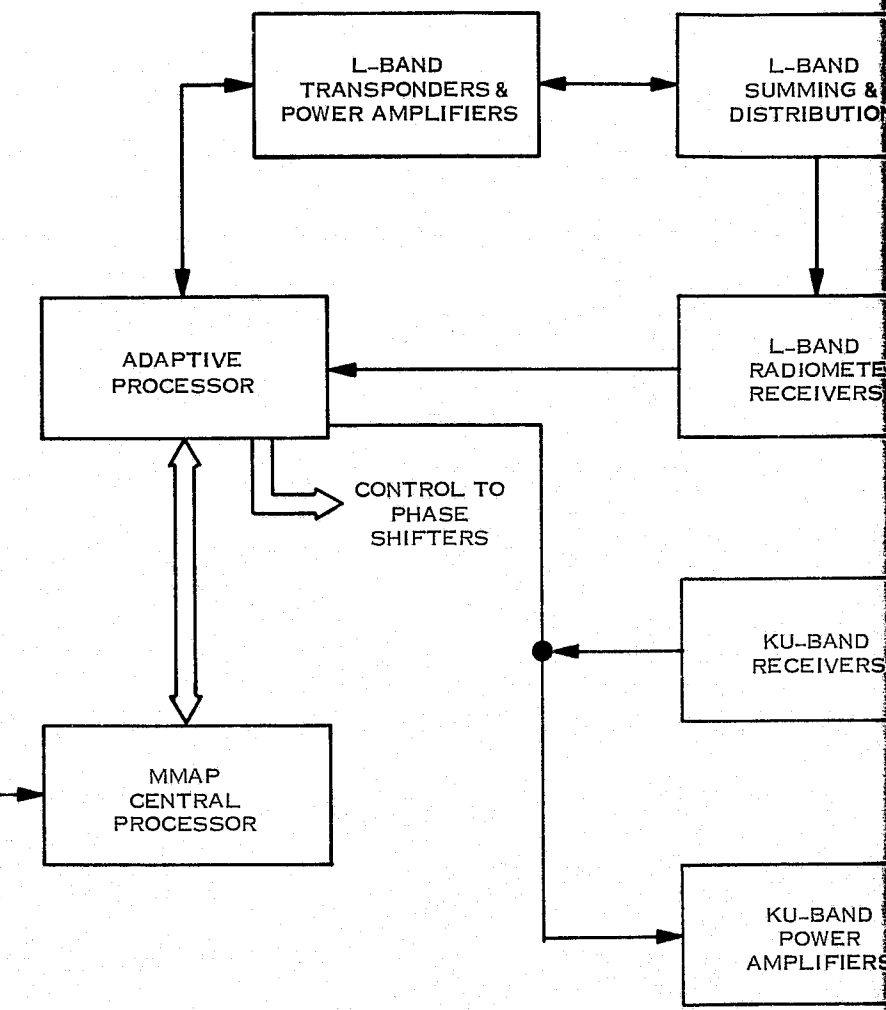

FOLDOUT FRAME)

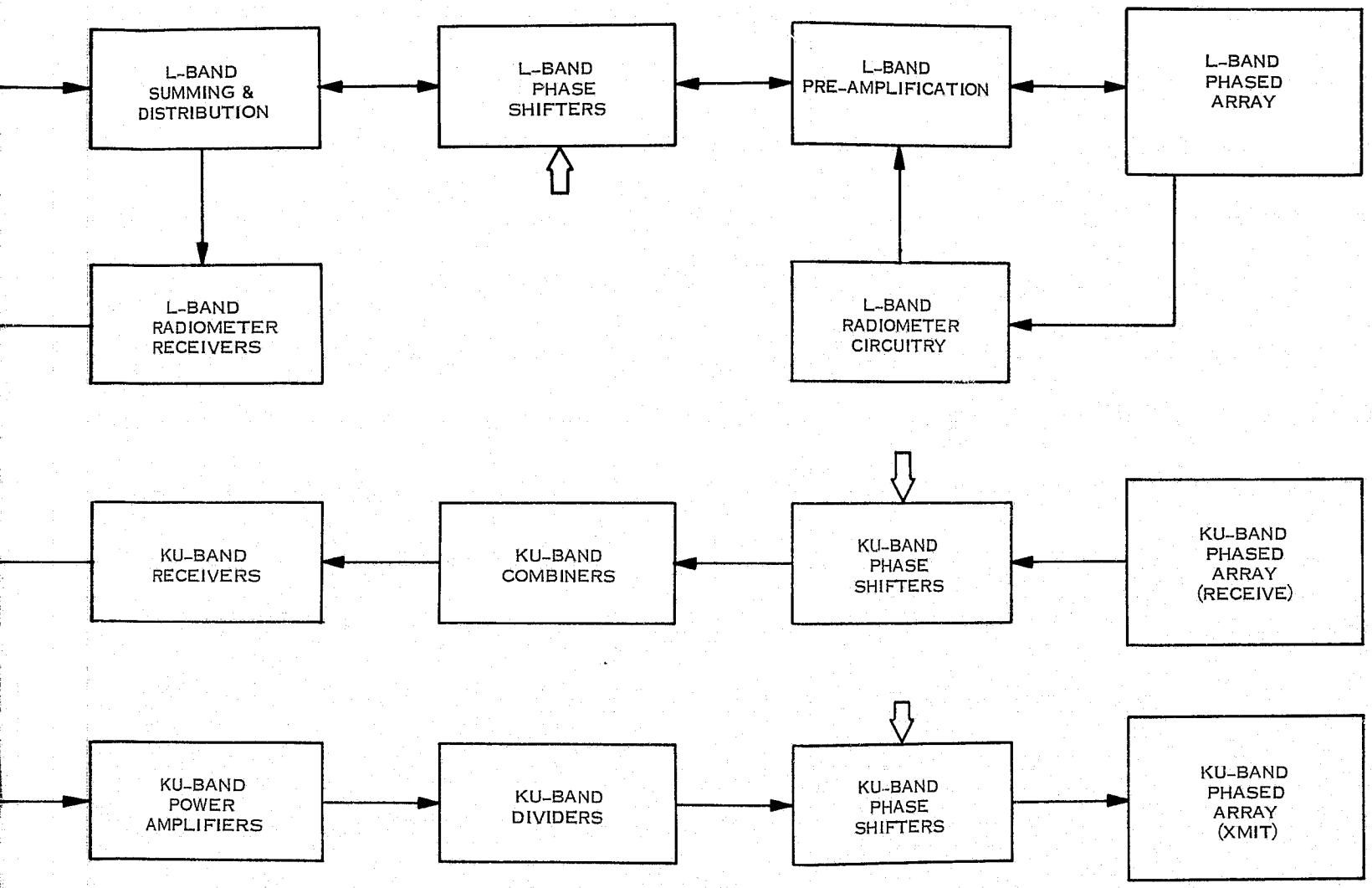

Figure 2-2. AMPA Antenna System Block Diagram (Integrated with MMAP)

FOLDOUT FRAME 2

signal acquisition, beamforming, tracking, and interference rejection are accomplished through processing of the signals from a 16-element subarray of pseudo-randomly-spaced, main-array radiating elements.

For the L-band Radiometer Experiment, much of the equipment is shared in common with the L-band Communications Array. This is accomplished by switching the connections to the dipoles used in the L-band Communications Experiment so that the wideband, elemental, low-noise amplifiers can be used for either linear or horizontal polarization. This reconfiguration of the RF circuitry permits utilization of the low-noise amplifiers, phase shifters, and strip transmission line combiner/divider networks in both the L-band Communications and the L-band Radiometer Experiments at the expense of only about 2 dB of system noise figure.

For the Ku-band Communications Experiment, a single broadband configuration of 576 orthogonal dipole elements hybrid-connected to achieve both right-hand and left-hand circularly polarized operation on transmit and receive was used as an initial reference array. This array was arranged in 16 subarrays of 36 elements and utilized 3-bit digital time-delay networks for broadband beam steering of a nominally 5° beam over the 12-14 GHz band. While the reference array was chosen primarily on a "least hardware" basis, a more practical implementation of a single broadband phased array is to use a combination of elemental phase shifters and time-delay steering at the subarray level. Further tradeoff considerations (discussed in Subsection 5.4) led to the choice of a two-array configuration for Ku-band.

The two-array Ku-band antenna system shown in the AMPA block diagram of Figure 2-2 was selected during the Phase A Feasibility Study as the preferred configuration. Using separate arrays for transmit and receive eliminates the requirement for broadband beam steering and eases the physical size constraints on the arrays, thus presenting a more attractive alternative in spite of the increased hardware requirement. The two-array approach has the added advantage that a proven GE developed Ku-band phase shifter is directly applicable without development. Also applicable is a dual-polarized crossed-bow-tie dipole element in which the dipoles are embedded in a cavity above cutoff for the fundamental waveguide mode. The design has excellent VSWR and circularity performance characteristics over more than a 14% bandwidth.

Thinning of the Ku-band arrays is both desirable and acceptable and would result in a considerable saving in hardware at the expense of some reduction in gain. Thinning each array 75% to 144 radiating elements, for instance, would reduce the gain about 6 dB. Adaptive signal acquisition, beamforming, tracking, and interference rejection are accomplished at Ku-band as in the L-band phased array through processing of the signals from a 16-element subarray of pseudo-randomly-spaced, main-array radiating elements. In addition, frequency re-use for orthogonally-polarized dual-channel communications is accomplished through adaptive polarization control.

An adaptive processor shown in Figure 2-2 would be shared by all arrays in the AMPA antenna system. This would provide control signals to the phase shifters for adaptive signal acquisition, beamforming, and tracking as well as for interference rejection. The block diagram of Figure 2-2 shows the AMPA antenna system integrated with other MMAP experiments and connected to an MMAP central processor. The AMPA antenna system can also be used alone effectively for conducting multiple Adaptive Multibeam Antenna (AMBA) experiments.

A photograph of the preferred AMPA antenna system design concept on a model of Shuttle/Spacelab is shown in Figure 2-3. In this model, the Ku-band phased arrays are mounted on the forward edge of the L-band phased array. Alternative AMPA antenna system configurations that result in more compact integrated apertures are to place the Ku-band arrays in the corners of the L-band array with either a cruciform or octagonal L-band array outline. Outline drawings of the AMPA antenna system and alternative configurations are given in Section 6.

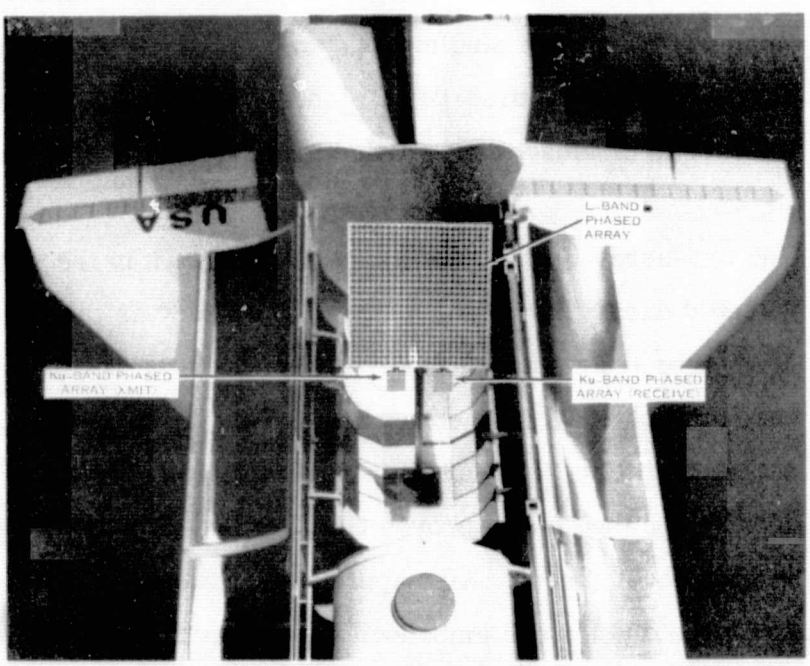

Figure 2-3. Adaptive Multibeam Phased Array Antenna System

A photograph of the AMPA antenna system integrated with the MMAP mission antennas is shown in Figure 2-4 with the antennas stowed and in Figure 2-5 with the antennas deployed.

2.3 CONCLUSIONS

Major conclusions reached during the Phase A Feasibility Study were the following:

- An Adaptive Multibeam Antenna (AMBA) can be used to conduct meaningful experiments on Spacelab.
- Several applications missions of interest were identified in three major categories: communications, radar, and radiometry. From these, an L-band Communications Experiment, an L-band Radiometer Experiment, and a Ku-band Communications Experiment were selected for conducting adaptive multibeam antenna experiments on Spacelab.
- The Adaptive Multibeam Phased Array (AMPA) is the preferred antenna system for conducting those experiments over multibeam reflector and lens antenna systems, because of its greater versatility, its ability to better meet the antenna performance requirements, the commonality of equipment achievable, its suitability for full adaptive control, its adaptability to other experiment configurations, and its greater growth potential.

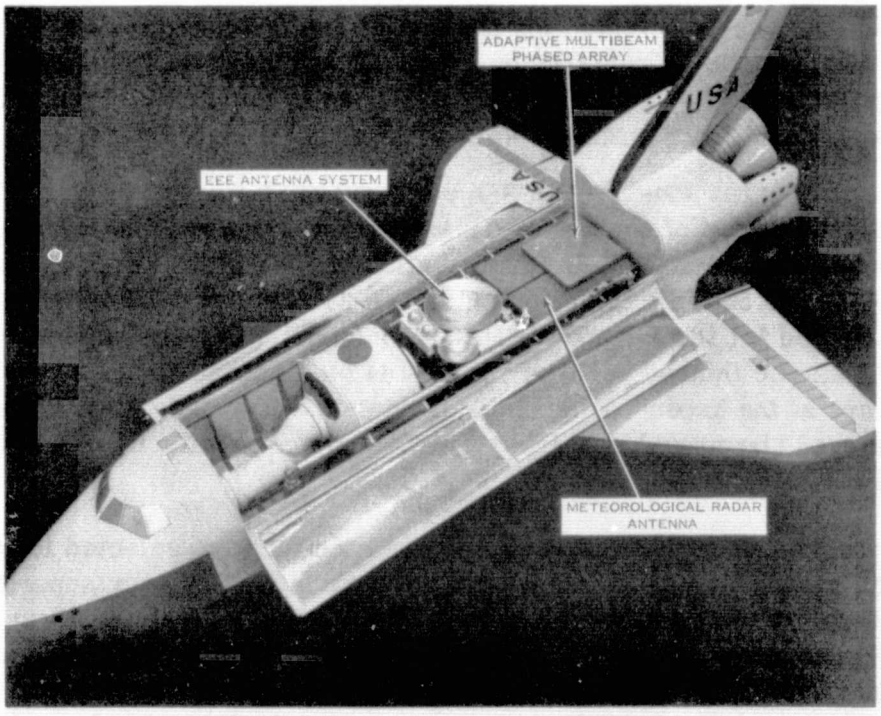

Figure 2-4. AMPA with MMAP Mission Antennas, Stowed

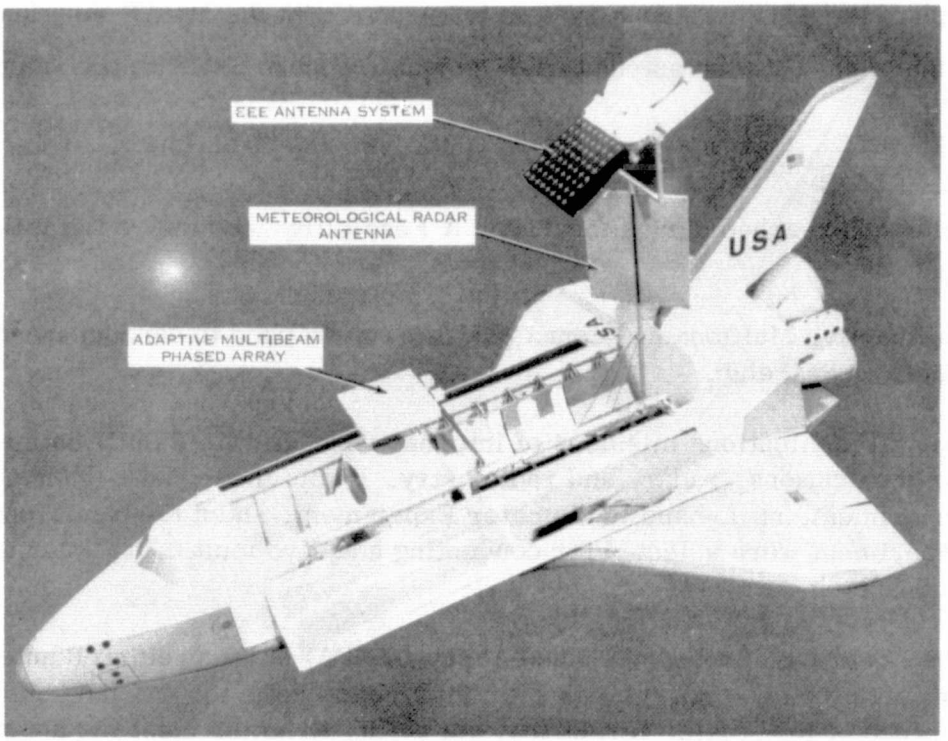

Figure 2-5. AMPA with MMAP Mission Antennas, Deployed

- The design concept selected for the AMPA antenna system uses a single phased array for both the L-band Communications and the L-band Radiometer Experiments, with much of the RF circuitry shared in common and reconfigured for the two experiments by switches operated from the control console.

- The L-band array must have a 3-meter by 3-meter aperture to achieve a minimum angular resolution of about 5^{o}. This aperture must be filled to obtain high radiometer beam efficiency, thus 576 radiating elements are needed in a rectangular grid or 430 to 500 in a triangular grid. A 24 x 24 array of crossed-dipole elements was selected for the L-band AMPA. For communications only, the 24 x 24 element array could be thinned perhaps 75% to 144 elements for a considerable saving in hardware at the expense of about 6 dB in gain. Two independently steerable diplexed beams would be provided initially, with adaptive beamforming and interference rejection.

- Separate phased arrays for transmit and receive were selected for the AMPA antenna system at Ku-band because of the greater frequency separation and bandwidth. Each array would have 576 crossed-dipole elements in a 0.4-meter by 0.4-meter aperture for a filled array. As at I-band, the Ku-band arrays could be thinned for a saving in hardware with a corresponding reduction in gain. Dual polarization is provided on each of two adaptively-formed independent beams on both arrays to permit experimental evaluation of frequency re-use by adaptive polarization control.

- Alternative single Ku-band phased-array configurations require less hardware but they must be broadband, have more complex circuitry, and are more difficult to package. The most attractive beam steering method for a single transmit/receive array at Ku-band is a combination of phase shift steering of the radiating elements and time delay steering of subarrays.

- Alternative array beamforming network (BFN) configurations considered were those with element level amplifiers, subarray level amplifiers, and beam level amplifiers in various combinations for transmit and receive. The BFN configuration selected for L-band uses element level receive amplifiers to achieve a low noise figure and beam level transmit amplifiers. At Ku-band, beam level amplifiers were selected for both receive and transmit based on hardware and packaging considerations. Element level amplifiers for receive at Ku-band would give a considerably lower noise figure, however, and would be the preferred BFN configuration for more than two beams.

- A new adaptive technique was conceived for adaptively controlling a full phased array with a much smaller fully-adaptive subarray of the main array. This technique provides adaptive signal acquisition, beamforming, tracking, and interference rejection. (See Section 9.) For the AMPA antenna system, the beams would be adaptively controlled by a 16-element pseudo-randomly-spaced subarray of the full phased array.

- The multibeam feature of the AMPA antenna system is highly desirable for passive microwave radiometry and radar scatterometry, since it permits the recording of large areas of the earth with high resolution and with high accuracy in either temperature or backscatter measurement within the time allotted by the given orbital parameters and transverse scan angle. This feature would be used with program controlled beams for optimum beam sequence and dwell time.

- The Adaptive Multibeam Phased Array (AMPA) antenna system can be used alone effectively for conducting multiple experiments, or it can be integrated readily with other MMAP experiments for greater commonality of equipment and system synergism. Eventually, the AMPA antenna system could be used on a free-flyer spacecraft for multiple applications missions.

- Man has a vital role to play in the Spacelab/AMPA experiments. The three basic operational areas requiring manned activity are experiment activation, operation, and deactivation. Man would configure the experiment, calibrate and select modes of operation, control and monitor the experiment, perform on-board data evaluation for experiment iterations, and prepare the AMPA antenna system for reentry. He would also perform contingency operations as required. Man's participation and observation in real time would result in numerous benefits and greater experiment effectiveness.

- The Adaptive Multibeam Phased Array (AMPA) could be implemented for Spacelab flights in the early 1980's. This implementation would start with a Phase B System Definition Study and the study of experiment related tasks, and proceed on through the Phase C and D Execution for the development, manufacture, test, and integration of the AMPA antenna system. A program plan and schedule for this implementation is given in Section 8.

SECTION 3

APPLICATIONS FOR ADAPTIVE MULTIBEAM ANTENNAS

A survey was made of possible applications for an adaptive multibeam antenna to satisfy the objective of conducting adaptive multibeam experiments on Spacelab to evaluate techniques and related applications. The applications considered fell into three major categories: communications, radar for search and detection, and radiometry for earth resources.

As the applications study progressed, a large list of possible applications was compiled. From these, three applications missions were selected by General Electric in consultation with the NASA/GSFC Technical Officer for the Adaptive Multibeam Antenna Study and with other interested personnel at NASA/Goddard.

Having selected the three applications, the study proceeded to define the necessary parameters and design for performing techniques-oriented experiments on the Shuttle/Spacelab, with the end objective being the application of these techniques to the three categories. The detailed survey of these categories and the selection of meaningful applications is the subject of Subsections 3.1 and 3.2. The three selected AMBA experiments/applications are described in Subsection 3.3.

3.1 ADAPTIVE MULTIBEAM ANTENNA APPLICATIONS

A preliminary list of possible applications missions for adaptive multibeam antennas was compiled, based upon an extensive literature search and discussions with research workers at General Electric and at NASA/Goddard. This preliminary list of possible AMBA applications is shown in Table 3-1. For each application area, the performance attainable with aperture sizes considered reasonable for the Shuttle/Spacelab was explored. The initial calculations were made for a 2 meter by 2 meter aperture, which was then increased to 3 meters by 3 meters for better spatial resolution.

3.1.1 MULTIBEAM FEATURE FOR RADIOMETRY

In compiling the list shown in Table 3-1, it was realized that for many applications in remote sensing and mapping, adaptive features might not be necessary but multibeam features,

coupled with adequate resolution and beam efficiency, were of primary importance. The salient feature of the multibeam approach to earth resources was considered to be the reduction in time to image the field of view desired, reducing it from the product of the number of beams and the integration time for a single resolution cell to just the integration time for a single resolution cell. This was pointed out by Dr. F. C. Jackson of General Electric, who supplied the basic reasoning for this view and several papers to support that view.

Table 3-1. Potential AMBA Applications

Communications
Data Collection (1 way and 2 way) - Satellites, Aircraft, Ships, Buoys, Platforms, and Herd Migrations
Ground Truth Determination
Search and Rescue
Interference Maps
Low Power Communications (small users)
TDMA/SDMA (Sync and non-Sync)
Space Traffic Control
Shaped Beam Patterns (Synthetic)
Shuttle Position and Location
Navigation Aids
Radar
Meterological Radar
Ocean Wave Height and Slope
Traffic Control - Ships, Aircraft, Cars, Trains
Search and Rescue
Terrain Mapping
Scatterometry
Multipath Experiments
Buoy Tracking
Radiometry
Soil Moisture
Sea Ice Tracking and Monitoring
Ocean Temperature
Ground Temperature
Snow Cover
Cloud Cover
Oil Slick Tracking and Monitoring

For microwave radiometry, the time τ needed for one independent measurement is:

$$\tau = \frac{1}{\Delta f} \cdot \frac{1}{\left(\frac{\Delta T}{T}\right)^2} \qquad (1)$$

where T is the temperature to be measured, ΔT is the temperature resolution or accuracy to which the measurement is to be made, and Δf is the bandwidth in Hertz, assuming an ideal noiseless system. As an example, with $\Delta T = 10^{\circ}K$ and $T = 300^{\circ}K$, for $\Delta f = 10^6$ Hz, $\tau = 900$ microseconds. With $\Delta T = 1^{\circ}K$ and the same source temperature and signal bandwidth, $\tau = 90$ milliseconds.

An antenna with effective aperture area A_e has an angular resolution in two dimensions equal to the beamwidth squared, or approximately $(\lambda/D)^2 = \lambda^2/A_e$. The number of resolution cells in a solid angle of unity is thus A_e/λ^2. The time needed to image a unit solid angle field of view is then:

$$\Delta t = \tau\left(\frac{A_e}{\lambda^2}\right) \qquad (2)$$

For a 2 meter by 2 meter square array at 1.5 GHz ($\lambda = 20$ centimeters), the time Δt required to image unit solid angle field of view for a $1^{\circ}K$ resolution is 9 seconds, while for a $10^{\circ}K$ resolution the time is only 90 milliseconds. Thus, the desired temperature resolution dictates the time required to image a given field of view with angular resolution cells of size (λ^2/A_e) steradians.

The time rate of scanned solid angle, however, is given by:

$$\Delta t_s = \beta \frac{h}{v} \qquad (3)$$

where β is the transverse scanning angle, h is the altitude, and v is the orbital velocity. For $\beta = 1$ radian, $v = 7700$ m/sec, and $h = 270$ km, $\Delta t_s = 35$ seconds. For both cases treated above, the time required to image the field of view is less than the scanned rate of solid angle and so these are compatible.

While it is clear that these two cases are compatible with the time rate of scanned solid angle, the angular resolution is only about $1.2\,\lambda/D = 0.12$ radians for a 2 x 2 meter tapered array at 1.5 GHz. At 300 km orbit altitude, this gives a 36 kilometer spot size, which is too coarse a resolution for many applications of radiometry. Increasing the frequency to 10 GHz gives a better resolution (5.4 kilometers), but from equation (2) this requires a total integration time Δt of 400 seconds to image unit solid angle field of view for a temperature resolution of $1^{\circ}K$. This is not only excessive, but is longer than the time rate of scanned solid angle.

The multibeam feature can be used to reduce the time to image unit solid angle field of view to the time to make one independent measurement in one resolution cell. Obviously, if (A_e/λ^2) beams are used, then:

$$\Delta t = \tau \frac{(A_e/\lambda^2)}{(A_e/\lambda^2)} = \tau \qquad (4)$$

For a 2 x 2 meter array, this would require 100 beams at 1.5 GHz (λ = 20 cm). If only n beams are used, on the other hand:

$$\Delta t = \frac{\tau\,(A_e/\lambda^2)}{n}\,, \qquad (5)$$

and if $n = \dfrac{(A_e/\lambda^2)}{k}$ then

$$\Delta t = k\,\tau \qquad (6)$$

Thus at 10 GHz, to keep $\Delta t \leqq \Delta t_s = 35$ seconds, with a temperature resolution of $1^{\circ}K$, only $n \geqq 400/35 = 12$ beams are required. It is in this respect that the multibeam feature for passive microwave radiometry becomes highly desirable: to record large areas of the earth with high resolution and with high accuracy in temperature, in the time allotted by the given orbital parameters and transverse scan angle.

The parameters discussed above can be interrelated to obtain:

$$\Delta t \leqq \Delta t_s, \text{ or:}$$

$$\frac{\tau}{n} \cdot \frac{A_e}{\lambda^2} \leqq \frac{\beta h}{v} \tag{7}$$

When for $n = 1$, $\Delta t > \Delta t_s$, it is seen that by choosing $n > 1$ beams, the time Δt to image unit solid angle field of view can be reduced so that $\Delta t \leqq \Delta t_s$.

The applications for multibeam passive radiometry lead to the suggested techniques proposed for the Shuttle/Spacelab. Using as little as 4 beams, a 2 x 2 meter array at 1.5 GHz (λ = 20 cm) would have the time Δt required to image unit solid angle field of view reduced from 9 seconds to 2.25 seconds for a temperature resolution of 1^{o}K. For a transverse scan angle of 0.25 radians at 300 km orbit altitude, the time rate of scanned solid angle Δts is 9.7 seconds and a single beam would be sufficient. With 4 simultaneous beams, however, the transverse scan angle can be increased by $\Delta t_s/\Delta t$ to (9.7/2.25) x 0.25 = 1.08 radians, or about 60^{o}.

An experiment to test these techniques would require only 4 simultaneous receiving channels and would evaluate the use of multiple beams to reduce the required time to image the field of view for microwave radiometry. At the same time, the resolution of 36 kilometers for an array of 2 x 2 meters at 1.5 GHz would permit studies of ground run-off soil moisture as suggested by Dr. J. Shiue of NASA/Goddard.

A similar situation exists in such areas as radar scatterometry where the time to take one independent measurement in wave slope is:

$$\tau = \frac{1}{\Delta f} \left(\frac{\sigma}{\Delta \sigma} \right)^2 \tag{8}$$

for a given fractional slope resolution of $(\Delta\sigma / \sigma)$. It was concluded that for earth resources mapping, either passively or actively, the application of multiple beams to reduce the time to image a field of view below that of the allotted time is a desirable primary feature, and adaptive processing is of secondary importance.

3.1.2 ADAPTIVE MULTIBEAM FEATURE FOR COMMUNICATIONS AND RADAR

Adaptive processing enters into the scene where signal acquisition, detection, and tracking in the presence of natural or man-made interference are important. The benefits of adaptive multiple-beam antennas are:

1. Improved link performance
2. Inherent antenna discrimination against intentional and unintentional interference.

The increased link performance is due to:

1. Larger satellite antenna gain
2. Ability to take advantage of frequency re-use.

The increased antenna gain can be used to reduce ground terminal requirements or to increase the data rate. With the same frequency bandwidths utilized in several beam locations, the capacity for communication systems that are bandwidth limited is improved. With crowded spectrum allocations, multiple-beam antennas provide valuable additional capabilities.

Adaptive processing further offers:

1. The potential of optimizing the performance for a given community of users
2. Rejection of interferring signals.

These two factors are of considerable importance in enhancing the efficiency and performance of communication systems. The spatial and temporal variation of the user community and of the man-made and natural interference must be fully considered in using adaptive processing to optimize antenna system performance.

After a survey of adaptive multibeam antenna applications for communications and radar, attention was focused on the important application of search and rescue at sea and on the technique of signal detection, acquisition, and tracking in the presence of interference. An important Shuttle/Spacelab experiment is the detection, acquisition, and tracking of low-power signals from a subject in distress as in a lifeboat or raft.

Since the spatial resolution of a 2 x 2 meter array at 300 km is about 37 km using a wavelength λ = 20 cm (1.5 GHz), this is the smallest resolution cell of that particular antenna that can be observed. Using doppler shift techniques, however, the range can be found very accurately, providing the location and velocity of the Shuttle/Spacelab is known very accurately. It is feasible that location to within 0.3 kilometers can be obtained based on the calculations performed. The requirements for this, determined from the required doppler slope sensitivity, would be a sender in distress with an antenna gain of 2 dB and 10 watts of power in order to get a signal-to-noise ratio of 46 dB with a 2 x 2 meter array at λ = 20 cm and 300 kilometers orbit altitude. With higher gain antennas, powers of only a watt or less would be required. Thus, the search and rescue experiment for the adaptive multibeam antenna at 300 km orbit altitude seems very feasible.

Many adaptive processing modes for interference rejection and for signal acquisition and tracking could be tested by utilizing low power systems on the earth. This important problem of rapidly locating senders in distress is, therefore, one of the prime applications for the Adaptive Multibeam Antenna system.

3.2 AMBA APPLICATIONS MATRIX

The survey discussed in Subsection 3.1 considered three basic categories of applications missions, explored values for the key operational parameters, and identified features and benefits of adaptive multibeam antennas for those application areas. An applications matrix was then prepared for each category to summarize the critical parameters, requirements, and basic antenna design features. These AMBA applications matrices are shown in Tables 3-2, 3-3, and 3-4 for the communications, radar, and radiometric applications, respectively. An evaluation of the AMBA potential for each application is given in the last column of each matrix.

Table 3-2. Possible Communications Applications and Requirements

Applications	Objective	Critical Parameters	Requirements*	Basic Design Features	Evaluation*
• Search and Rescue	Locate sender in distress	Low power sender with low gain antenna; Search, detect, acquire, and track; Locate sender within 0.01 km	Multibeam antenna; Adaptive processing; Scan large area and track; Doppler source location	3 x 3 meter array; 500 MHz to 1.5 GHz (λ = 60 to 20 cm); Adaptive processing	Ideal application for AMBA experiment
• Small User Communications	Low power communications between small users	Detect, acquire, and relay message; Large no. channels; Frequency re-use; Adaptive spatial and temporal processing	Adaptive multi-beam antenna; Acquire, beam-form, and track; Identify users; Interference rejection	3 x 3 meter array; 500 MHz to 1.5 GHz; Adaptive processing	Excellent for AMBA; 2 beam experiment initially
• Navigation and Traffic Control	Guide aircraft and ships	Search, detect, acquire, and track sender; Locate to 0.1 km accuracy	Frequency re-use; Interference rejection; Adaptive signal processing	3 x 3 meter array; 500 MHz to 1.5 GHz	Good AMBA potential
• Data Collection	Readout data from buoys, herd migrations, etc.	Low power sender with low gain; Activate trans-ponder; Accept coded information; Locate within 0.01 km	Multibeam antenna; Adaptive processing; Scan large area and track; Doppler source location	3 x 3 meter array; 500 MHz to 1.5 GHz; Adaptive processing	Excellent for AMBA

*For meaningful experiment on Shuttle/Spacelab.

Table 3-3. Possible Radar Applications and Requirements

Applications	Objective	Critical Parameters	Requirements*	Basic Design Features	Evaluation*
• Oceanography	• Determine sea state	Mean wave slope; Mean wave height to 1%	1m resolution; 100 MHz bandwidth; 0.1m sec. int. time	Large array; High frequency	Not feasible for Shuttle experiment
	• Sea ice extent	Radar imagery	25 km resolution; 100 MHz bandwidth; Negligible int. time	3 x 3 meter array; 1.5 GHz feasible	Good for AMBA; 4 beams for reduced mapping time
• Meteorology	Determine cloud cover, storms, etc.	Radar imagery	25 km resolution; 100 MHz bandwidth; Negligible int. time; f = 19 GHz	0.3 x 0.3 meter array; 19 GHz (λ = 1.58 cm)	Good for AMBA; 4 beam experiment
• Terrain Mapping	Geographic mapping and prediction	• Altitude	1m range resolution; 100 MHz bandwidth; 1m sec. int. time	Not applicable	Multibeam antenna not needed
		• Radar imagery	30 km resolution; 100 MHz bandwidth; Negligible int. time	3 x 3 meter array; 1.5 GHz usable	Good for AMBA; 4 beam experiment

*For meaningful experiment on Shuttle/Spacelab

Table 3-4. Possible Radiometric Applications and Requirements

Applications	Objective	Critical Parameters	Requirements*	Basic Design Features	*Evaluation
• Oceanography	• Determine sea state	$\Delta T = 0.5^{o}K$ $T = 300^{o}K$ f = 60 GHz	10 m resolution; 100 MHz bandwidth; 4m sec. int. time	Large array; 60 GHz and up	Not feasible for Shuttle experiment
	• Ocean temperature	$\Delta T = 0.5^{o}K$ $T = 300^{o}K$	25 km resolution; 100 MHz bandwidth; 4m sec. int. time	3 x 3 meter array; 1.5 GHz (λ = 20 cm) adequate	Good for AMBA; 2 or 4 beam experiment initially
	• Sea ice distribution	$\Delta T = 0.5^{o}K$ $T = 273^{o}K$	25 km resolution; 100 MHz bandwidth; 3m sec. int. time	3 x 3 meter array; 1.5 GHz adequate	Good for AMBA; 2 or 4 beam experiment
• Soil Moisture	• Determine farm moisture	$\Delta T = 0.5^{o}K$ $T = 300^{o}K$ f = 1.4 GHz	100 m resolution; 100 MHz bandwidth; 4m sec. int. time	Large array; 60 GHz and up	Not feasible for Shuttle experiment
	• Watershed distribution	$\Delta T = 0.5^{o}K$ $T = 300^{o}K$ f = 1.4 GHz	25 km resolution; 100 MHz bandwidth; 4m sec. int. time	3 x 3 meter array; 1.5 GHz adequate	Good for AMBA; 2 or 4 beam experiment
• Meteorology	Determine cloud cover, storms, etc.	$\Delta T = 0.5^{o}K$ $T = 200^{o}K$ to $300^{o}K$ f = 19 GHz	10 km resolution; 100 MHz bandwidth; 2 to 4m sec. int. time	0.6 x 0.6 meter array; 19 GHz (λ = 1.58 cm)	Good for AMBA; 4 beam experiment

*For meaningful experiment on Shuttle/Spacelab

3.3 SELECTED AMBA EXPERIMENTS

The three applications missions selected by General Electric and NASA/GSFC as suitable for conducting meaningful Adaptive Multibeam Antenna experiments on Spacelab are the L-band Communications Experiment, the L-band Radiometer Experiment, and the Ku-band Communications Experiment. These three experiments offer the opportunity to evaluate a variety of antenna system techniques for a diversity of applications. The experiments are defined in the following three sections. Key measurement parameters are given, and some suggested modes of operation for a systematic experimental evaluation are listed. The antenna performance requirements for the three selected experiments are tabulated at the end of each section. Detailed analyses are given in Appendices A and B for the communications and radiometer experiments.

3.3.1 L-BAND COMMUNICATIONS EXPERIMENT

The L-band Communications Experiment is defined in Figure 3-1. The purpose of the experiment is to demonstrate the feasibility of low power, point-to-point communications via low orbiting spacecraft using narrow beams. It is based on short term communication between ships and assumes low power cooperating shipboard terminals having near hemispheric overhead coverage operating at the maritime L-band communications frequencies.

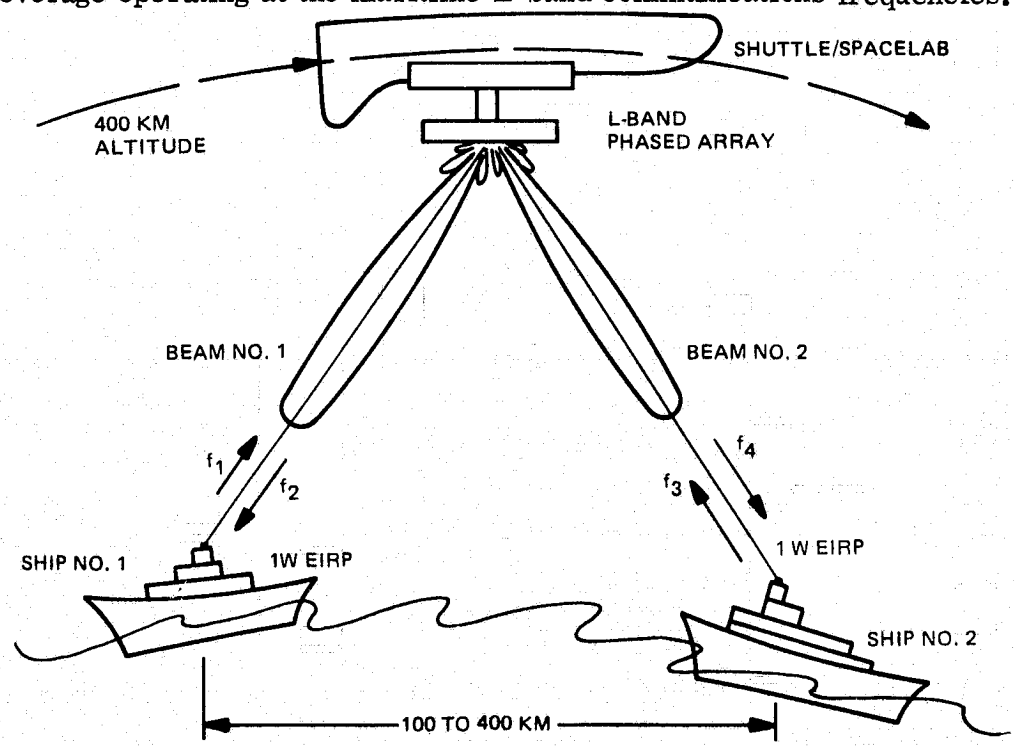

Figure 3-1. L-band Communications Experiment Definition

The key measurement parameters for the L-band Communications Experiment are:

1. Acquisition time
2. Track accuracy
3. Signal to noise ratio (S/N) at Spacelab
4. Doppler compensation achieved at Spacelab
5. Received signal quality
6. Interference cancellation ratio

The following modes of operation are suggested for this experiment:

1. Adaptively form one or two receive beams pointed toward cooperating shipboard transmit terminals and record data received. Antenna performance parameters such as acquisition time, S/N, doppler compensation achieved, and angle tracking will also be recorded for later analysis.

2. Adaptively form two receive beams and two corresponding transmit beams to establish a communications link between two cooperating shipboard terminals within the coverage area. Record data relayed via the antenna system and record the antenna performance parameters.

3. Adaptively form a communications link as in mode 2 above, but in the presence of a third cooperating shipboard terminal that transmits a controlled interference signal, and adaptively reject the known interference to maximize S/N for the desired transmission under various conditions. Record data relayed and the antenna performance parameters, including measures of interference rejection/ cancellation.

The Adaptive Multibeam Antenna (AMBA) performance requirements established for this experiment are given in Table 3-5.

Table 3-5. Antenna Performance Requirements for L-band Communications Experiment

Transmit Frequency Band	1530 to 1550 MHz
Receive Frequency Band	1630 to 1650 MHz
Antenna Gain	27 dB min.
-3 dB Beamwidths	5^{o}
Number of Independent Receive Beams	2
Number of Corresponding Transmit Beams	2
Coverage Angle	$\pm 40^{o}$ cone about Nadir
Beam Steering Method	Adaptive Control
Beam Pointing Accuracy	0.5^{o}
Side Lobe Levels	-20 dB max.
Transmit Polarization	RH Circular
Receive Polarization	LH Circular
Transmit Power	10 W
Signal Acquisition Time	< 5 Seconds
Signal Tracking Rate	$> 2^{o}$ per Second

3.3.2 L-BAND RADIOMETER EXPERIMENT

The L-band Radiometer Experiment is defined in Figure 3-2. The purpose of the experiment is to demonstrate the feasibility of radiometric soil moisture measurement from low orbiting spacecraft using multiple narrow beams. Because of the coarse resolution obtained at L-band with a 3 meter aperture (about 35 km), measurements of greatest significance will be those of gross water sheds in mountainous regions and of ground-water runoff and soil moisture distribution in valleys and plains. The techniques developed with this experiment will be applicable, however, to the design of systems having greater resolution.

The key measurement parameters for the L-band Radiometer Experiment are:

1. Beam control versus beam sequence
2. Optimum beam stepping and dwell time

3. Temperature reading and calibration

4. Temperature resolution

5. Optimum combination of beams and receivers

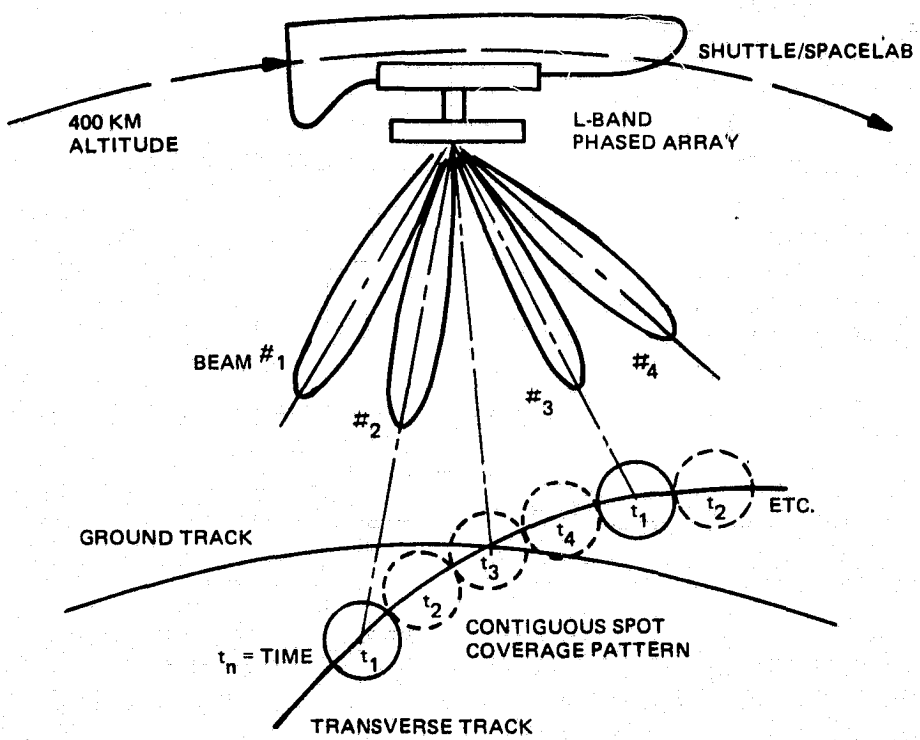

Figure 3-2. L-band Radiometer Experiment Definition

The following modes of operation are suggested for this experiment and indicate the great variety of beam sequences that could be used:

1. Form four program-controlled, equally spaced beams spaced four beamwidths apart in a plane perpendicular to the flight plane and dwell for the radiometer integration time with correction for motion along the flight path. Step the group of beams one beamwidth to effect contiguous beam coverage and dwell as before; then, repeat the step and dwell sequence two more times to complete the cycle. Return beams to initial position relative to the spacecraft so as to form contiguous beams along the flight path, and repeat entire cycle. Record all radiometry data and antenna performance data for later analysis.

2. Form four program-controlled contiguous beams in a plane perpendicular to the flight plane and dwell for the radiometer integration time with correction for motion along the flight path. Step the group of beams four beamwidths to effect contiguous beam coverage and dwell as before; then repeat the step and dwell sequence two more times to complete the cycle. Return beams to initial relative position so as to form contiguous beams along the flight path, and repeat the entire cycle. Record data as before.

3. Form four program-controlled contiguous beams in a square cluster and dwell as for modes 1 and 2, step the beam cluster two beamwidths to effect contiguous beam coverage and dwell as before, and repeat the step and dwell sequence six more times to complete the cycle. Return the beam cluster to its initial relative position so as to form contiguous beams along the flight path, and repeat the cycle. Record data as before.

4. Form and steer four program-controlled beams in other geometrical coverage patterns that it may be desired to investigate, such as circular or spiral scan, and record data as before.

These modes of operation will be developed further in Section 4.1.

The Adaptive Multibeam Antenna (AMBA) performance requirements established for this experiment are given in Table 3-6.

Table 3-6. Antenna Performance Requirements for L-band Radiometer Experiment

Radiometer Frequency	1400 MHz
Bandwidth	50 MHz
Antenna Gain	27 dB min.
-3 dB Beamwidths	5^{o}
Number of Independent Beams	4
Individual Beam Efficiency	85%
Side Lobe Levels	-20 dB max.
Polarization	Dual Linear
Coverage Angle	$\pm 40^{o}$ cone about Nadir
Beam Steering Method	Program Controlled
Beam Pointing Accuracy	0.5^{o}
Beam Repositioning Time	0.1 msec. max.

3.3.3 KU-BAND COMMUNICATIONS EXPERIMENT

The Ku-band Communications Experiment is defined in Figure 3-3. The purpose of the experiment is to demonstrate the feasibility of low power, wideband, point-to-point communications via low orbiting spacecraft using narrow beams and to demonstrate the feasibility of frequency re-use by means of adaptive dual polarization. It is based on short term communication between ground stations and assumes moderate power cooperating ground terminals of moderate gain (40 to 50 dB) that will track Spacelab.

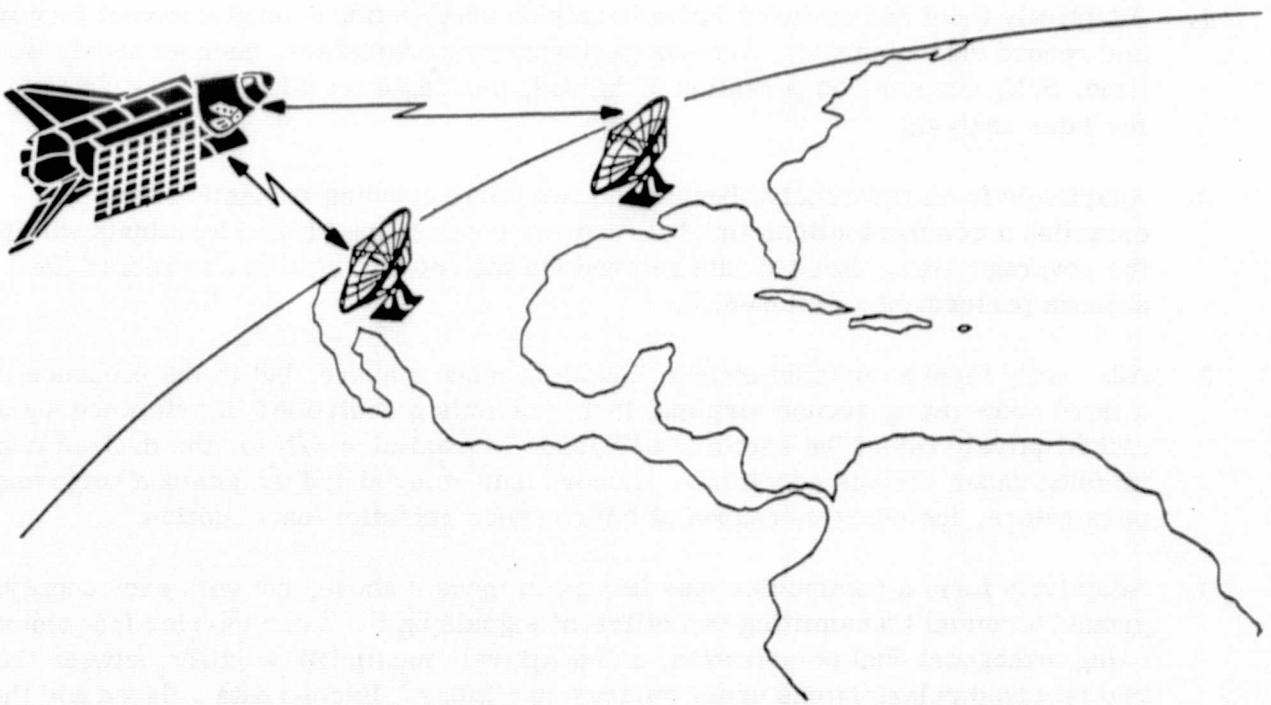

Figure 3-3. Ku-band Communications Experiment Definition

The key measurement parameters for the Ku-band Communications Experiment are:

1. Acquisition time
2. Track accuracy
3. Signal to noise ratio (S/N) at Spacelab

4. Doppler compensation achieved at Spacelab

5. Received signal quality

6. Interference cancellation ratio

7. Dual polarization isolation

The following modes of operation are suggested for systematically evaluating the techniques to be investigated in this experiment:

1. Adaptively form one or two receive beams on cooperating ground transmit terminals and record data received. Antenna performance parameters, such as acquisition time, S/N, doppler compensation achieved, and angle tracking will also be recorded for later analysis.

2. Adaptively form two receive beams and two corresponding transmit beams to establish a communications link between two cooperating ground terminals within the coverage area. Record data relayed via the antenna system and record the antenna performance parameters.

3. Adaptively form a communications link as in mode 2 above, but in the presence of a third cooperating ground terminal that transmits a controlled interference signal, and adaptively reject the known interference to maximize S/N for the desired transmission under various conditions. Record data relayed and the antenna performance parameters, including measures of interference rejection/cancellation.

4. Adaptively form a communications link as in mode 2 above, but with each cooperating ground terminal transmitting two different signals on the same carrier frequency using orthogonal dual polarization, and adaptively maximize isolation between the two received polarizations under various conditions. Record data relayed and the antenna performance parameters, including measures of the orthogonally polarized signal isolation.

The Adaptive Multibeam Antenna (AMBA) performance requirements established for this experiment are given in Table 3-7.

Table 3-7. Antenna Performance Requirements for Ku-band Communications Experiment

Transmit Frequency	12 GHz
Receive Frequency	14 GHz
Bandwidth	500 MHz
Antenna Gain	27 dB min.
-3 dB Beamwidths	5^{o}
Number of Independent Receive Beams	2
Number of Corresponding Transmit Beams	2
Coverage Angle	$\pm 40^{o}$ cone about Nadir
Beam Steering Method	Adaptive Control
Beam Pointing Accuracy	0.5^{o}
Side Lobe Levels	-20 dB max.
Transmit Polarization	RH and LH circular, or orthogonal linear
Receive Polarization	LH and RH circular, or orthogonal linear
Transmit Power	10 W
Signal Acquisition Time	< 5 Seconds
Signal Tracking Rate	$> 2^{o}$ per Second

SECTION 4

ANTENNA PERFORMANCE REQUIREMENTS AND DESIGN TRADEOFFS

The three Adaptive Multibeam Antenna (AMBA) experiments that were defined in Section 3 are summarized at the beginning of this section. The antenna performance requirements established for those experiments in Section 3 are then discussed in more detail. The results of communications link and radiometer analyses are given, and the operational modes for the experiments are expanded into functional requirements. Some additional considerations presented are alternative radiometer scan sequences and means of increasing experiment operational time.

The characteristics of several types of antenna systems that were considered during the Phase A Study are discussed in Subsection 4.2 with respect to the specified antenna performance requirements. The various design tradeoff features for each antenna type are considered in relation to the requirements. It became evident early in the study that a phased-array antenna system offered the greatest versatility for performing the desired experiments and was actually the most practical means of achieving the desired capability. As a result of these design tradeoff considerations, the phased array was selected as the preferred type of antenna. Design concepts that were developed for an Adaptive Multibeam Phased Array (AMPA) antenna system are presented separately in Section 5.

4.1 ANTENNA PERFORMANCE REQUIREMENTS

The three Adaptive Multibeam Antenna (AMBA) experiments that were selected during the Phase A Feasibility Study are the L-band Communications Experiment, the L-band Radiometer Experiment, and the Ku-band Communications Experiment. These were discussed in Section 3 and are summarized in Figures 4.1-1, 4.1-2, and 4.1-3.

The antenna performance requirements established for these three experiments are summarized in Table 4-1. A detailed discussion of these requirements is given in this section for each of the experiments. The modes of operation given in Section 3 for each experiment are interpreted here in terms of functional requirements.

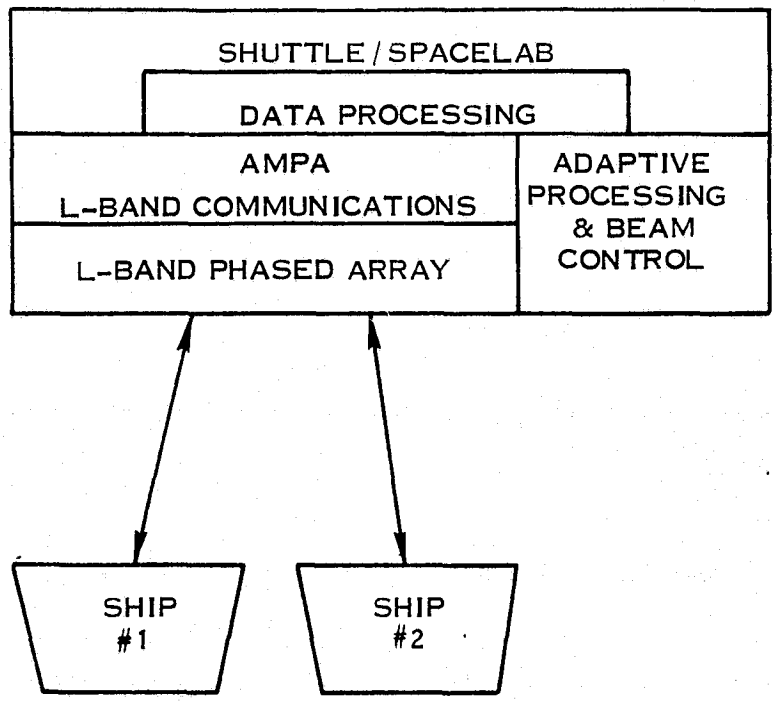

Figure 4.1-1. L-Band Communications Experiment Block Diagram

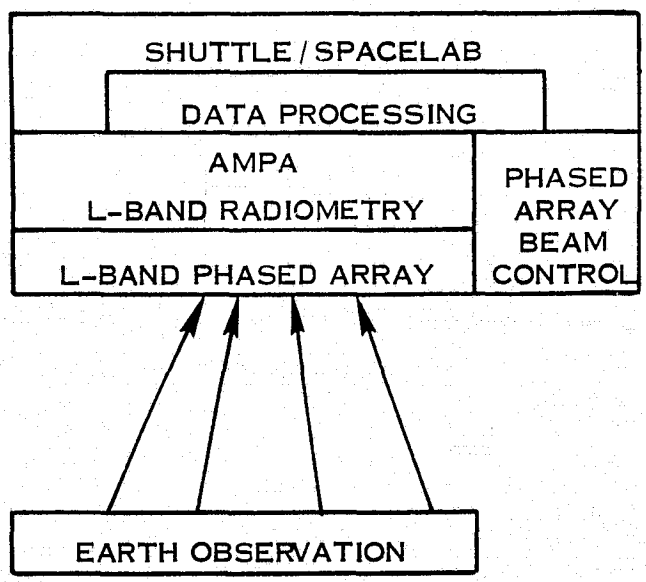

Figure 4.1-2. L-Band Radiometer Experiment Block Diagram

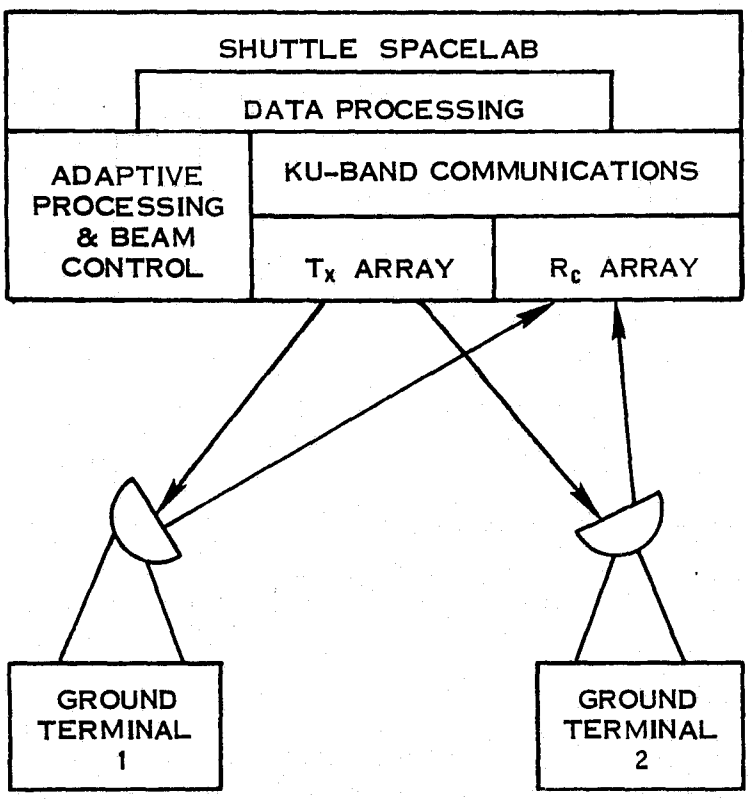

Figure 4.1-3. Ku-Band Communications Experiment Block Diagram

Table 4-1. Summary of Antenna Performance Requirements

Parameter	L-band Communications	L-band Radiometer	Ku-band Communications
Transit Frequency, GHz	1.54	N/A	12
Receive Frequency, GHz	1.64	1.4	14
Bandwidth, MHz (each band)	20	50	500
Minimum Antenna Gain, dB	27	27	27
-3 dB Beamwidth, degrees	5	5	5
Number of Independent Receive Beams	2	4	2
Number of Corresponding Transmit Beams	2	N/A	2
Beam efficiency (in main beam), %	N/A	85	N/A
Coverage Angle Rel. to Nadir, degrees	±40	±40	±40
Beam Steering Method	Adaptive Control	Program Controlled	Adaptive Control
Beam Pointing Accuracy, degrees	0.5	0.5	0.5
Beam repositioning time, millisec.	N/A	0.1	N/A
Maximum Sidelobe Level, dB	-20	-20	-20
Transmit Polarization	RH circular	N/A	R&L circ. or Dual 4 in.
Receive Polarization	LH circular	Dual Linear	Orthog. to Tx
Transmitter Power, Watts	10	N/A	10
Signal Acquisition Time, sec.	<5	N/A	<5
Signal Tracking Rate, degrees/sec.	>2	N/A	>2

A detailed analysis was made of the communications experiment constraints for the L- and Ku-band experiments. These are detailed in Appendix A. Link calculations, carrier acquisition for PCM/PSK-PM, acquisition (and data) for FM, data margins in the PCM/PSK-PM System, ground antenna considerations, etc., are analyzed to determine the optimum design approach.

The pertinent results of that analysis for the L-band Communications Experiment are that a ground transmitted power of 275 mw is required with a 3 dB-gain ground antenna in order to achieve 3 KBps data transmission over a PCM/PSK-PM data link for a 47.7 second contact time. The corresponding Spacelab/AMPA transmitted power required was established as 138 mw, which leaves 18.6 dB of signal margin with 10 watts of Spacelab transmitted power.

For the Ku-band Communications Experiment, two fully duplex communications links of 50 MHz bandwidth are planned. A ground transmitter power of only 6.18 watts and a ground antenna gain of 54.7 dB (15-foot reflector) are required for a reference AMPA configuration, which has a worst-case noise figure of 15 dB. The downlink transmitted power required from Spacelab is only 0.168 watts. A best-case noise figure of 8 dB is obtained with an alternative AMPA configuration having more hardware, as discussed in Section 5.

An additional performance requirement applicable to both the L-band and Ku-band communications antenna systems is that any adjacent transmit carrier intermodulation products be down greater than 130 dB in the receive band. This requires carefully designed diplexer circuitry. In-band intermodulation products, on the other hand, are compatible with a saturating transmit amplifier and would be acceptable in a system having separate amplifiers per transmit beam.

A detailed analysis was also made for the L-band Radiometer Experiment constraints, and these are given in Appendix B. For a Shuttle orbit altitude of 400 km, the analysis gives an available dwell time per spot of 1.2 seconds for four radiometer beams, or 0.6 seconds for

two radiometer beams. The corresponding temperature resolution attainable is $\Delta T = 0.33^{o}K$ or $0.46^{o}K$, respectively, with a 5 dB noise figure for the radiometer receiver. With regard to the radiometer bandwidth, 27 MHz would probably be used instead of 50 MHz because of the availability of the 1.4 to 1.427 GHz radio astronomy band and because the achievable temperature resolution is suitable.

The modes of operation given in Section 3 for the three selected AMBA experiments are expanded here into functional requirements. The functional requirements of the L-band Communications Experiment include:

1. The system should be capable of automatically locating two RF transmitting sources in an interference-free environment. The sources may be located sequentially or simultaneously. It is highly desirable that the locating process be as rapid as possible because the available communication time between two ground stations simultaneously within the satellite's AMPA field-of-view is short (approximately 50 seconds).

2. The system should automatically form beams in the direction of the two sources using the full array area for both beams.

3. These beams should be maintained on the sources as the directions to the sources change because of the satellite motion.

4. The AMPA should receive data from source 1 via beam 1 and retransmit the data to source 2 via beam 2 and vice versa.

5. The AMPA shall measure and record all data necessary to evaluate the system performance. These shall include, as a minimum, the following:

    a. GMT of acquisition time of each beam which together with the GMT of initiation of transmission by the ground station sources will be used to determine acquisition time.

    b. Received signal levels vs. time to assess the signal to noise ratio in each receive channel continuously.

    c. Frequency of each received signal to obtain a continuous record of beam tracking performance vs. doppler shift.

    d. The direction of the two beams as measured by the phases automatically attained in the AMPA to track the transmitting sources. These directions

will later be compared to the computed directions between the satellite and signal sources to assess the accuracy of the AMPA automatic angle tracking.

e. The two received signals at the satellite will be demodulated and recorded. By this means the uplink performance can be evaluated separately from the downlink performance.

f. In addition to measurements performed and recorded on the satellite a comparable set of measurements will be made at the two ground receivers to evaluate both the individual downlink performance and the full two-way performance (earth station to satellite to earth station).

6. The system should be capable of achieving the above full duplex link between the two earth stations in the presence of a controlled interfering RF source. This source will be within the AMPA field-of-view at the same time as the two transmitting-receiving sites.

   The AMPA design will incorporate automatic sidelobe interference rejection features to minimize the effect of the interference source. The interference source will initially be a noise modulated carrier in the AMPA acceptance bandwidth. Later more sophisticated interference sources may be employed.

7. The experiment will be designed for repeated signal acquisition, beam tracking, and data transfer with varying levels and types of interference over many satellite passes. The measurements will be same as above except that all measurements will be made at points in the circuitry where the effect of interference rejection can be monitored.

The functional requirements for the L-band Radiometer Experiment are:

1. The system shall provide several beam sequences and dwell times to permit evaluation of alternate approaches to soil moisture measurement using simultaneous programmed beams.

2. The system shall provide at least two and preferably four simultaneous beams.

3. The radiometer beams shall yield spatial resolution (spot size) equivalent to that available from the full array aperture when used for one beam only.

4. The system shall provide the same coverage (a continuous swath of ± 40 degrees) as a single scanned beam.

5. The system shall provide four times the integration time per spot with four beams (or twice with two beams) as would one beam covering the same swath, and the corresponding temperature resolution.

At least the three scan modes or sequences shown in Figures 4.1-4,5, and 6 should be considered for a four-beam system. The design may provide all three modes, or if no particular advantage exists from one mode to the next, the design may provide only one scan mode with a saving in programming and/or RF hardware complexity. Program flexibility will permit special scan modes, however, such as circular or spiral scan modes.

Note that the dwell time per spot is the same for all three cases. It is uniquely determined by the number of spots each beam must illuminate during the time interval in which the satellite advances one spot size. In Appendix B, the dwell time was found to equal 1.212 seconds per spot for a 4-beam radiometer system. For a 2-beam system, the dwell time would be 0.606 seconds per spot. The 1.212 seconds dwell time would be allocated 1.2 seconds to integration and 12 milliseconds to beam switching in a 4-beam radiometer system. For a 2-beam system, the integration time would be about 0.6 seconds.

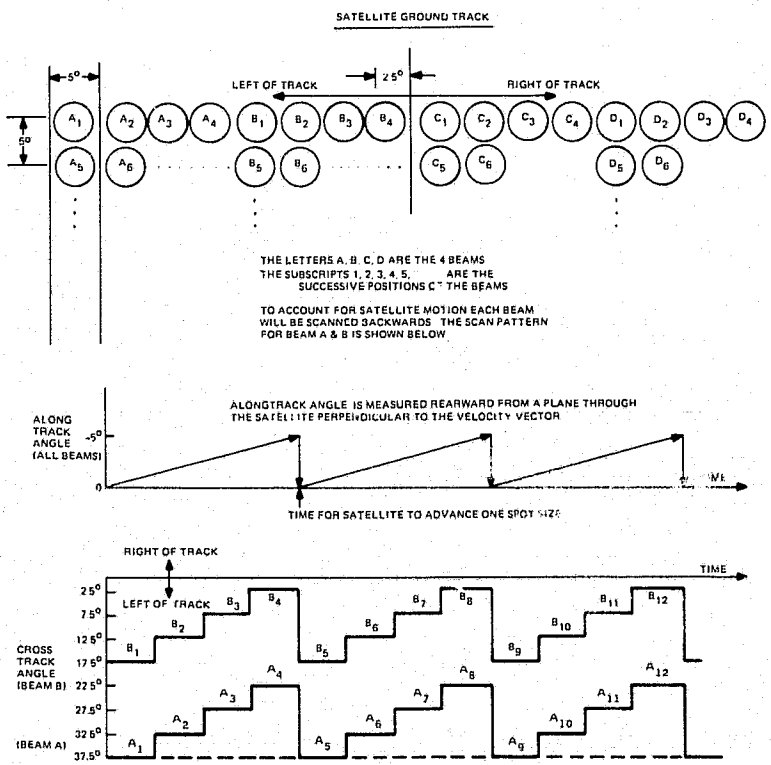

Figure 4.1-4. Radiometer Scan Mode, Case 1

The functional requirements for the Ku-band Communications Experiment include all those of the L-band Communications Experiment; that is, automatic locating of two signal sources, establishing a full duplex link between the earth (or ship) stations, and interference rejection. In addition, the AMPA must have capability at Ku-band of a full duplex link where each terminal will transmit and receive using dual orthogonal polarizations at the same frequency to double the data capacity in the same bandwidth. Thus, there will be in effect two full duplex links between the two terminals instead of the one full duplex link of the L-band experiment case. This will be accomplished in an interference-free environment initially, and then evaluated in the presence of controlled interference. The design should adaptively maximize the isolation between the two received polarizations from each transmitting source under various conditions.

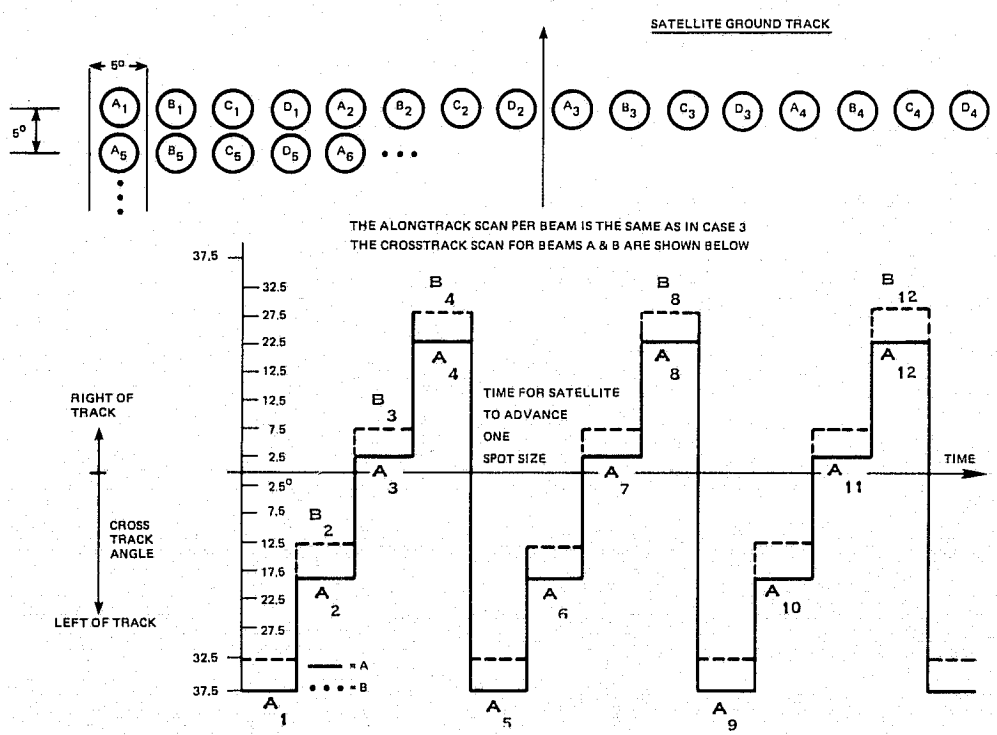

Figure 4.1-5. Radiometer Scan Mode, Case 2

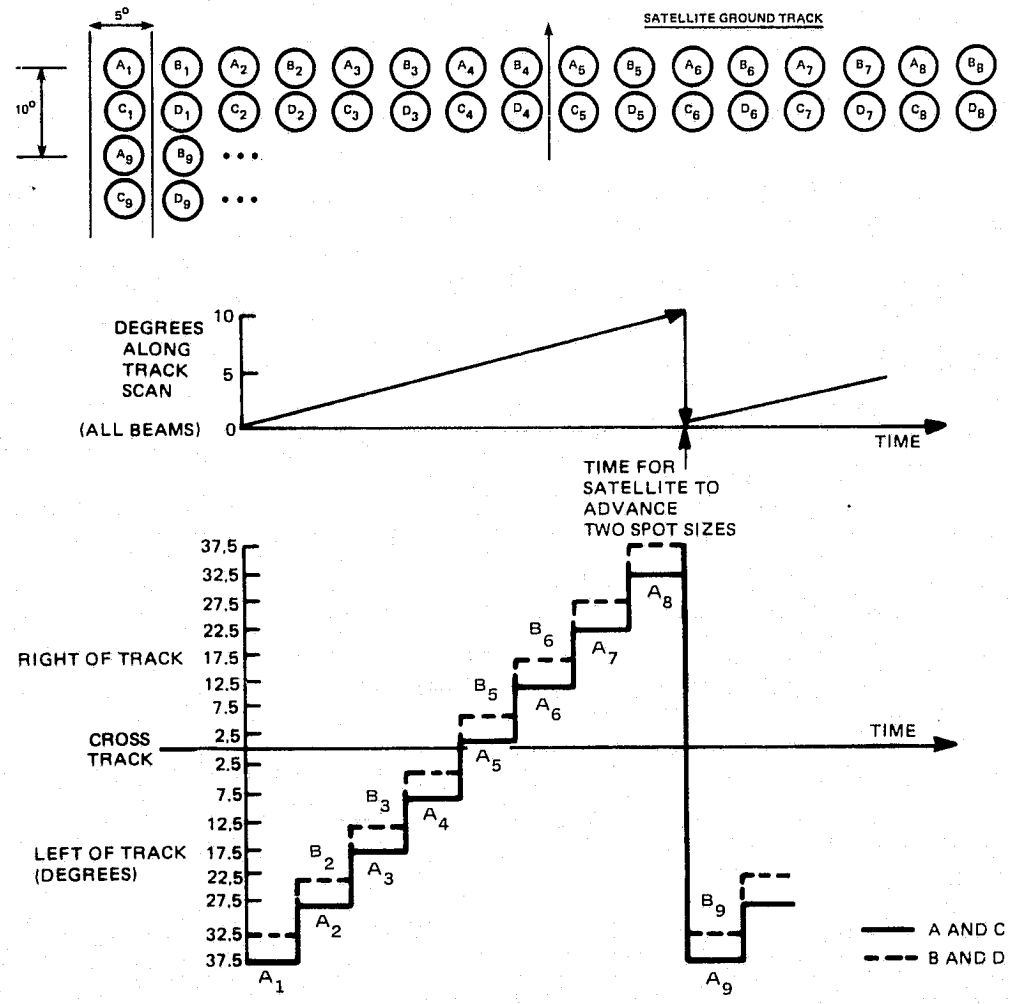

Figure 4.1-6. Radiometer Scan Mode, Case 3

Techniques are discussed in Paragraph 5.5.4 for isolating and tracking two signals which are transmitted with orthogonal polarization, and arrive at the AMPA with changed relative polarizations. This is illustrated in Figure 4.1-7 for five typical pairs of polarization conditions.

The same types of measurements will be made in the Ku-band Experiment as in the L-band Communications Experiment except that for Ku-band they will be repeated four times instead of twice; i.e., once for each received polarization from each of the two sources.

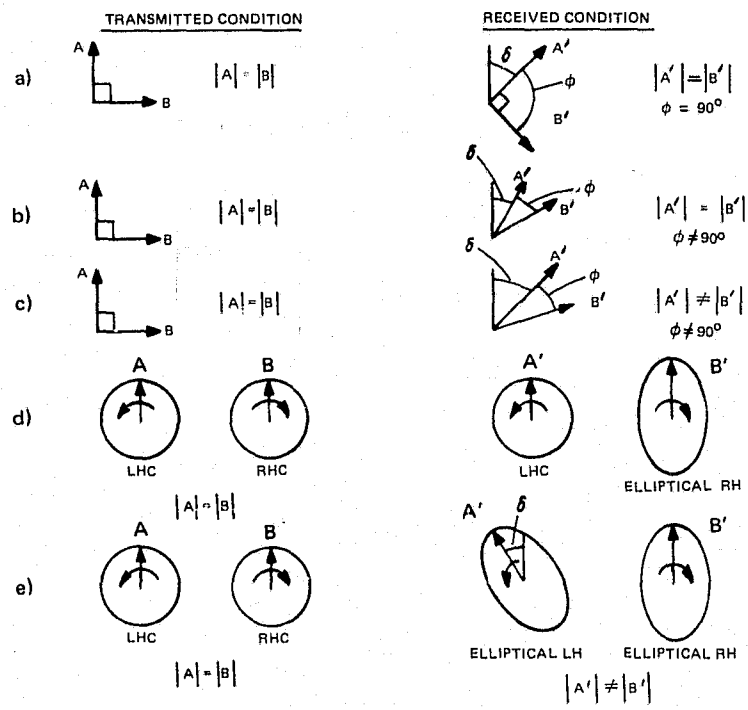

Figure 4.1-7. Typical Changes in Received Polarization

One further consideration that deserves some additional study is the problem of how to increase the limited experiment operational time. Typical AMPA/Spacelab orbit traces for one day are shown in Figure 4.1-8. It is seen that only one or two passes per day occur over a given global area. This could possibly be increased to four or more, if programmed roll of the Shuttle/Spacelab (or tilt of the AMPA antenna system) were employed to aim the Adaptive Multibeam Phased Array (AMPA) for coverage to one side of the ground track and then the other on two or more subsequent passes.

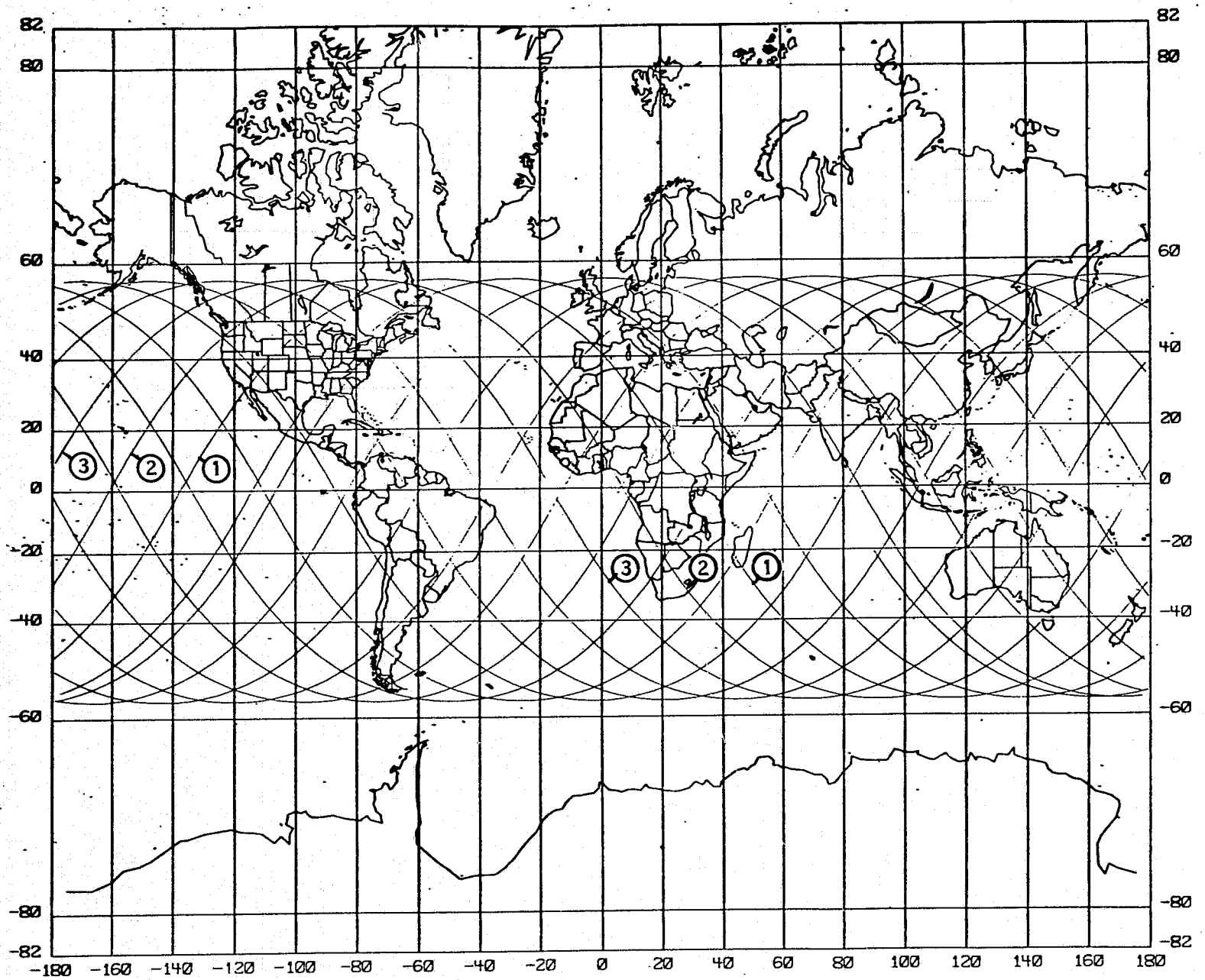

Figure 4.1-8. Typical AMPA/Spacelab Orbit Traces for One Day

4.2 ANTENNA TYPES AND DESIGN TRADEOFFS

As indicated earlier, the multibeam phased array was chosen as the preferred antenna system over multibeam reflector and lens antenna systems during the AMBA Phase A Feasibility Study. The various types of antenna systems considered and the reasons for choosing the phased array are presented in this subsection. The large number of multibeam antenna configurations that exist may be generally classified into four categories. These are the reflector, the passive (waveguide and dielectric) lens, the active (bootlace) lens, and the phased array types of antenna systems. The characteristics of each of these antenna systems were considered with respect to their inherent capabilities and their ability to meet the antenna performance requirements of the selected Adaptive Multibeam Antenna experiments.

Examples of the various types of antenna systems considered are presented, and their major performance features and limitations are discussed. Evaluation criteria are then described, and a tradeoff chart is presented to summarize the results.

4.2.1 REFLECTOR ANTENNA SYSTEMS

Reflector antennas are ideally suited for single beam operation. Reflector antenna systems can also be used to generate multiple beams over a limited field of view and may be constructed in a wide variety of configurations, each with its own desirable features. Several advantages of reflector antenna systems which made them contenders for the AMBA experiments are listed below:

1. Reflectors are inherently broadband, with the bandwidth limited primarily by the feed.
2. For large sizes, the cost per unit area is low.
3. Reflector antennas are relatively lightweight.
4. Analysis and design procedures are simpler than for lenses and phased arrays of comparable performance.

Several shortcomings of reflectors when compared with lenses and phased arrays, however, are:

1. Single reflector systems have fewer degrees of freedom than lenses or phased arrays, which results in poorer pattern performance.

2. Aperture blockage in symmetrical reflector systems causes gain loss and an increase in sidelobe levels, especially when multiple feeds are used.

3. The patterns degrade rapidly for feeds located off the optical axis of a single reflector system.

4. Multiple reflector systems also have limited angle coverage, and are more complex.

5. Offset reflector systems avoid aperture blocking, but introduce system asymmetry.

Representative reflector antenna systems are shown in Figures 4.2-1 and 4.2-2. Figure 4.2-1 illustrates a single symmetrical paraboloid fed by a primary feed cluster. Each beam in space is associated with an individual feed element in this configuration. The system has limited scan capability, poor off-axis patterns, and excessive aperture blockage. Figure 4.2-2 illustrates one of many offset dual reflector systems, which overcome the aperture blockage problem. This system has limited scan capability also, however, and suffers addtional pattern degradation due to reflector asymmetry.

4.2.2 PASSIVE LENS ANTENNA SYSTEMS

Lens antenna systems perform better than reflector systems in several respects. They maintain better patterns over moderate coverage angles, and wide angle lenses can be designed to achieve relatively low phase errors over much larger angles. They have no aperture blockage because the feed system is behind the lens and transmits or receives through it.

Passive lens antennas may be of either the constrained waveguide or the dielectric type. The waveguide lens has greater freedom in design, but the dielectric type has a greater bandwidth. An example of a zoned waveguide lens with multibeam feed, which was developed by General Electric, is shown in Figure 4.2-3.

Passive lens antenna systems have individual beams in space associated with individual feeds, as do the reflector systems. In general, they cannot meet the wide coverage angle required for conducting experiments at low orbit altitudes without sacrificing beam agility and incurring pattern degradation. Passive lens antenna systems also have limited adaptive capability.

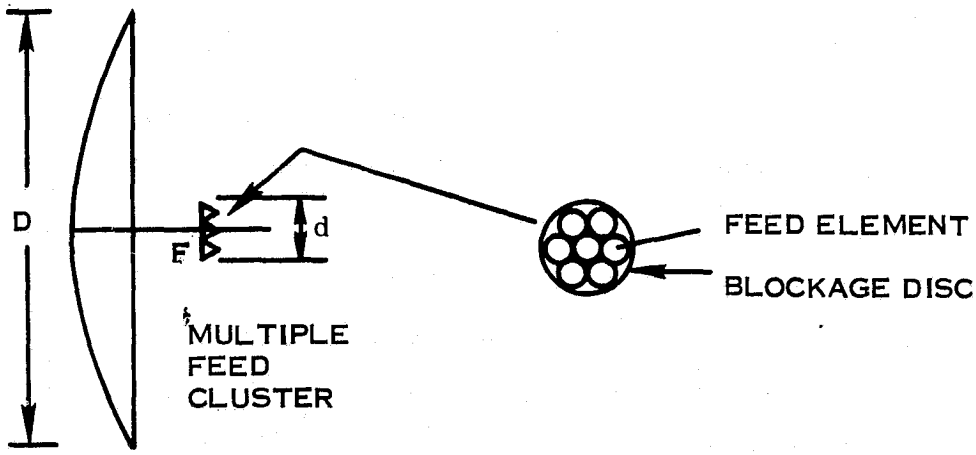

Figure 4.2-1. Paraboloidal Reflector with Feed Cluster

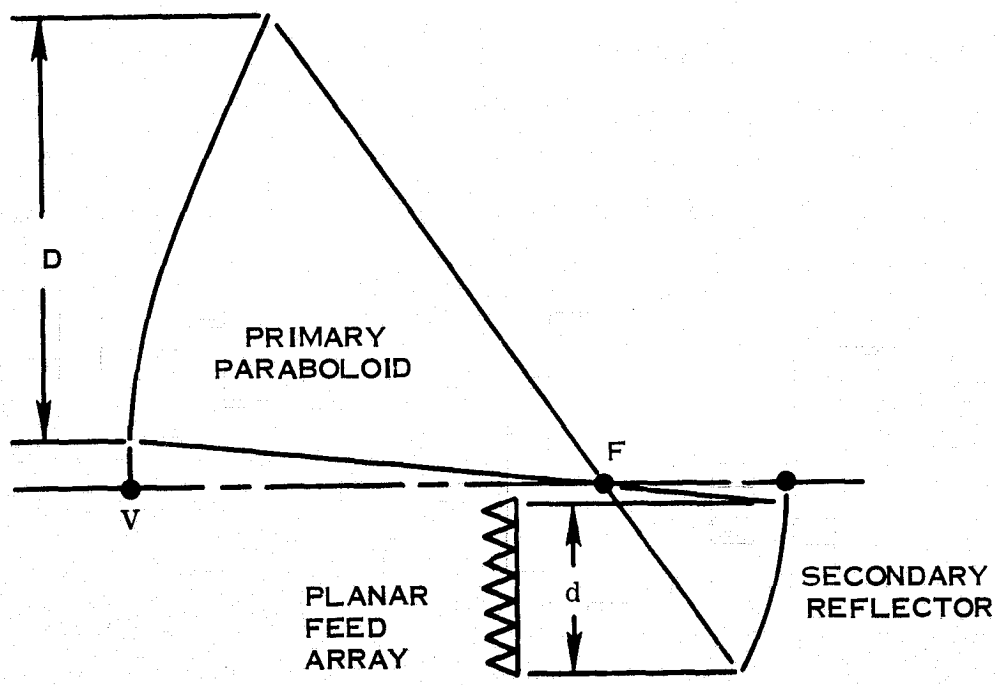

Figure 4.2-2. Offset Confocal Dual Reflector Antenna System

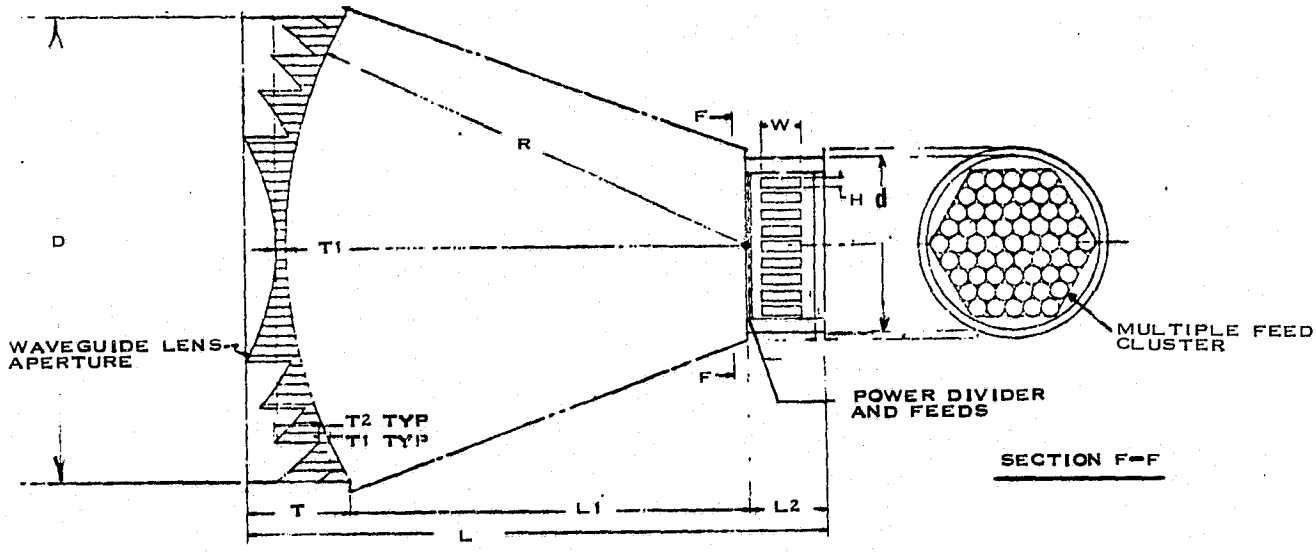

Figure 4.2-3. Zoned Waveguide Lens with Multibeam Feed

4.2.3 ACTIVE LENS ANTENNA SYSTEMS

The active or bootlace lens antenna system is similar in geometry to the constrained passive lens antenna except that the external aperture surface can be planar. This is so because focusing and control of an individual beam or a multiple beam cluster is accomplished by means of a phase shifter incorporated into each individual lens cell. The lens cells may also contain individual amplifiers or even complete transmit/receive modules. Because of this, considerable control over the aperture distributions can be obtained for the set of multiple beams. Such a bootlace lens with a multibeam feed (reference 8) is shown in Figure 4.2-4.

The surface on the feed side of the bootlace lens is chosen to be spherical, preferably, in order to minimize the cubic phase error term when the radiating element density of both sides of the lens is identical. The bootlace lens is inherently capable of producing lower sidelobes than the waveguide lens since amplitude tapering is readily accomplished. This advantage has less impact, however, when the incorporation of adaptive aperture control is considered. As with the passive lens antennas, no aperture blockage occurs because the

feed is behind the lens. Aperture thinning with the bootlace lens is also readily implemented by connecting the elements of a filled input aperture on the feed side of the lens to radiating elements of an expanded, thinned output aperture.

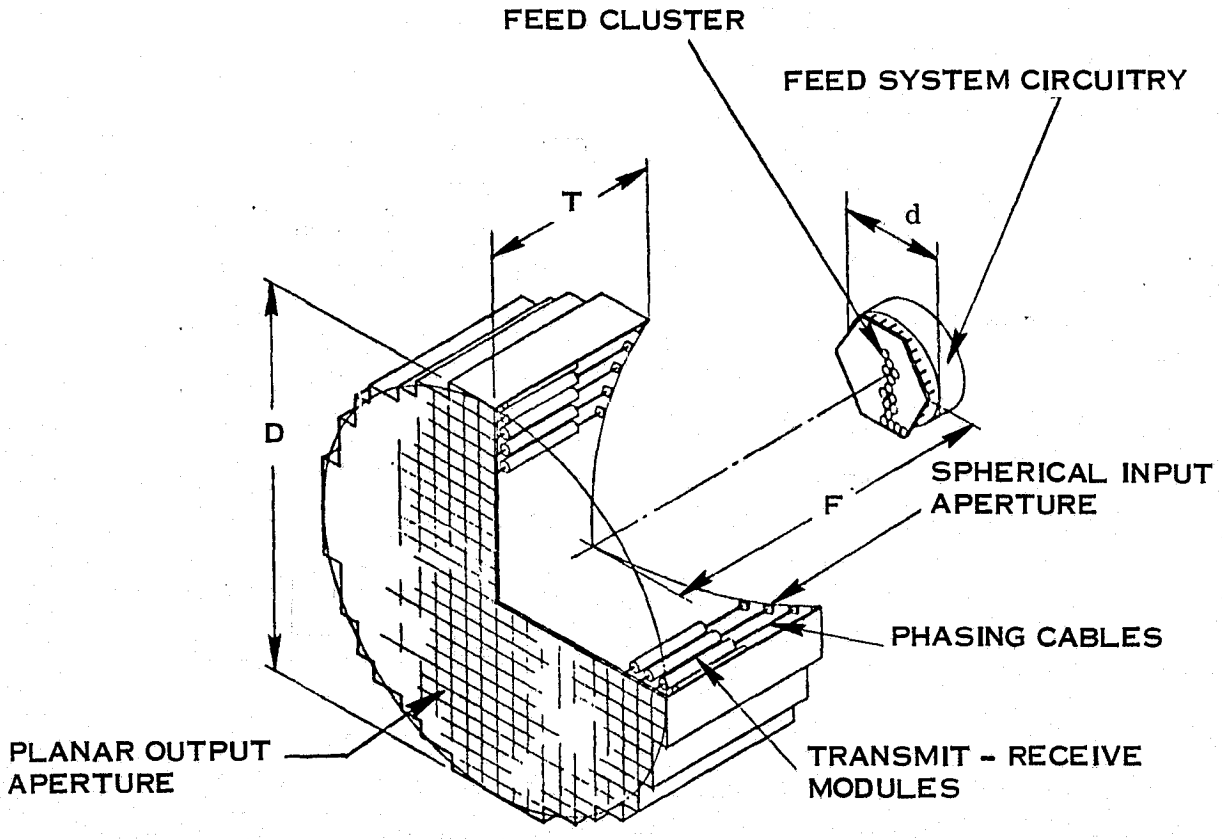

Figure 4.2-4. Bootlace Lens with Multibeam Feed

4.2.4 PHASED ARRAY ANTENNA SYSTEMS

The network-fed phased array antenna system is the most attractive method of forming multiple beams insofar as flexibility, conceptual simplicity, and theoretical performance capability are concerned. The attractiveness of the phased array antenna is due to the ability to control the amplitude and phase at each radiating element from a non-radiating feed network. This provides much more flexibility in the choice of circuitry, and it also eliminates the feed system spillover losses which occur with reflector and lens antenna systems.

A generalized phased-array antenna block diagram is shown in Figure 4.2-5. The essential characteristics of the phased array antenna are embodied in the beamforming network and the radiating structure. The radiating structure consists of radiating elements placed on a grid, and the design procedure is basically concerned with choosing the type of radiating element to be used and the placement of the elements on the ground plane. These choices influence the bandwidth and angular coverage region possible. The radiating elements are normally placed on a regular grid, which results in a far-field pattern which is periodic. These pattern periodicties are called grating lobes. The dimensions of the element grid are normally determined so that at the highest frequency of interest and at the largest scan angle of interest, the first grating lobe remains just outside the visible region. It is evident from this discussion that the coverage region and the array bandwidth parameters are closely interrelated. A great deal of effort has been expended on the problem of providing wide angle designs, but relatively little has been done on the design of phased arrays for extremely wide-band performance (i.e., for bandwidths with edge frequencies in the ratio of 2:1 or more; see reference 2).

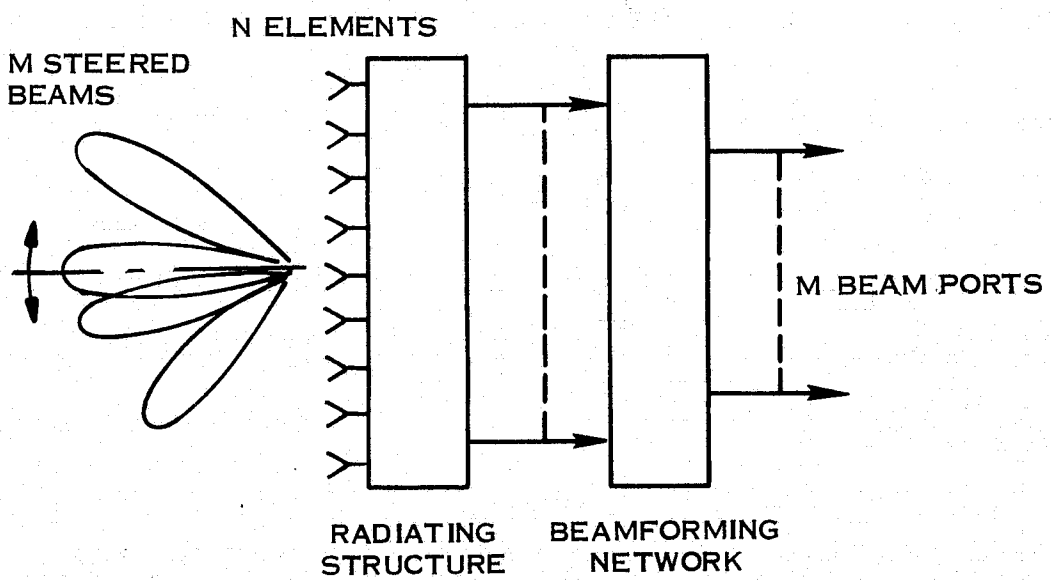

Figure 4.2-5. Generalized Phased Array Block Diagram

The function of the beamforming network is to weight the radiating element outputs prior to summation on receive, or to provide the desired amplitude distribution on transmit. Generally, a symmetrical radiation pattern is desired so that the amplitude weighting on each element is solely a function of the desired sidelobe level, and the phase shift impressed on each element output is a function only of the angle to which the beam is to be steered.

A significant amount of work has been reported on choosing the element amplitude taper in such a way as to produce a radiation pattern with low sidelobes and high gain (see references 3 through 7). In practice, however, the effects of component tolerances limit the sidelobe levels which have been achieved. The present state-of-the-art does not permit the design of arrays with peak sidelobe levels more than about 30 dB below the main lobe peak.

The most significant advantage of the phased array antenna system over the other systems is its great versatility. It is possible to continuously scan a single beam over a given coverage area, or to design a network that produces many narrow beams to provide simultaneous as well as independent coverage of the same region. It is also possible to scan several beams simultaneously as well as independently. The problems which have, in the past, resulted in a dampened enthusiam for phased array antennas are the complexity required on the spacecraft in order to achieve these advantages, the weight of the specific phase shifting devices used to scan the beams, the effects of using separate low noise receive amplifiers at each radiating element, and the effects of using either many low-power amplifiers or a few high-power amplifiers for the transmit function. It is clear from the potential advantages available, however, that the phased array antenna system must rank high in any tradeoff of antenna configurations considered, because of its ability to better meet the antenna performance requirements for the selected AMBA experiments.

4.2.5 ANTENNA SYSTEM TRADEOFF RESULTS

The antenna performance requirements for the selected Adaptive Multibeam Antenna (AMBA) experiments form the basis for the antenna system design tradeoffs. Major differences between these tradeoffs and those for similar studies of multibeam antennas for synchronous satellite applications are the much greater coverage angle (80^{o} versus 18^{o}) and the greater

beam agility required. Another significant difference is the greater allowable system weight on Spacelab.

In a study conducted by General Electric (see reference 8) for a multibeam X-band communications antenna system for a synchronous satellite, the bootlace lens was chosen as the prefered type. In a similar study conducted by Lockheed (see references 1 and 9), it was concluded that a phased array would not meet the bandwidth requirement imposed for a single transmit/receive antenna, and an artificial dielectric lens antenna configuration was selected instead.

The choice of a particular antenna system to satisfy the performance requirements of a given application depends upon the analyses of many parameters as well as upon experienced judgement. From the two examples given above, it is seen that the preferred antenna system can differ considerably with different requirements.

Five basic criteria were used in performing the tradeoffs needed to select the preferred type of antenna system for the AMBA experiments. These criteria are described below:

Radiation Pattern Performance encompasses those parameters which describe the shape of the radiation pattern. These represent the traditional parameters: gain, beamwidth, monopulse sensitivity, and sidelobe level.

Beamforming Capability refers to the performance of the network which controls the amplitude and phase of the aperture illumination. Specifically, the questions of the number of beams possible and whether the beams are steered independently or as a group will be considered in this category.

Bandwidth Capability is measured by two parameters; the agile bandwidth and the instantaneous bandwidth. The agile bandwidth refers to the total frequency range over which an antenna may be expected to successfully transmit or receive a narrowband signal. The instantaneous bandwidth represents the maximum signal bandwidth which may be accommodated by the antenna. This distinction is particularly important when considering phased array techniques.

Adaptive Aperture Compatibility refers to the complexity involved in incorporating adaptive processing within a given multibeam configuration. Included in this category are adaptive signal acquisition and beamforming, interference rejection, and adaptive polarization control.

Tracking Capability represents the accuracy of maintaining a single beam in the direction of a desired user. The distinction has been made between the process of maximizing the antenna gain in the direction of a desired signal and minimizing directional interference, even though these are not fundamentally separable problems. The reason for this is that in many practical situations, separate treatment of these two problems leads to a practical successful implementation.

These factors relate directly to the performance of a communications system in that they represent measures of the ability of the system to receive or transmit data in a desired direction, to suppress interference which is spatially resolved, and to maintain a link over a specified period of time.

The results of the Adaptive Multibeam Antenna tradeoffs are summarized in Table 4-2. Nine evaluation factors derived from the five basic criteria and from practical considerations are rated for each of the four types of antenna system discussed in this subsection.

Table 4-2. Adaptive Multibeam Antenna Tradeoffs

	Reflector	Waveguide Lens	Bootlace Lens	Phased Array
Bandwidth	1	3	2	4
Continuous/Rapid Scan	3	2	2	1
Scan/Coverage Angle	5	5	5	1
Sidelobes	4	3	2	1
Adaptive Ability	4	3	2	1
Tracking Ability	4	3	2	1
Large No. of Beams	3	1	1	2
Simplicity	1	2	3	4
Weight	1	2	3	4

Rating Scale: 1 = Excellent
2 = Good
3 = Fair
4 = Acceptable
5 = Unacceptable

This table clearly shows the superiority of the phased array antenna system in all areas related to antenna performance except for bandwidth. The price paid for this superiority is seen to be greater weight and complexity, but both are acceptable for the Spacelab/AMBA applications. The other three types of antenna system are all unacceptable for the required coverage angle with two or more simultaneous beams. The phased array antenna system has an added advantage over the other three in that it permits independent control of individual beams. The latter is a result of the phased array being a steered beam antenna system rather than a switched beam system.

Because of these results, the phased array was selected as the preferred antenna system for the Adaptive Multibeam Antenna for Spacelab. Design concepts for an Adaptive Multibeam Phased Array (AMPA) antenna system are presented in Section 5.

SECTION 5
AMPA DESIGN CONCEPTS

The tradeoff considerations required to converge on a preferred Adaptive Multibeam Phased Array (AMPA) antenna system design concept are discussed in this section. A reference phased-array design approach is presented for each of the three selected Spacelab experiments: L-band Communications, L-band Radiometry, and Ku-band Communications. A summary of the candidate tradeoff parameters and their associated impact is included. Some basic phased array considerations common to all three experiments are presented first, however, since the required antenna beamwidths, gain, side lobe levels, and beam efficiency are closely interrelated.

5.1 BASIC PHASED ARRAY CONSIDERATIONS

For the L-band Communications and Radiometer Experiments a minimum angular resolution of 5 degrees requires an aperture width of about 3 meters. For a radiometer beam efficiency of 85%, this aperture must be essentially filled, and the spacing between radiating elements must be small enough to prevent the formation of grating lobes at the maximum scan angles. This basic array relationship is given in Figure 5.1-1. For a radiometer frequency of 1.4 GHz, this maximum radiating element spacing is about 12.5 cm which results in a 3 meter square array of 24 x 24 = 576 radiating elements in a rectangular grid. Alternatively, a 3 meter square array with a triangular element grid could be used with about 500 radiating elements, or a 3 meter hexagonal array with a triangular grid of about 432 radiating elements. The basic array parameters for the rectangular and triangular element grids are shown in Figures 5.1-2 and 5.1-3.

For the L-band Communications Experiment, grating lobes could be allowed to enter visible space provided that they are sufficiently suppressed by the radiating element pattern to prevent reducing the array gain significantly. With a $\pm$ 40 degree scan angle, a radiating element spacing that would normally produce grating lobes near $\pm 75^{\circ}$ (about 0.6 wavelength spacing) can be used with less than 0.5 dB loss in gain, if the radiating element is well designed for low mutual coupling effects to obtain good side lobe control and freedom from

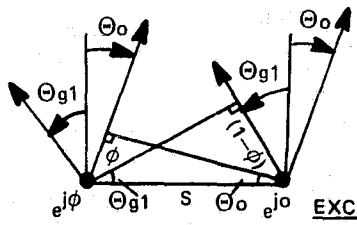

S = ELEMENT SPACING IN WAVELENGTHS

ϕ = RELATIVE ELEMENT EXCITATION IN WAVELENGTHS

Θ_o = BEAM SCAN ANGLE

Θ_{g1} = 1st ORDER GRATING LOBE ANGLE

- GIVEN S AND Θ_o: $\Theta_{g1} = \text{SIN}^{-1}\left(\frac{1 - S \sin \Theta_o}{S}\right)$
- GIVEN Θ_o AND MIN. ALLOWABLE Θ_{g1}: $S_{max} = \left(\frac{1}{\sin \Theta_{g1} + \sin \Theta_o}\right)$

Figure 5.1-1. Basic Array Relationships

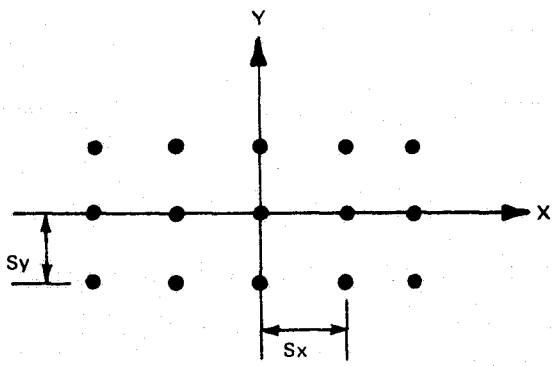

- 2 CARDINAL PLANES
- SQUARE GRID: Sy = Sx = S
- NO. ELEMENTS = Nx Ny = N^2
- GRATING LOBES AT:

$$\Theta_{g1} = \sin^{-1}\left(\frac{1 - S \sin \Theta_o}{S}\right)$$

IN X AND Y PLANES

RECTANGULAR ELEMENT GRID

Figure 5.1-2. Basic Array Parameters (Rectangular)

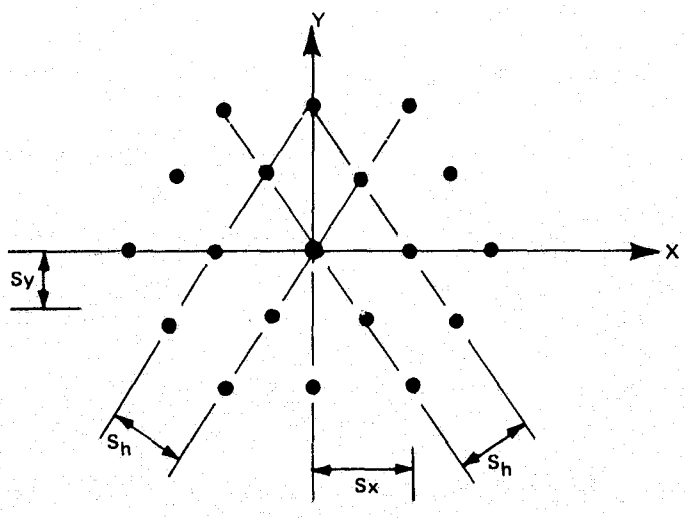

- 3 CARDINAL PLANES
- EQUILATERAL GRID: Sy = 0.866 Sx = S_h
- NO. ELEMENTS = 0.866 N^2
- GRATING LOBES AT:

$$\Theta_{g1} = \sin^{-1}\left(\frac{1 - S_h \sin \Theta_o}{S_h}\right)$$

IN 30°, 90° AND 150° PLANES

Figure 5.1-3. Basic Array Parameters (Triangular)

"blind spots" with scan. Assuming that the 1.54 GHz transmit/1.64 GHz receive maritime communications frequencies are used for the L-band communications experiment, a radiating element spacing of about 11.5 cm would be satisfactory, which results in 26 x 26 = 676 radiating elements for a 3 meter square array.

Since commonality of equipment is an important consideration in the design of experiments to be flown in Spacelab, it is highly desirable to use the same phased array for both the L-band Radiometer and the L-band Communications Experiments. This can be readily done, as seen from the above discussion, by using the radiating element spacing required for for the L-band Communications Experiment and appropriately switching the RF circuitry behind the array to obtain the desired experiment configurations. A plot of grating lobe angle versus frequency is given in Figure 5.1-4, which shows that even better radiometer performance would be obtained at 1.4 GHz with the smaller element spacing. A 24 x 24 = 576 element array with a rectangular element grid has been chosen as a reference array configuration, as discussed further in Section 5.2. Suitable dipoles are the high performance, bent dipole elements developed by GE and shown in Figure 5.1-5, or broad band printed circuit dipoles similar to those used in the GE TPS-59 radar and shown in Figure 5.1-6.

For the Ku-band Communications Experiment, the same considerations apply with regard to radiating element spacing as discussed above for the L-band Communications Experiment, except that the 12 GHz transmit and 14 GHz receive frequencies are more widely spaced. While a single array could be used for both transmit and receive with satisfactory radiating element spacing and has been used as a reference array design in Subsection 5.4, other factors such as excessive beam shift with frequency and the more limited space behind each radiating element for RF circuitry at Ku-band indicate that separate transmit and receive arrays may be preferable. A two-array system configuration, as shown in Figures 2-2 and 2-3, was selected for the Ku-band Communications Experiment during this study.

Thinning of the Ku-band arrays would be permissible, since the high beam efficiency required for L-band radiometry is not needed for Ku-band communications. A considerable saving in hardware would result from thinning, together with some reduction in gain. Thinning from 576 to 144 radiating elements, for instance, would decrease the gain about 6 dB.

For all three of these experiments, a special beam control computer will be incorporated as part of the experiment configuration in order to achieve the desired flexibility and agility of beam control. For the L-band and Ku-band Communications Experiments, the beams will be controlled adaptively from a 16-element pseudo-randomly-spaced subarray of the full phased array while the beams will be controlled with a commanded sequence program for the L-band Radiometer Experiment. The on-board Spacelab/MMAP processor will be used for the processing of experimental data.

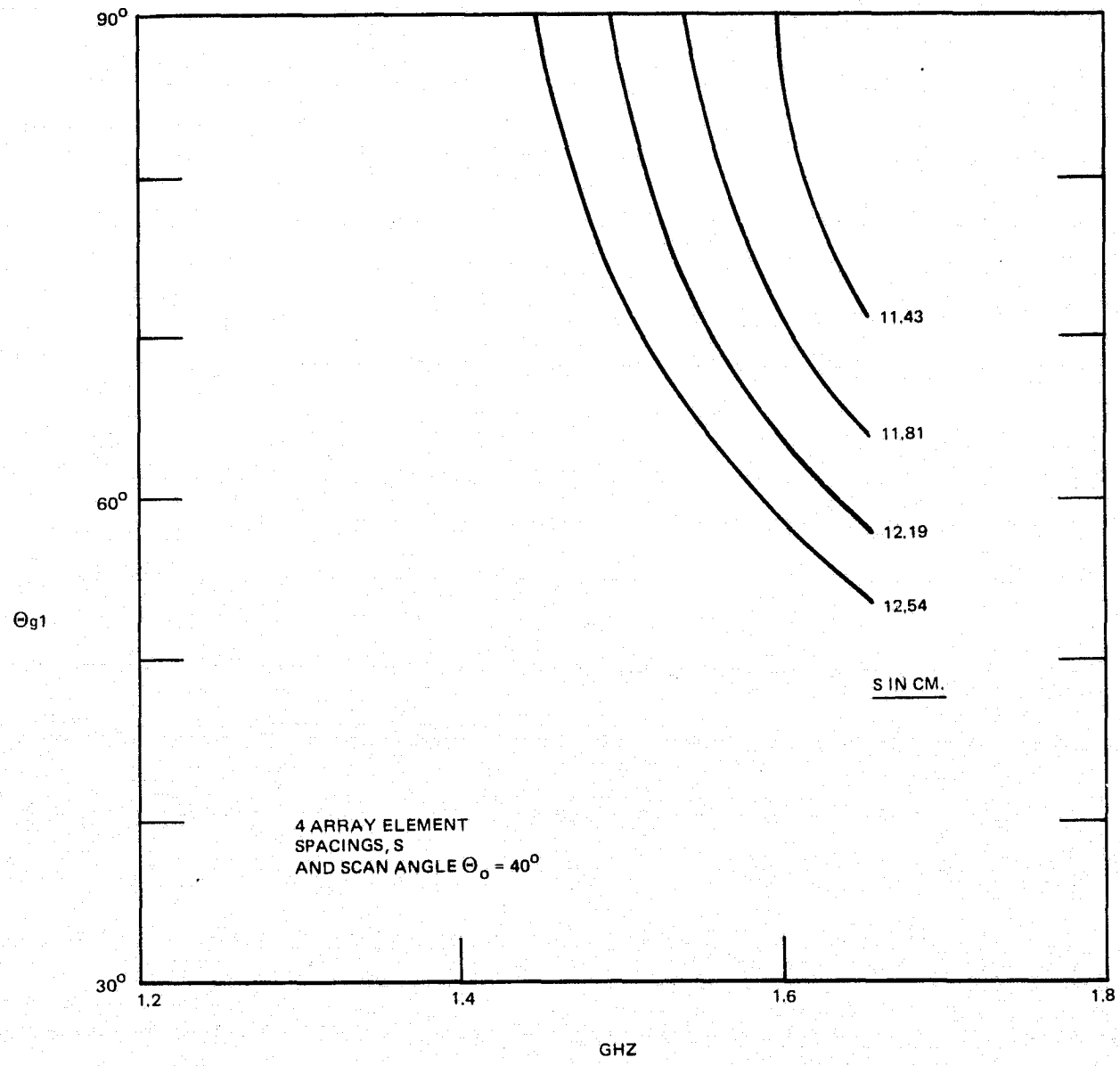

Figure 5.1-4. Grating Lobe Angle, $\theta g1$ vs Frequency

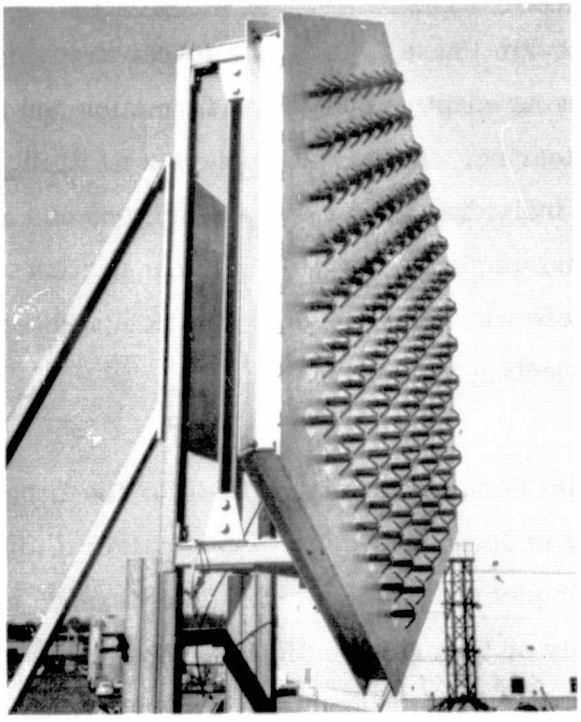

Figure 5.1-5. 127 Element L-band Array

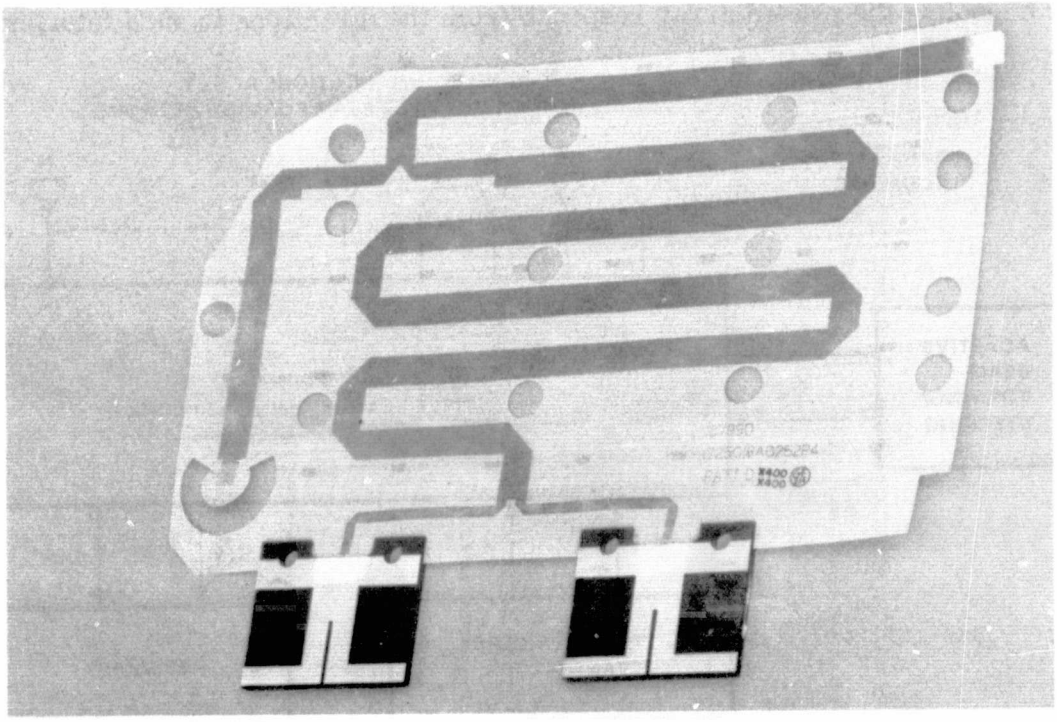

Figure 5.1-6. Stripline Center Board with Integral Stripline Dipole

5.2 L-BAND COMMUNICATIONS AMPA DESIGN CONCEPTS

The L-band Adaptive Multibeam Phased Array is a planar array configuration intended for two-way communications using adaptive dual-beam formation and for radiometry using programmed multiple-beam steering. The array employs a multiplicity of crossed dipole elements under the control of individual bilateral phase shifters and associated polarized feed networks. Solid-state signal amplification is used in conjunction with a strip transmission line sum and distribution network. The design is also compatible with adaptive side lobe canceling techniques for rejecting interference.

A generalized multiple Beam Forming Network (BFN) for the L-band Communications Experiment adaptive phased array is shown in Figure 5.2-1. Several different phased array configurations can be used to implement this network. In all cases, a receive beam is formed on one user either adaptively or by a combination of adaptive and programmed control. The received signal is then translated in frequency and transmitted on another beam which has been similarly formed on a second user, so as to establish a communications link between the two users. A further adaptive feature is the rejection of interference from undesired signals by canceling the phased array response from the directions to such interfering signals.

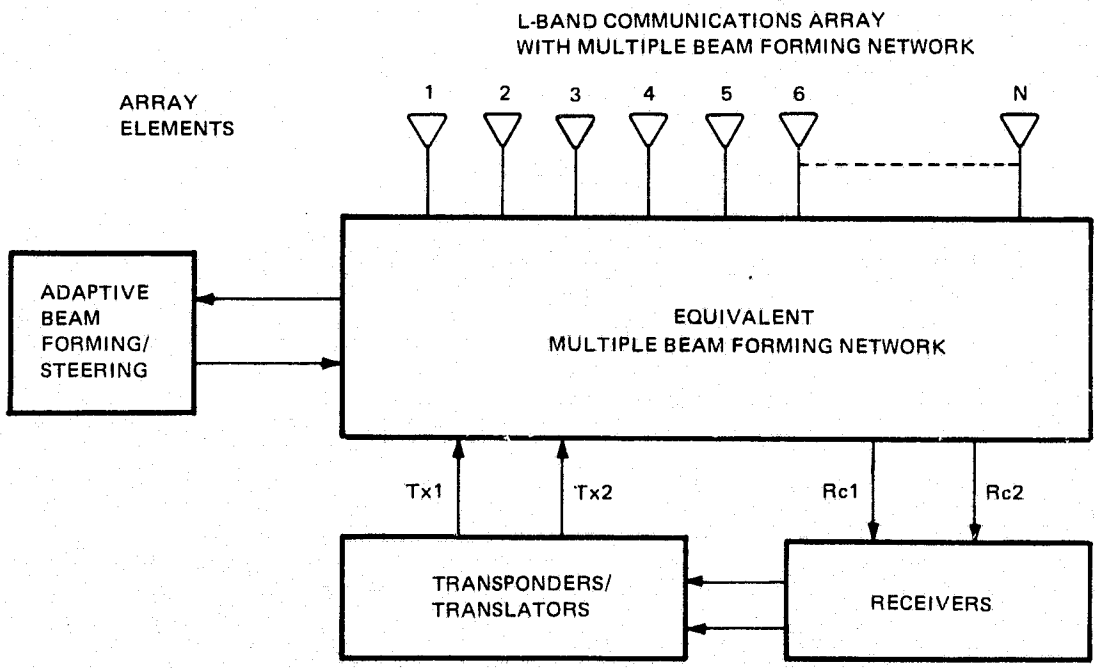

Figure 5.2-1. L-band Communications Array with Multiple BFN

Configuration 1. The most versatile means of implementing the multiple BFN is to use element level amplifiers for both transmit and receive with a diplexer for each element, as shown in Figure 5.2-2. This configuration has the advantage of establishing the receive signal-to-noise ratio at the elemental amplifier before the signal is divided for multiple beam forming. Two sets of phase shifters (or equivalent adaptive weighting signals) are then used to form the two receive beams in sum networks 1 and 2. Similar sets of phase shifters can be used after the transmit dividers and drivers (not shown) to feed the elemental transmit amplifiers, or the same phase shifters can be used that are used on receive with additional diplexing circuitry. Beam level transmit amplifiers could be used with this configuration as an alternative to element level transmit amplifiers. In any case, the amount of hardware is considerable in this configuration and warrants considering alternative configurations.

Configuration 2. A configuration using subarray level amplifiers is shown in Figure 5.2-3. This has considerable flexibility as to the number of elements used for a subarray and their arrangement. For instance, a 24 x 24 element array could be arranged as 8 x 8 9-element subarrays, 4 x 4 36-element subarrays, or 24 24-element columns, amongst many others. There is a diplexer, a receive amplifier, and a transmit amplifier per subarray in this configuration, which saves considerably on hardware at the expense of receive signal-to-noise ratio. A major contributor to the latter is the 3 dB hybrid divider at each element before the two sets of elemental phase shifters used to form the two receive beams. The transmit amplifiers would be fed from transmit dividers following the two-beam translators/transponders. Again, the transmit amplifiers could be at the beam level feeding the transmit dividers. A major advantage of this configuration is that the same two sets of phase shifters are used for both transmit and receive, without the need for additional diplexing circuitry. While at first glance it appears disadvantageous that half the transmit power for each beam is lost in the elemental hybrids, this is no worse than with the elemental transmit amplifiers of the first configuration, since the latter must operate linearly over the full dynamic range of the composite signal level and thus at 50% of the full amplifier efficiency.

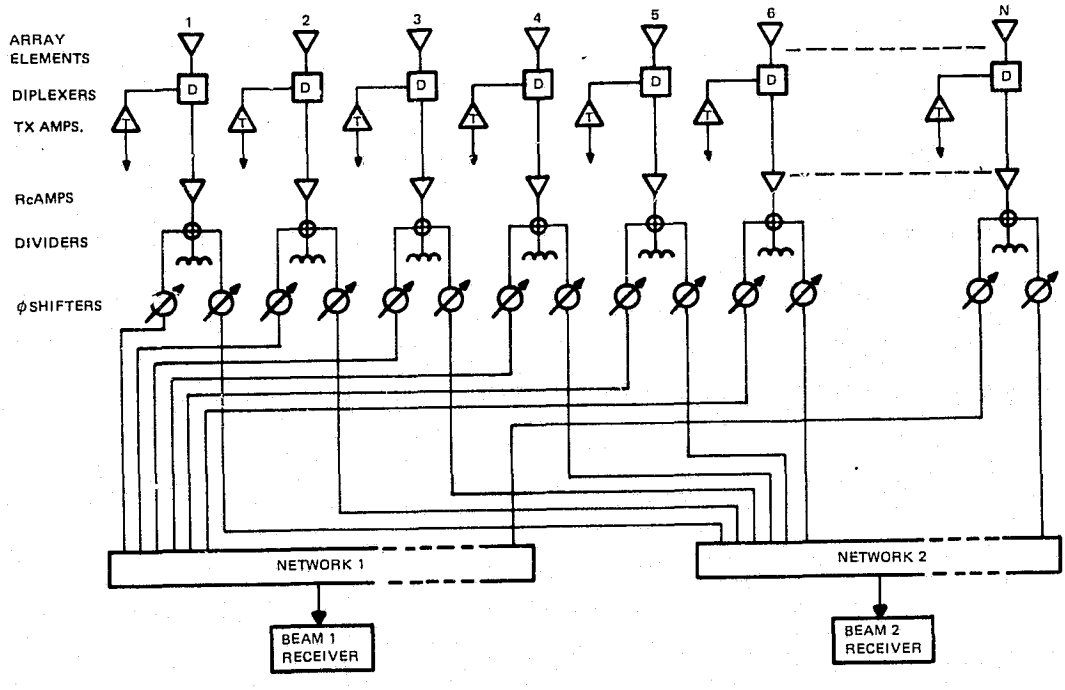

Figure 5.2-2. L-band Communications Array with Element Level Amplifiers

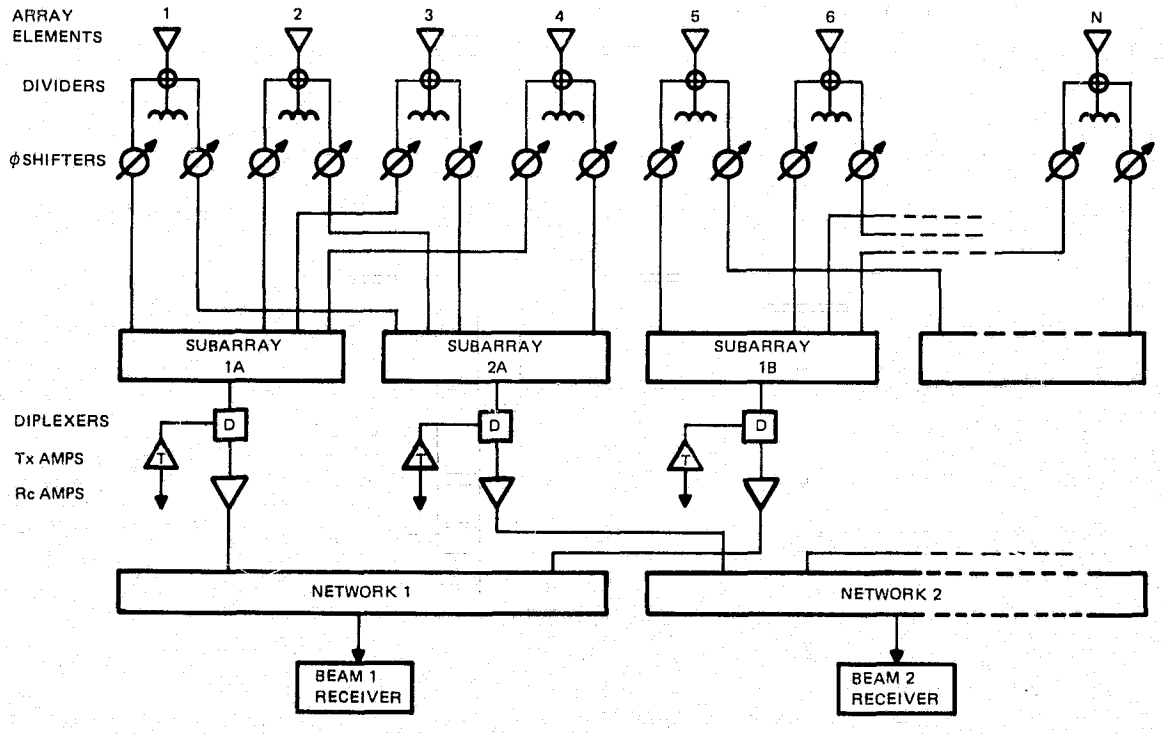

Figure 5.2-3. L-band Communications Array with Subarray Level Amplifiers

Configuration 3. A third configuration using beam level amplifiers is shown in Figure 5.2-4. In this case, only a single diplexer, receive amplifier, and transmit amplifier is needed per beam. The receive signal-to-noise ratio is the worst in this case, however, because of all the sum network losses before the receive amplifier. Other advantages and disadvantages are the same as discussed above for the subarray level amplifiers.

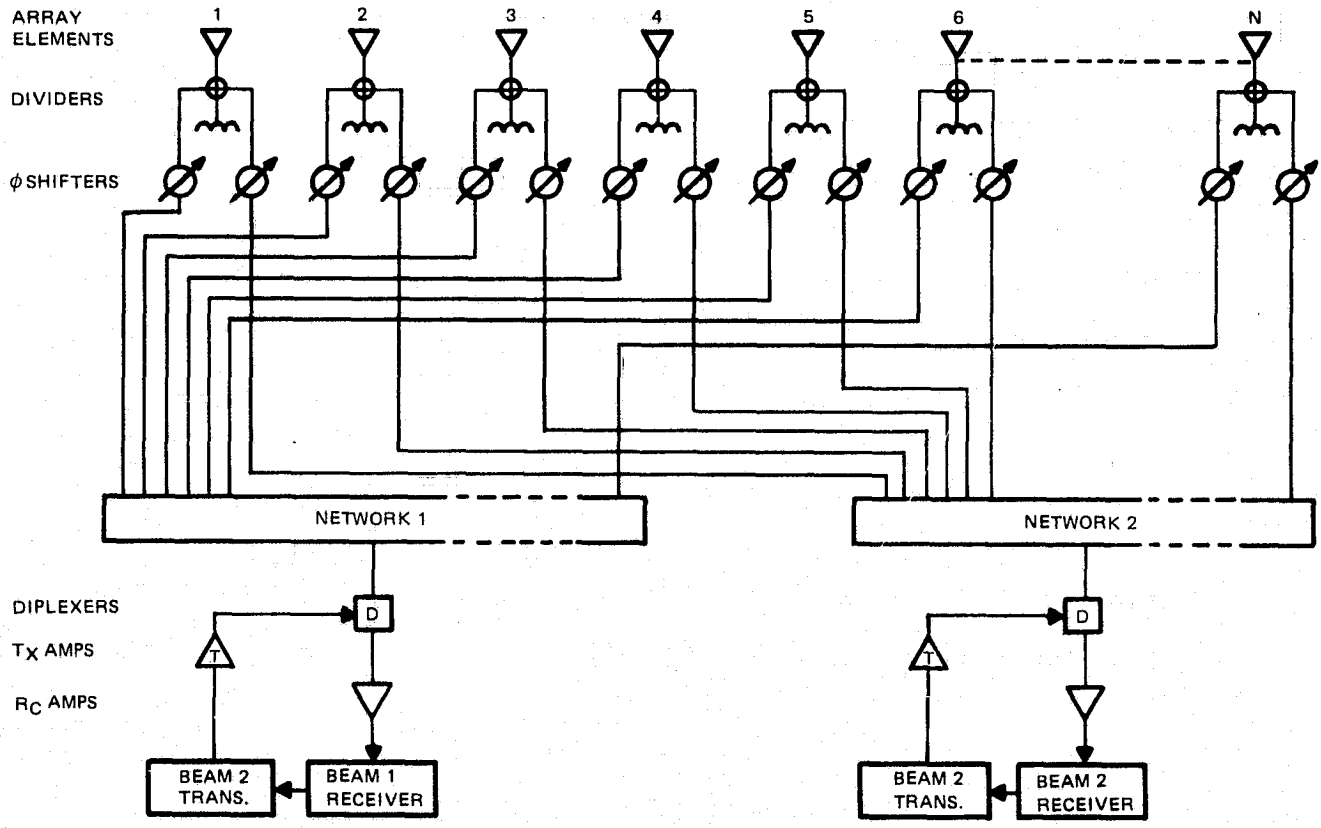

Figure 5.2-4. L-band Communications Array with Beam Level Amplifiers

5.2.1 REFERENCE L-BAND ARRAY DESCRIPTION

A functional block diagram of the reference L-band communications array is shown in Figure 5.2-5. Tradeoff comparisons of alternative AMPA design concepts will be made with this array. The adaptive and frequency translation equipments are omitted in the figure for simplification. The array is planar and is configured for 24 x 24 = 576 individual crossed dipole elements capable of orthogonal receive and transmit circular polarization (RHC-Xmit, LHC-receive). The receive noise figure is minimized by employing receive amplifiers on a per-element basis. Transmit power and complexity is minimized by using power transmitters on a per-beam basis. One bilateral, 3-bit phase shifter is employed per element per beam in order to minimize the hardware complement and supply the required beam resolution. Bilateral power summers and splitters are used as well. The high isolation required to achieve greater than 130 dB intermodulation rejection in the receive band is provided by the low loss diplexer circuitry.

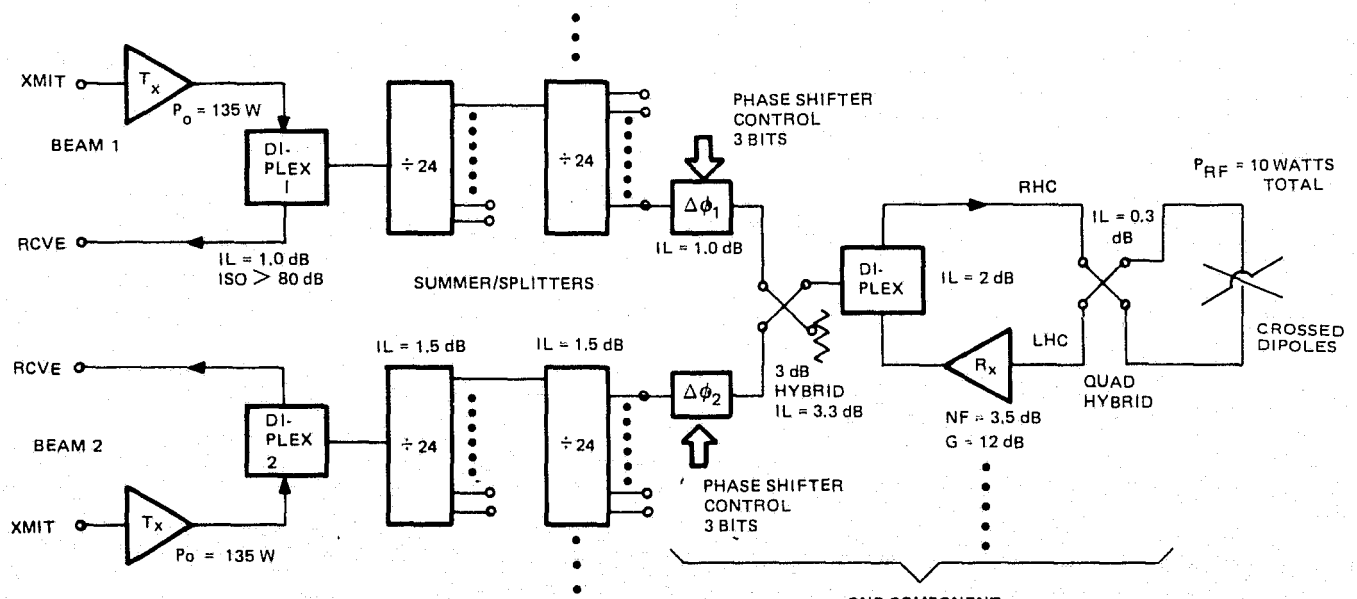

HARDWARE COMPLEMENT

CROSSED DIPOLES	– 576
QUAD HYBRIDS	– 576
RECEIVERS	– 576
DIPLEXERS	– 576
3 dB HYBRIDS	– 576
$\Delta\phi_1$	– 576
$\Delta\phi_2$	– 576
SUMMERS	– 25
SPLITTERS	– 25
DIPLEXER 1	– 1
DIPLEXER 2	– 1
TRANSMITTERS	– 2

Figure 5.2-5. L-band Communications Reference Array Functional Block Diagram

Maximum beam shift caused by the difference in frequency between transmit and receive will be $\pm$ 1.5 degrees, which is comfortably within the 5 degree beam width. The instantaneous array bandwidth is well in excess of the 20 MHz required.

5.2.2 ARRAY TRADEOFF ALTERNATIVES

Table 5.2-1 presents the salient results of deviating from the reference array implementation of Figure 5.2-5. This tradeoff matrix is representative and is not intended as a complete list. The four options listed are described below:

Option 1 - This option considers a low level amplifier for each crossed dipole radiating element. The amplifier is placed at the RHC input to this quadrature hybrid. The 10.3 dB loss differential results in a corresponding reduction in the RF power losses. Class A operation of the amplifiers is likely in order to reduce out-of-band intermodulation products between adjacent transmit carriers since a filter per element having adequate rejection would be prohibitive in size. A marked reduction in amplifier efficiency results from Class A operation; however, in-band intermodulation performance is improved. In addition, amplifier failures result in a graceful degradation in beam performance.

Option 2 - This option considers a single amplifier for each beam. The 10.3 dB loss between antenna elements and the receiver input port results is a significant noise figure degradation and therefore may not be compatible with radiometer operation. Non-graceful array degradation results from an amplifier failure, but reliability may be improved by employing a commandable redundant receiver.

Option 3 - This option considers the use of non-reciprocal phase shifters and power summers and splitters. This necessitates twice as many components, but the component design is more straightforward. Since the phase shifters and summers/splitters are not common between the transmit and receive frequencies, beam steering effects are negligible.

Option 4 - This option considers placing the transmit and receive amplifiers at intermediate locations between the array input and the antenna radiating elements. A firm set of array requirements would be needed to make a meaningful location selection. This option permits a compromise, however, between achieveable noise figure and intermod product performance, reliability, size, weight, power and cost.

Table 5.2-1. L-Band Communications Tradeoff Matrix Summary

Tradeoff Options	Size	Weight	DC Power	Cost	Comments
1. Transmit amplifiers at each antenna element	Larger	Greater	Higher	Higher	• Graceful degradation for amplifier failures • Beam diplexer isolation requirement relaxed • Class "A" Operation required • Lower in-band intermodulation products
2. One receiver for each beam	Smaller	Less	Lower	Lower	• Array N.F. 10.3 dB higher and not radiometer compatible • Beam diplexer requirements more severe • Non-graceful degradation
3. Separate phase shifters and summer/splitters for transmit and receive	Larger	Greater	Slightly higher	Higher	• Non-reciprocal phase shifters and summer/splitters used • Negligible beam steering between transmit and receive channels
4. Subarray configuration	Larger	Greater	Higher	Higher	• Possible to achieve better compromise between tradeoffs 1 and 2, i.e., modest N.F., graceful degradation and acceptable in-band intermod products

5.3 L-BAND RADIOMETER AMPA DESIGN CONCEPTS

For reasons of overall economy of cost, weight, power and size it is desirable to utilize L-band equipment in common for the communications and radiometer experiments. The reference array design and the various options for the L-band Communications Experiment described above in Section 5.2 meet the L-band radiometer experiment requirements except for the following necessary modifications:

1. Dual linear or linear horizontal polarization must be provided for radiometric mapping,

2. Adaptive beam forming must be replaced by commanded beam forming with programmed control to obtain the required single and/or multiple beam scan modes,

3. Additional equipment is required for switching, timing, calibration and data processing of the radiometer data stream, and

4. The design for the receive line components must meet the combined bandwidth requirements for both the radiometer and the communications receive frequency bands.

Figure 5.3-1 shows a schematic diagram with these basic modifications from the communication system diagram of Figure 5.2-5.

A polarization switch is added to provide sequential access to vertical and horizontal polarization (bypassing the hybrid used for circular polarization in the L-band Communications Experiment). Additional filtering may be required to limit the noise bandwidth. Diplexers, hybrids, phase shifters, combiners, and receivers must accommodate both the communications and radiometer bandwidths.

In all other respects, the reference array design exhibits the desired commonality:

1. The proximity of the radiometer band (assumed 1400-1427 MHz) and the L-band communications band (1500-1600 MHz) allows both experiment objectives to be achieved with a common array.

2. The 3m x 3m array provides the required 5 degree beamwidth with a conical scan angle of ± 40 degree from nadir. The array design in terms of number of radiating elements, element spacing, and element weighting (low sidelobes) will be optimized for the radiometer beam to provide maximum beam efficiency over the scan volume. Insertion loss, integration time, and bandwidth will be optimized to provide the best possible radiometer resolution consistent with the specified system parameters (single/dual linear polarization, mapping requirements, orbital geometry).

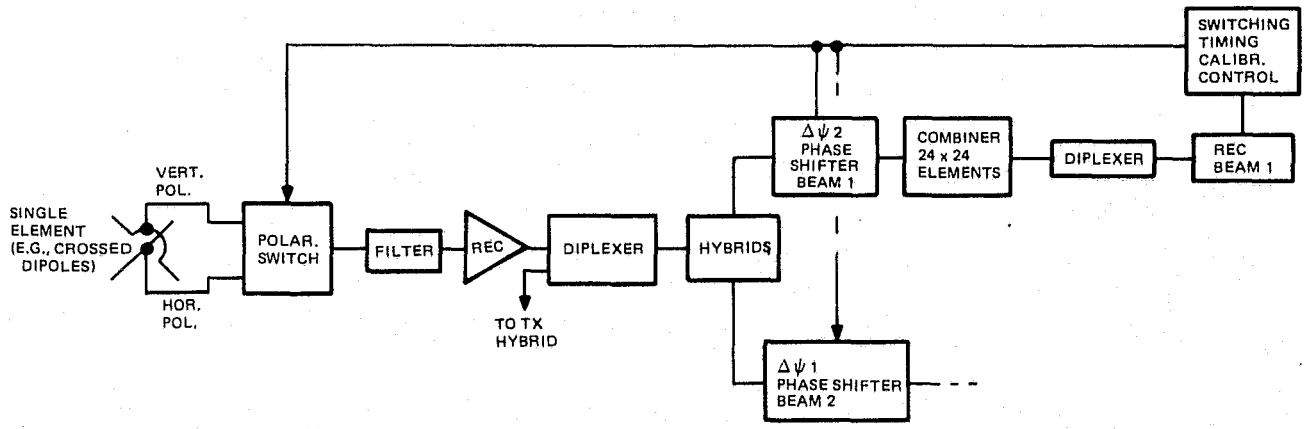

Figure 5.3-1. L-band Radiometer Array Functional Block Diagram (Single Element)

The required polarization switching between the L-band communication and radiometer systems is shown schematically in Figure 5.3-2. These switches could be implemented in either coaxial or stripline configuration to obtain minimum insertion loss ahead of the pre-amplifiers. Control and synchronization of the switches will be provided by a master controller for switching between the communications and the radiometer experiments and selecting the desired polarization mode.

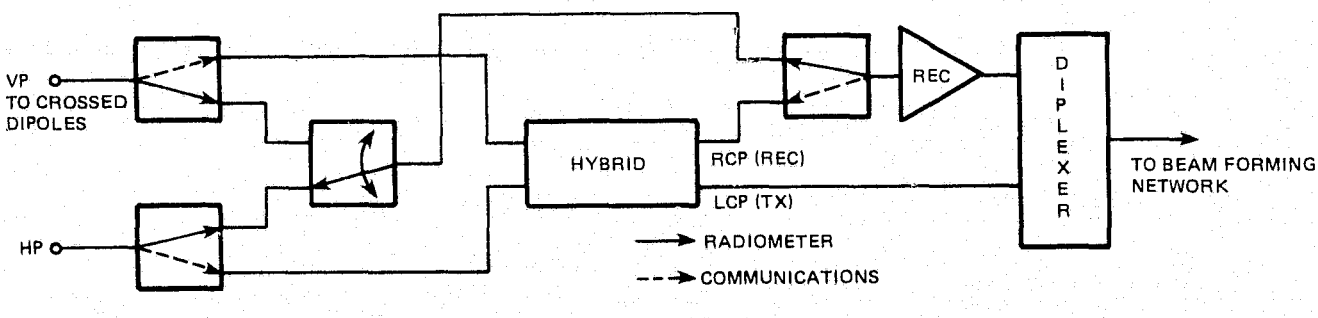

Figure 5.3-2. Polarization Switching for Radiometer (Linear Pol) and Communications (Circular Pol) Experiments

5.4 KU-BAND COMMUNICATIONS AMPA DESIGN CONCEPTS

The Adaptive Multibeam Phased Array (AMPA) antenna system illustrated in Figure 5.4-1 is a two dimensional, broadband, electronically scanned, multibeam array intended for multichannel Ku-band communications with dispersed non-static terminal locations. Dual-polarized feeds at each subarray element provide for frequency re-use in each beam. Bilateral feed networks and time delay steering provide simultaneous transmission at 12 GHz and reception at 14 GHz through a single array. Adaptive sidelobe cancelling implemented through selected array elements reduces interference in each receive beam. Adaptive polarization cancellation nullifies the undesired orthogonal signal in each channel, thereby maximizing the signal to cross-polarized interference ratio during multibeam dual-polarized operation.

This phased array antenna system is not intended as an optimum baseline design, but it is presented initially as a reference array design concept for the tradeoff discussions which follow. It is a broadband, single array antenna system design which is economical of equipment but fairly complex. Alternatives to this reference array are then presented which are simpler but require greater numbers of components. An alternative design concept using separate arrays for transmit and receive is finally selected as the most practical means for implementing the AMPA Ku-band antenna system.

5.4.1 REFERENCE ARRAY DESIGN CONCEPT

The Ku-band AMPA reference array design shown in Figure 5.4-1 has been segmented and expanded in Figures 5.4-2 through 5.4-4.

A single phased array of 24 x 24 = 576 radiating elements arranged in 16 subarrays of 36 elements each has been chosen for the reference array design. A subarray and subarray feed structure is shown in Figure 5.4-2. Crossed-dipole radiating elements coupled through a 90 degree hybrid provide independent RCP and LCP feed ports for each element. Each port is split through a 3 dB hybrid into a time delay network for dual beam forming on each polarization. The desired signal on the four ports labeled a, b, c and d of each radiating element are as shown in the matrix below:

Port	Desired Signals			
	Receive at 14 GHz		Transmit at 12 GHz	
	From Terminal #	Polarization	To Terminal #	Polarization
a	1	RCP	1	RCP
b	2	RCP	2	RCP
c	1	LCP	1	LCP
d	2	LCP	2	LCP

The signals at port (a) are combined in a matched hybrid network with the corresponding signals from the remaining 35 subarray elements, and similarly for the signals of ports b, c, and d, producing 4 distinct ports for the subarray, which are labeled R1, R2, L1, L2 as shown. Circulator-coupled frequency diplexers are used to separate the transmit and receive signals at the subarray level.

The corporate feed system for the array is shown in Figure 5.4-3 where the individual beams for each polarization from each subarray are summed into the receive array beams using matched hybrid 16-way summers. Conversely, the transmit beams are divided 16 ways for distribution to each subarray transmit port. Single preamplifiers are incorporated after full receive array beam forming. Single power amplifiers are used in each transmit beam.

The Signal Flow Diagram of Figure 5.4-4 illustrates a method for implementing adaptive sidelobe cancellation and adaptive polarization cancellation (discussed in Paragraph 5.5.4) using the single reference array antenna system. Array tradeoff discussions will include the adaptive equipment only to the extent of indicating whether more or less equipment is required, since the functional features of the adaptive equipment are necessary regardless of the array design and do not change.

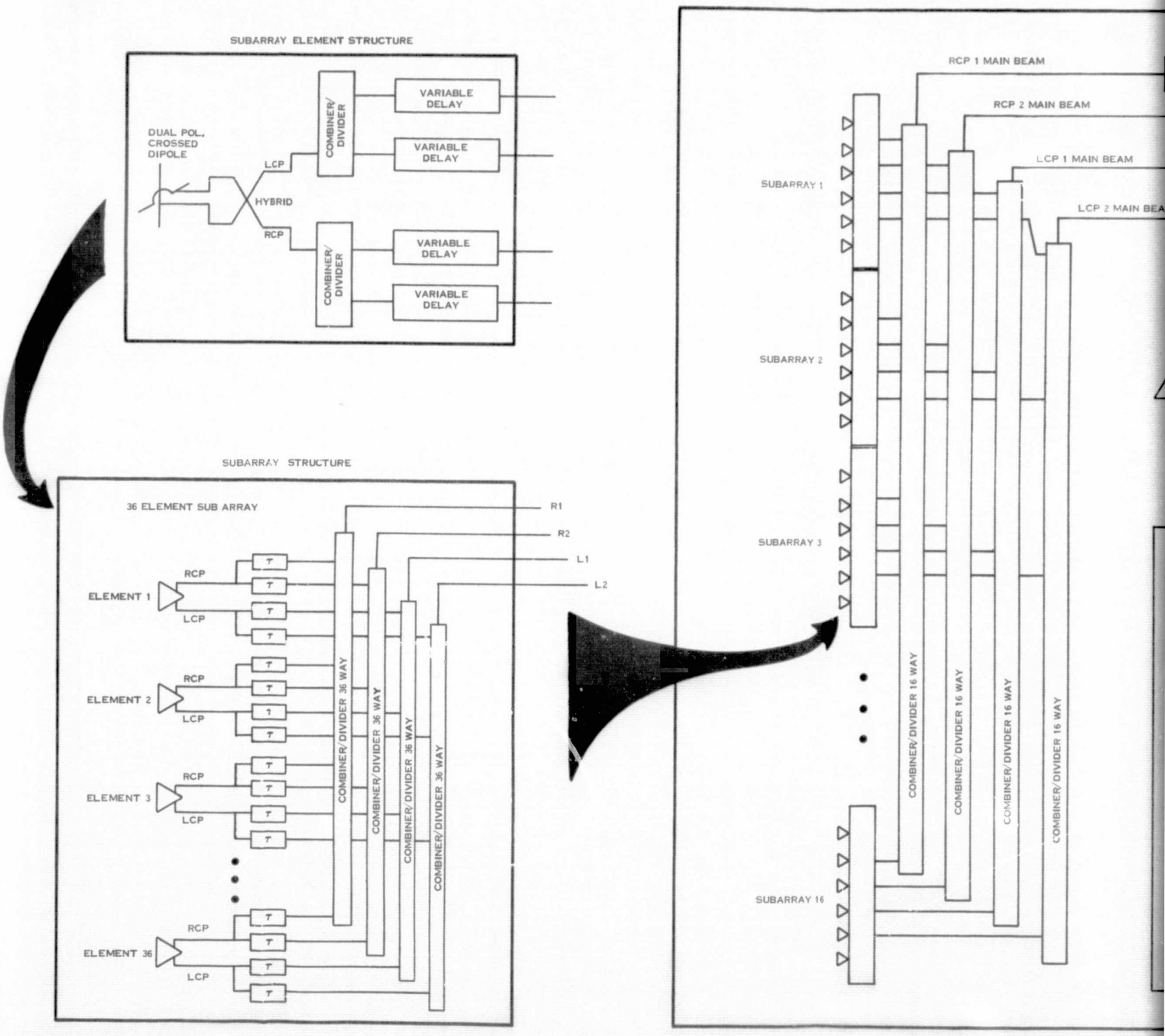

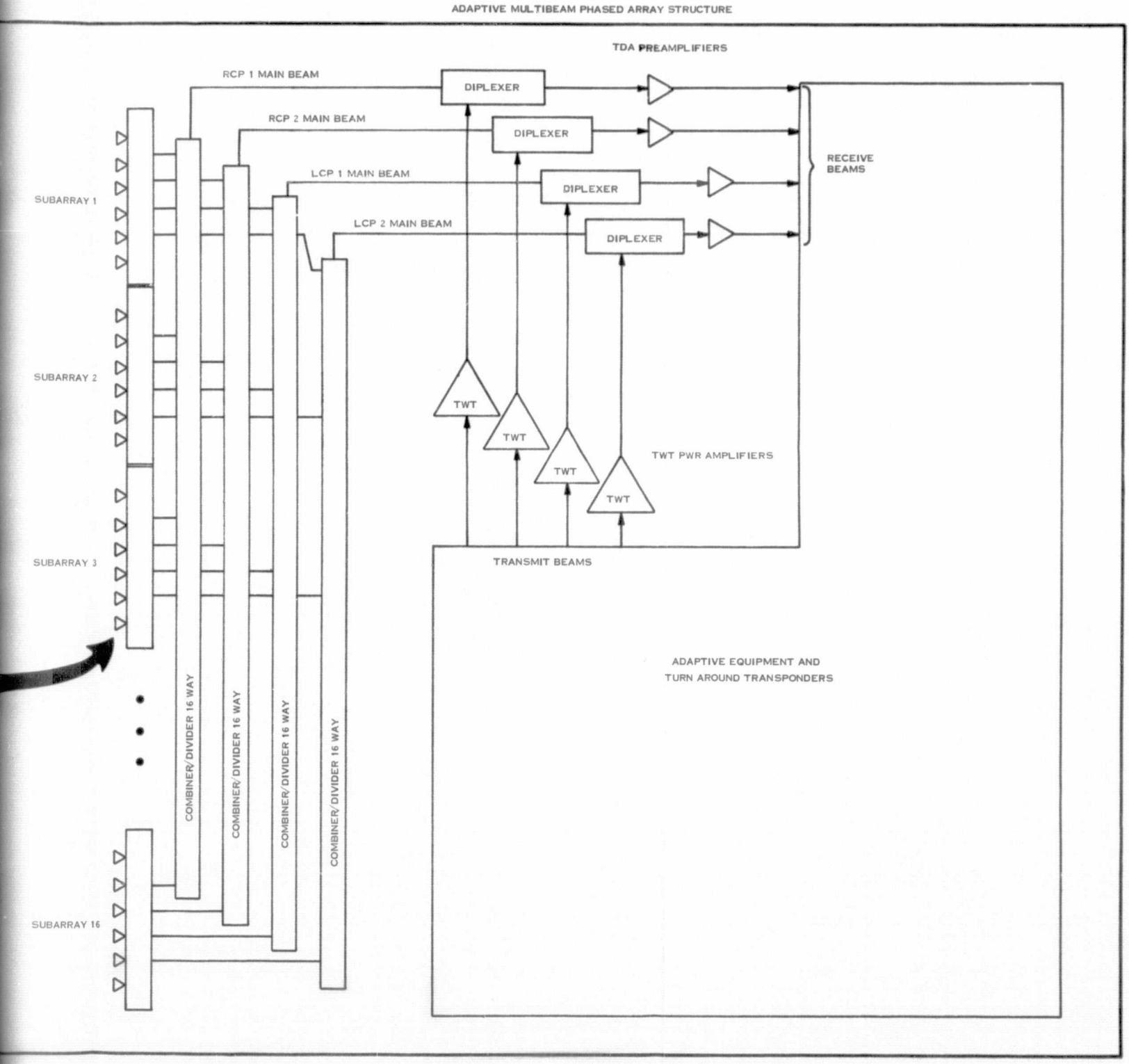

Figure 5.4-1. Ku-band AMPA Reference Array Design

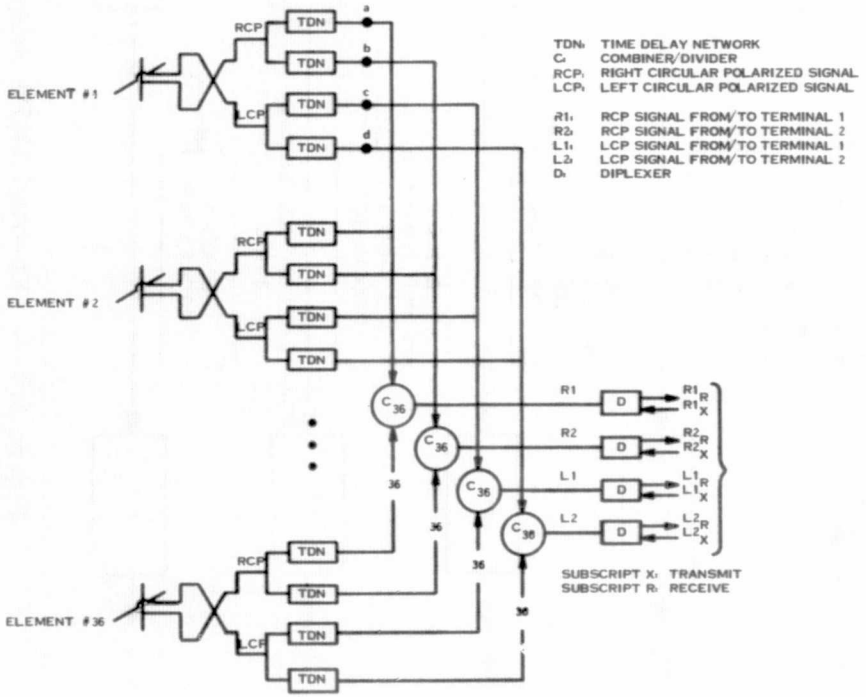

Figure 5.4-2. Subarray and Subarray Feed for Ku-band AMPA

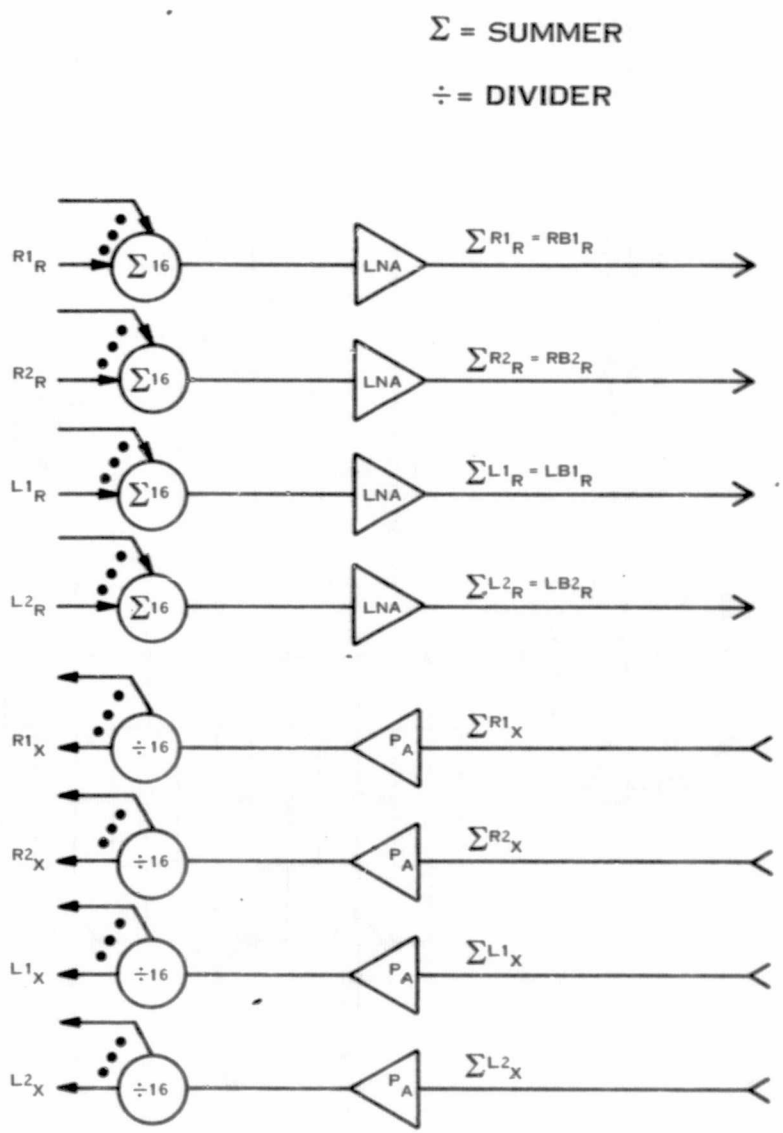

Figure 5.4-3. Array Feed for Ku-band AMPA

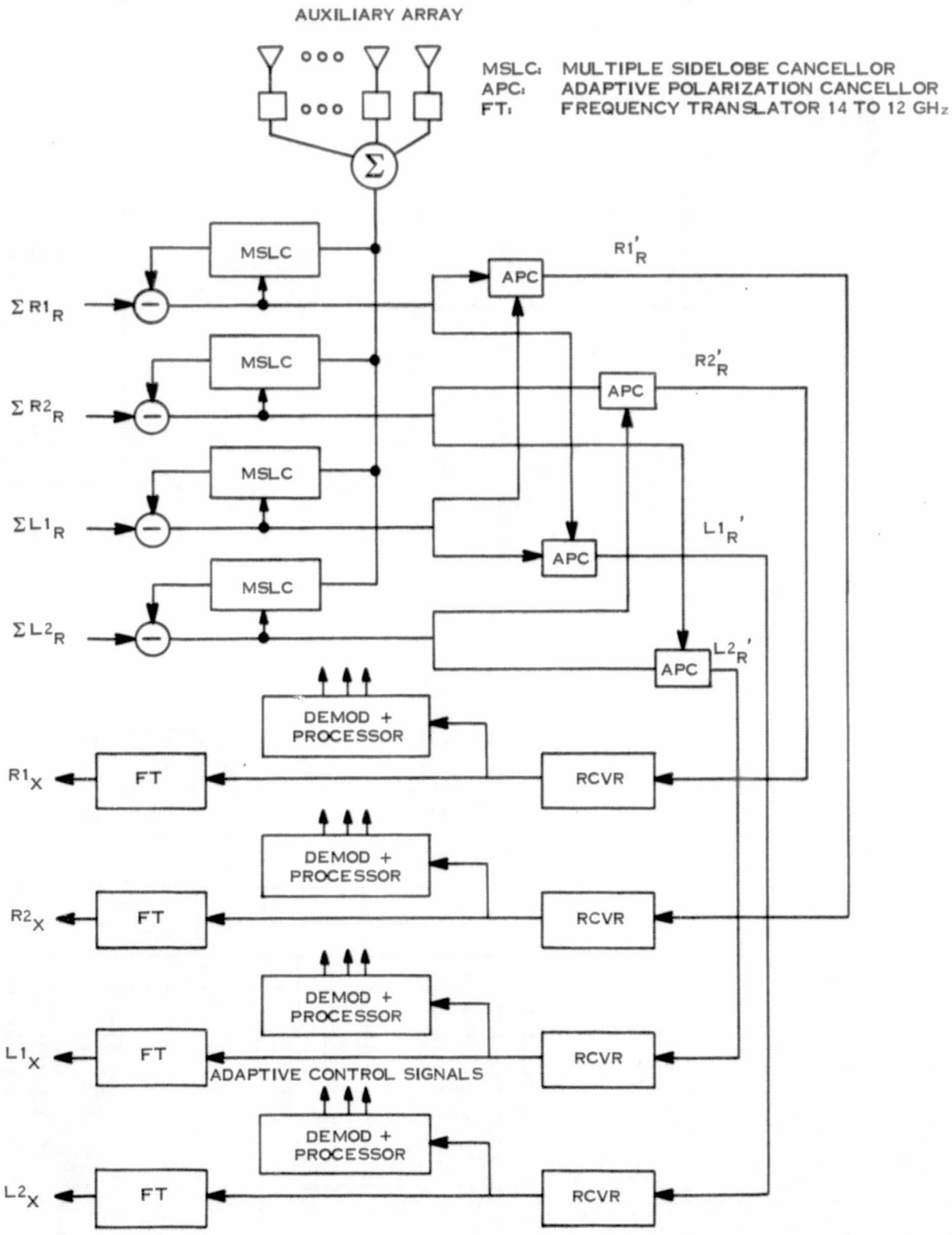

Figure 5.4-4. Ku-band AMPA Adaptive Equipment

5.4.2 ARRAY TRADEOFF ALTERNATIVES

The relative merits of alternatives to the reference array design are clear when comparisons are made with the reference array equipment matrix of Table 5.4-1 and with the list of salient features for the reference array design.

Table 5.4-1. Reference Array Hardware Matrix for Ku-band AMPA

Item	Type	Qty
Subarray Element	Crossed Dipole with Dual-Polarized Hybrid Feed	576
Beam Steering Elements	Digital Control 3-Bit Time Delay Network	2,304
Subarray Feed	Hybrid Networks (36 way)	64
Array Feed	Receive Beam Summers: 16-way Hybrid Network Transmit Beam Dividers: 16-way Hybrid Network	4 4
Diplexers	Circulatory	4
Low Noise Amplifiers	Tunnel Diode Amplifiers	4
High Power Amplifier	TWT	4
Adaptive Equipment	As per Figure 3.2.3-4	1

Some of the significant features of the reference array design are:

Positive

- Satisfies multibeam dual-polarization requirements with a single array
- Offers the widest bandwidth
- Parallel feed system capitalizes on similarity of equipment
- Subarray approach simplifies driver systems for the array
- Requires minimum hardware (quantity)

Negative

- Poor noise figure relative to other design configurations
- High-cost, difficult time-delay steering compared to phase steering

5.4.2.1 Array Feeding and Phasing Bandwidth Considerations and Tradeoffs

Aiming toward better noise figure performance and more practical beam steering techniques, alternatives for feeding and beam steering networks are discussed in this section. A comparison is made between phase steering and time delay steering based on bandwidth considerations, and configuration tradeoffs are discussed. The best alternative to pure time delay steering for a single array is shown to be a combination of phase steered radiating elements and time-delay steered subarrays.

Replacing the time delay networks of the reference array design with phase shifter networks would reduce the equivalent bandwidth such that bilateral use of each radiating element for transmission at 12 GHz and reception at 14 GHz would result in approximately 8.5^{o} shift in beam angle due to the frequency difference. This amount of beam shift is prohibitive where the beam width is in the order of 5^{o}, but may be practical with systems having greater than 10^{o} beam width and reduced gain requirements.

Rather than use each phase shifter bilaterally, separate phase shifters for transmit and receive could be used. The primary impact is 4,608 steering elements as opposed to half this number needed in the reference array. Examination of the feed system complexity argues also for two separate arrays, which essentially doubles the hardware quantities in Table 5.4-1. Multiple arrays have much merit with regard to packaging, however, as will be discussed further in Paragraph 5.4.4.

The most attractive beam steering alternative for a single transmit/receive array is one which combines phase shift steering of the radiating elements and time delay steering of the subarrays. This combined beam steering method is illustrated in Figure 5.4-5 for a single-beam linear array. The net result of this technique is to reduce the losses resulting from beam shift due to frequency, or to increase the corresponding bandwidth.

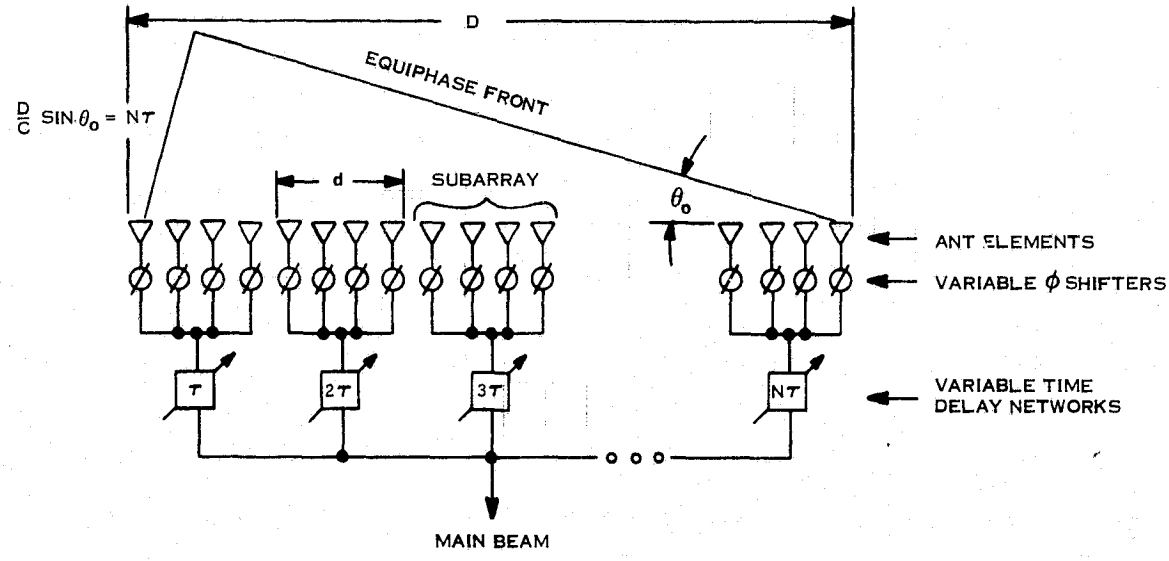

Figure 5.4-5. Combined Phase and Time Delay Beam Steering

As shown in Figure 5.4-5, a signal incident at angle θ_o travels a distance D Sin θ_o further to the last element of the array than to the first. The time to travel this distance is T = (D/C) Sin θ_o, which is the aperture fill time and may be expressed as the reciprocal of a bandwidth Δf. It is apparent from the following expression that if D is reduced, the bandwidth available will be greater:

$$\Delta f \alpha 1/T = \frac{C}{D \text{ Sin } \theta_o}$$

Expressing the aperture fill time as $N\tau$ and employing the time delays at each subarray as shown, the aperture fill time is reduced to the aperture fill time of the subarray dimension d, and the bandwidth is increased to that of the subarray bandwidth. The gain degradation resulting from frequency scanning is thus reduced considerably. This technique is highly desirable for the single array approach. Grating lobes are avoided through the use of separate time delay networks for each beam at the subarray level. The price paid for this alternative is 256 beam steering elements added to the reference array matrix. Suitable interleaving of subarrays may reduce this quantity by one half, but interleaving is difficult to accomplish at Ku-band because of the small element spacing.

An additional design consideration is to configure the time delay networks within the corporate feed network for the subarrays. This recognizes that long time delays are not needed in all subarray positions and thus reduces the total number of networks.

Thus far, we have considered only constrained feed networks, in which the individual signal paths are confined by the networks and feed lines. Space feed networks, in which portions of the signal paths between the array or subarray elements and a feed or combining point are in free space (i.e., between the feed horn and excitation elements of a bootlace lens), also merit consideration. Space feeds for the subarrays are not compatible with the single reference array, which requires maintaining isolation of four separate bidirectional beams from each antenna element, since the space feed cannot be physically configured in such a small array to combine more than two bidirectional beams per antenna element. Other system requirements, such as lower noise temperature and packaging considerations, favor a two- or four-array configuration, however, and space feeds are therefore considered further in Section 5.4.5.

5.4.2.2 Noise Temperature Tradeoffs

The reference array design produces the least desirable noise temperature performance for two reasons. First, 3 dB of loss is incurred in the formation of two beams from a single antenna radiating element. Second, in order to minimize the complexity and quantity of hardware, the preamplifiers are inserted after the main beams are formed. Approximately 7 dB of additional loss is thus sustained prior to preamplification. For an amplifier noise figure of 5 dB, the overall system noise figure is therefore 15 dB in this case.

Design alternatives which produce better noise temperature performance than the reference array system do so at the cost of additional hardware. The best noise temperature performance is achieved in the single array approach by placing the preamplifiers as close as possible to the antenna radiating elements and using minimum loss feeds to the elements. An optimum performance system would provide two diplexers and preamplifiers for each radiating element, thereby improving the system noise figure by 7 dB (4.0 dB less circuit loss and 3 dB resulting from preamplification prior to beam forming). For phased array systems requiring multibeam performance with a large number of simultaneous beams, preamplifiers at each radiating element are essential for good performance.

The single array configured for best noise temperature performance contains significantly more hardware per system than the reference array design. Compared to the reference array matrix of Table 5.4-1, an additional 1148 preamplifiers, 1148 diplexers, and 2304 phase shifters are required. The structure of each radiating element network is as shown in Figure 5.4-6. Physical and mechanical considerations preclude direct implementation of this technique in a single Ku-band array without further development work in packaging techniques. Considerable growth in the physical system dimensions to a size greater than the aperture size is necessary.

Best noise temperature performance produces maximum packaging difficulty, while minimized packaging design complexity produces the worst noise temperature performance. Little improvement in noise temperature performance (less than 2 dB) can be achieved with designs between the two extremes. As indicated above, expansion of the system for more beams in the multibeam array introduces a 3 dB loss for each doubling of the number of beams, unless preamplifiers and diplexers are incorporated at each radiating element prior to beam forming.

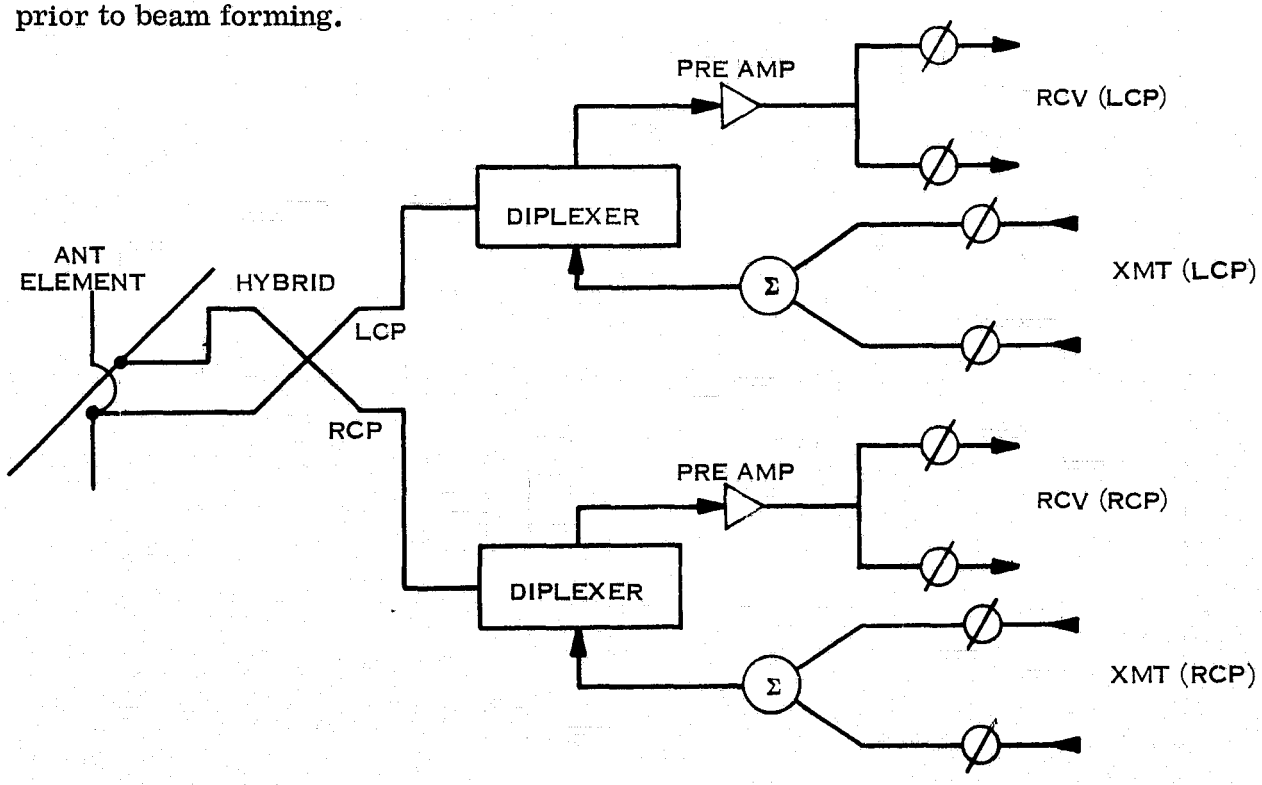

Figure 5.4-6. Multibeam Radiating Element Network Configured for Best Noise Performance

An alternative to the 3 dB loss per beam is to perform frequency selective filtering; however, this reduces the frequency ability of the system and requires tailoring each phased array system for specific applications. The tradeoff of noise figure vs packaging constraints is based on specific system requirements; for the AMPA experiment at Ku-Band, noise figure is not critical.

5.4.3 PHASED ARRAY PACKAGING CONSTRAINTS AT KU-BAND

Packaging of the phased array microwave components becomes increasingly difficult at Ku-band due to four primary considerations:

1. Critical microwave dimensions are difficult to maintain at 14 GHz (λ = 2.14 cm.), since dipole lengths, cavity dimensions, and antenna phase errors are typically held to 1/32 to 1/100 wavelength

2. All per-element processing must take place in the 0.6 λ x 0.6 λ (1.27 cm. x 1.27 cm.) cross section of the array element grid.

3. Transmission line losses are high because of the small line dimensions that are necessary in order to avoid higher-order modes on these lines.

4. Diode switches necessarily have high losses because of the small diode area that must be used to avoid excessive diode shunt capacity.

A very high packaging density is required at Ku-band if loss is to be minimized, and the number of beams at which the microwave hardware outgrows the array aperture size is smaller than at lower frequencies. For the AMPA Ku-band array, which requires two dual channel transmit and receive beams, it is therefore likely that two arrays - one for transmit and one for receive - is the most practical solution for a low loss design, as was indicated in Subsection 5.1.

5.4.4 ALTERNATIVE RADIATING ELEMENT TYPES

The choice of dual-polarized radiating element types is severely limited by the available per-element area in the phased array, approximately 0.6 λ x 0.6 λ (1.27 cm x 1.27 cm). It is desirable to process two independent channels in this area to avoid the need of duplicating full arrays for each polarization and for each of two beams. A ferrite waveguide phase shifter

has an active cross section approaching these dimensions when control coils are included, so it appears impossible to process two independent channels per element using ferrite shifters. This section therefore concentrates on the use of microstrip diode phase shifters for the AMPA array.

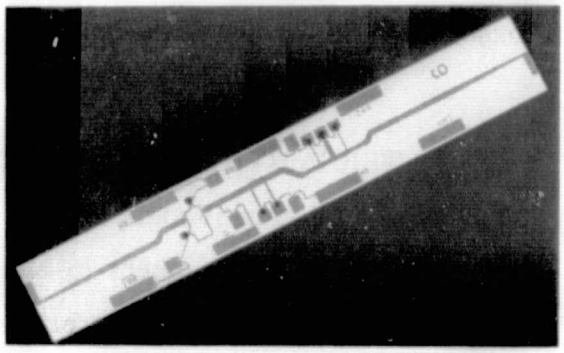

Figure 5.4-7. Ku-band Phase Shifter Used in an Active Lens

A Ku-band microstrip phase shifter developed by General Electric is shown in Figure 5.4-7. This phase shifter requires a cross sectional area of only 0.161 square cm (roughly 10% of the available cross section) for its RF transmission line portion, so that it is a good candidate for the AMPA array. Figure 5.4-8 illustrates a 37-element linearly polarized space-fed array using this microstrip phase shifter.

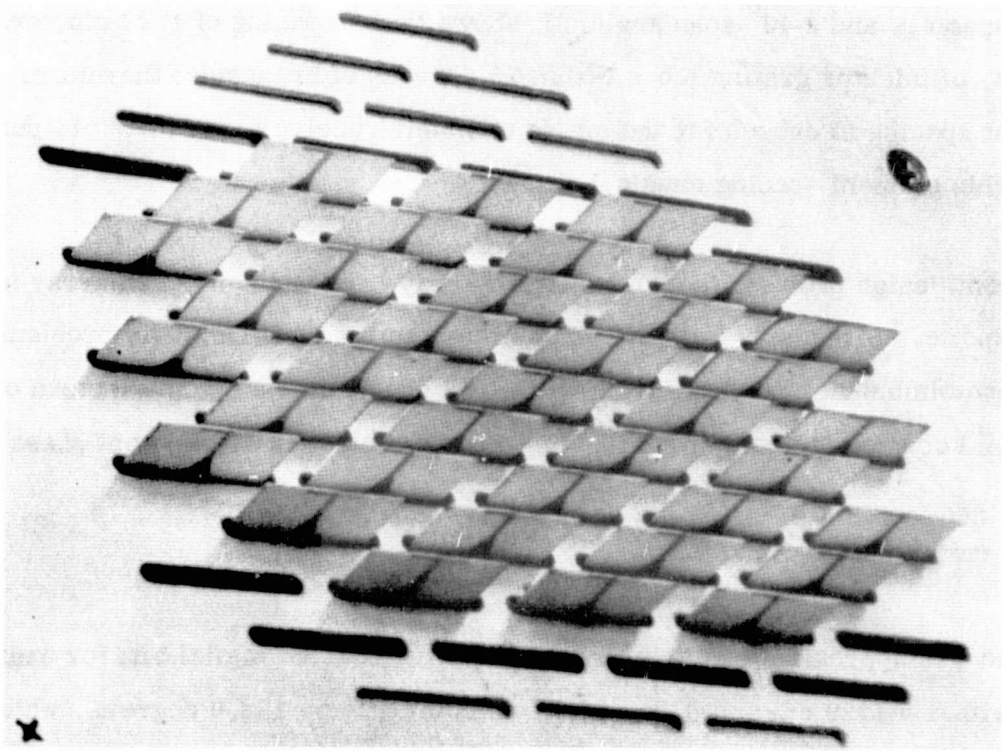

Figure 5.4-8. Ceramic Dipole Array

A dual-polarized radiating element can be formed by mounting two microstrip phase shifter boards on two adjacent sides of a 0.787 cm square dielectric rod as shown in Figure 5.4-9a.

Coupling to the dielectric rod may be accomplished either by simple short probes or by crossed-bow-tie dipoles embedded in the rod as shown in Figures 5.4-9a and b.

5.4.5 ALTERNATIVE ARRAY APPROACHES

The allotted radiating element area in the array face must be chosen so as to preclude grating lobes based on element-to-element spacing to avoid both interference and loss of aperture gain. The expression relating the beam scan angle θ_o, the grating lobe angle θ_{gl}, and the element spacing S is, as given in Subsection 5.1:

$$\theta_{gl} = \text{Sin}^{-1}\left(\frac{1 - S \text{ Sin } \theta_o}{S}\right)$$

where S is in wavelengths. The curve of Figure 5.4-10 is a plot of this function for five element spacings and a 40^o scan angle. It shows that a spacing of 1.29 cm, or 0.60 λ at 14 GHz, eliminates grating lobes within 75 degrees of broadside; therefore, this value of element spacing is chosen for the single transmit/receive array aperture design. At 12 GHz, this element spacing equals 0.516 λ.

A significant design problem is avoided if two arrays are used and each array is operated narrow band; e.g., one array at 12 GHz and the other at 14 GHz. This problem is concerned with the establishment of a phase front with fixed phase shift elements instead of time delay elements. For two elements spaced S cm apart, the element-to-element phase slope is:

$$\psi = \frac{360^o \cdot S \text{ Sin } \theta_o}{\lambda}$$

The phase ψ is approximated by setting phase to the nearest digital bit; for example, at 14 GHz with S = 1.29 cm and $\theta_o = 40^o$, ψ calculates to be 138.9 degrees, which to the nearest bit is 135 degrees. The actual phase front direction is

$$\theta'_{14} = \text{Sin}^{-1}\left(\frac{135^o}{360^o} \cdot \frac{\lambda}{S}\right) = \text{Sin}^{-1}\left[\frac{135}{360} \times \frac{1}{0.6}\right] = 38.68^o$$

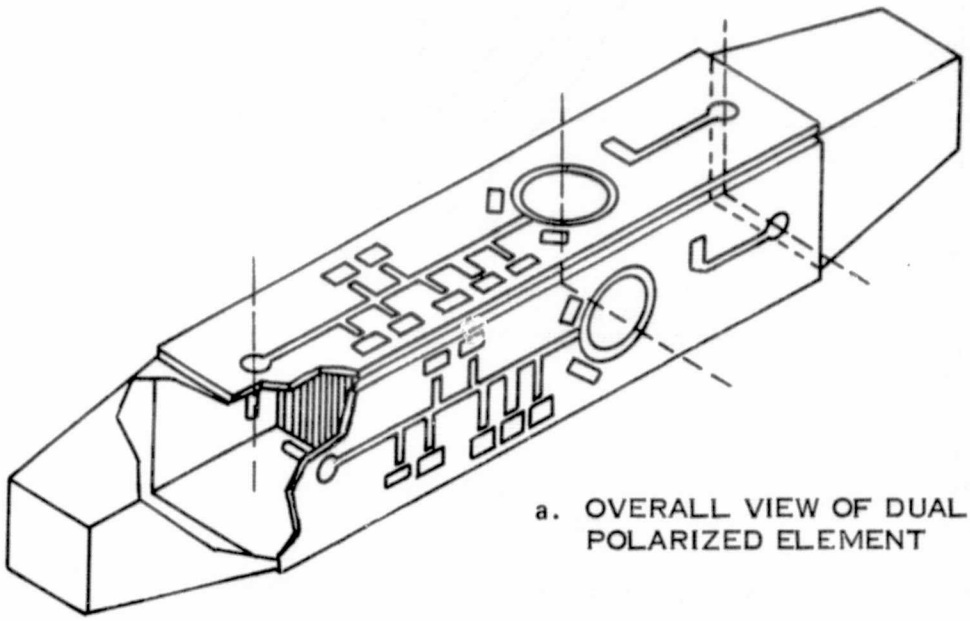

a. OVERALL VIEW OF DUAL POLARIZED ELEMENT

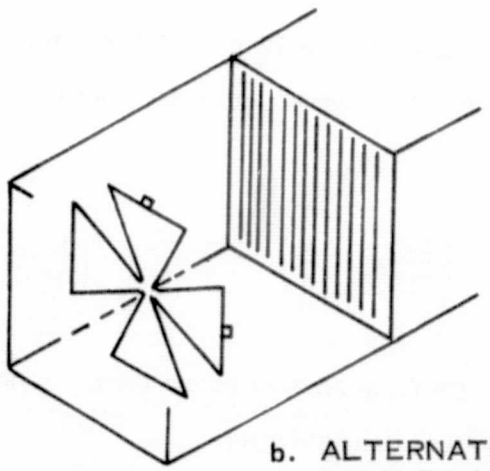

b. ALTERNATE CROSSED DIPOLE LAUNCHER

Figure 5.4-9. Ku-band Dual Polarized Element

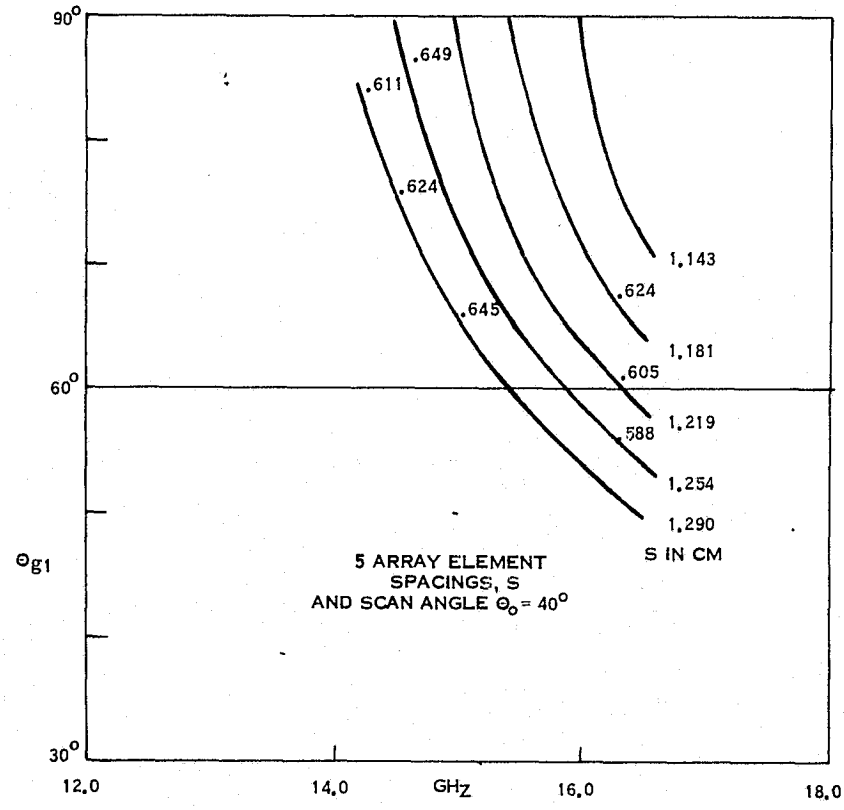

Figure 5.4-10. Grating Lobe Angle, θg1 vs. Frequency

If one array were used at both 12 and 14 GHz and this same phase shifter setting were used at 12 GHz, the different wavelength would give the following angle for the phase front:

$$\theta'_{12} = \text{Sin}^{-1}\left(\frac{135^o}{360^o} \cdot \frac{\lambda}{S}\right) = \text{Sin}^{-1}\left(\frac{135}{360} \times \frac{1}{0.516}\right) = 46.61^o$$

This beam shift with frequency of more than one beamwidth would be avoided by using the two-array system configuration.

The Ku-band array choice is heavily influenced by simplicity of the design approach as well as by insertion loss performance. The design candidates listed below and shown in Figure 5.4-11 are arranged in order of decreasing circuit desirability and also decreasing network complexity. These are:

1. Constrained "expanding feed" system: two transmission lines per element cell are led to a larger grid that maps the aperture. Larger dimensions permit use of four phasers per element cell without size restrictions. The number of ports to be combined in further processing is thus:

$$N_P = 4 N_E$$

N_P = Number of ports

N_E = Number of elements

2. Constrained space-fed system: two space-fed combiners per element cell conduct vertically and horizontally polarized signals to separate subarray output ports. The number of ports to be paralleled in further processing is:

$$N_P = \frac{2 N_E}{M}$$

where M = number of elements combined in one column subarray.

3. Fully Space-Fed System: dual-polarized elements in an M x M subarray reradiate to a conical dual-polarized feedhorn having two output ports. The number of ports paralleled in further processing is thus:

$$N_P = \frac{2 N_E}{M^2}$$

The "expanding feed" system would permit the use of lower loss ($\cong$ 1 dB) ferrite phase shifters, instead of the diode phase shifter with 2.7 dB loss. The 2 dB reduction in loss will be offset by the roughly 0.75 dB per foot increase in attenuation in stripline or microstrip. Thus in this design, the full flexibility and reduced attenuation are bought at the price of added complexity and weight.

The constrained space-fed design represents a solution of intermediate complexity since the number of splitters, mixers, etc. used in further processing is reduced by M, the number per column combiner. This system can employ two diode phase shifters per element cell. The two elemental channels can be connected two ways:

1. Two orthogonal linear dipoles connect to the two constrained column feeds. This system would then employ H-plane parallel-plate guide feeders having different launchers for entering vertical- and horizontal-polarization signals into the parallel plate regions. These transitions represent a difficult but not insurmountable design problem.

2. One linear dipole connects to a splitter ahead of two phasers. This system calls for a 15% bandwidth dipole and splitter or diplexer design, but may have two narrow band (4%) phase shifters operating at 12 and 14 GHz. In this system, the dual-polarized element problem is avoided.

The fully space-fed subarray design represents the simplest concept and has the fewest ($2N_E/M^2$) ports to be combined in further processing. The narrow-band dual-polarized radiating element is most advantageous, and the solution of this design problem is used both at the radiating surface and at the combining space-fed surface. $2N_E/M^2$ processors are needed beyond this structure, and there is now sufficient space to consider lower-loss waveguide combining systems between subarray feeds.

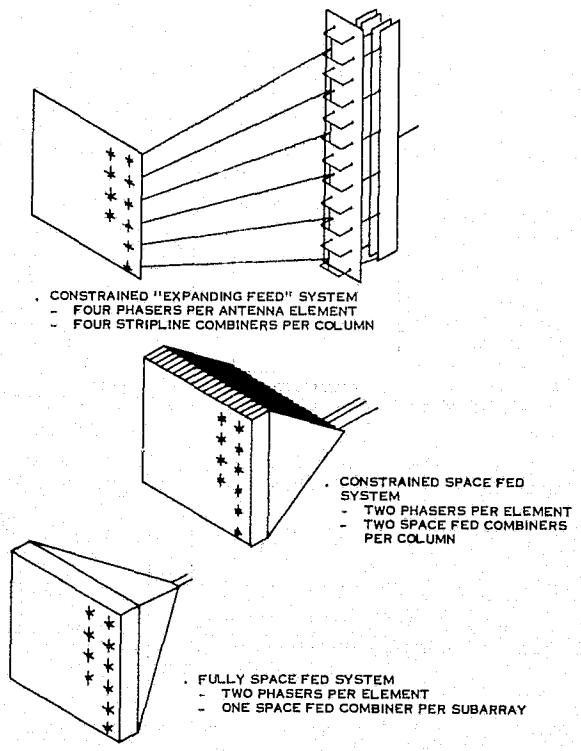

Figure 5.4-11. Comparison of Alternative Subarray Configurations

5.4.6 KU-BAND AMPA DESIGN SUMMARY

A single Ku-band phased array conceptually meets the functional system requirements for the AMPA Ku-band antenna system; however, the limited space behind each antenna radiating element indicates the desirability of separate transmit and receive arrays. Multiple arrays minimize the required packaging density and simplify the design. Four arrays provide the most efficient, most easily packaged system but require significantly more hardware than a single-array system configuration. The primary disadvantages of a four-array system are the hardware requirements and the space required for the four array apertures.

Although multiple-array approaches ease the mechanical design difficulty, the single-array approach is lighter, more compact, and most reliable due to minimum hardware quantity requirements. Alternatively, multiple arrays have the potential for highest reliability through the addition of redundant hardware.

Separate transmit and receive arrays allow each array to be optimized for operation in its narrower frequency band and provide an efficient system. Separate arrays for transmit and receive also eliminate the need for time-steered subarrays and permit implementation with only phase shifter networks throughout the system. Based on all these considerations, a two-array system configuration was selected for the Ku-band Communications Experiment during the Phase A Feasibility Study, as mentioned in Subsection 5.1.

5.5 ADAPTIVE PROCESSING TECHNIQUES AND CIRCUITRY

Array functions to be performed adaptively in both the L-band and the Ku-band Communications Experiments are the acquisition of valid transmitting sources, multiple beam formation, and suppression of interference. For Ku-band, an additional function to be performed is adaptive polarization control for frequency re-use experiments.

In any application, the benefits to be derived from a particular technique must be weighed against the complexity and associated costs for that technique. This Subsection discusses considerations involved in selecting and configuring the adaptive processing techniques required for adaptive multibeam experiments. Alternative configurations for each application, and considerations in their implementation, are presented.

5.5.1 APPLICATIONS OF ADAPTIVE ARRAYS

A great deal of work was done in the early 1960's on self-steering arrays (also called self-phased or self-focused arrays). Most techniques only attempted to phase-cohere the array for the desired signal direction. With modern adaptive array techniques, one can be more demanding and ask for adaptive weighting of the array that will maximize signal-to-noise plus interference ratio. In general, this requires weighting in amplitude as well as phase (i.e., complex adaptive weighting). Adaptive processing can be used for two distinct but closely related functions. One function is the rejection of undesired signals. A complementary function is the automatic acquisition, beamforming, and tracking of desired signals.

5.5.1.1 Sidelobe Interference Rejection

The performance of a satellite antenna in many applications will be considerably improved by suppressing intentional or unintentional sidelobe interference. Rejection of sidelobe interference is particularly important for multibeam communications. It will improve interbeam isolation permitting more frequency re-use among the multiple beams, and therefore increase the system capacity for a given bandwidth allocation. Suppressing sidelobe interference will increase the signal-to-noise plus interference ratio in each beam and provide protection against jamming for military applications. The only

alternative to adaptive sidelobe control would be a heavily tapered precision antenna having ultra-low sidelobes, which is a high-risk, costly approach for spacecraft application.

5.5.1.2 Spatial Acquisition and Tracking

Adaptive processing may be used to automatically acquire a user (i.e., form a beam pointed to a user) while simultaneously placing nulls in the antenna pattern in the direction of sidelobe interference. The same processor will also cause the beam to track the user as the relative angle between the spacecraft antenna and the user changes. Adaptive self-steering can compensate for phase errors originating between the user and the summing point of the array. This not only includes array motion and array geometry but also internal hardware errors, multipath errors due to reflections from other parts of the Shuttle, and effects of mutual coupling between the radiating elements.

5.5.2 CONSIDERATIONS IN ADAPTIVE ARRAY CONFIGURATION CHOICE

The choice of an appropriate adaptive processing configuration for sidelobe interference rejection depends upon many factors such as the type of antenna and its parameters, the number and distribution of intentional and unintentional interfering sources, the information bandwidth, and the cancellation (rejection) requirements. A system with 16 degrees of freedom would be able to demonstrate interbeam isolation for say 10 beams with a reasonable margin for cancellation of unintentional interference.

The antennas considered earlier in Section 5 for the Spacelab AMPA are phased arrays with 576 elements, (24 x 24). This disparity between the large number of elements in the array and the small number of degrees of freedom required for interference rejection suggests the multiple sidelobe canceller (MSLC) configuration. The MSLC configuration makes very efficient use of its degree of freedom, is compatible with any type and size antenna, and can be designed so that the number of degrees of freedom can be readily increased at a later date. The MSLC has been intensively studied, developed, and field-tested and therefore entails a lower risk than other configurations. However, the MSLC designed for communication applications is more complex than the typical radar MSLC

because of the continuous presence of the desired user signal. The MSLC must be constrained from attempting to cancel the desired signal. Two techniques may be employed to contend with this problem - mainbeam angle constraints, and signal removal from the feedback path. The MSLC configuration is described in Section 5.5.2.1.

A fully-adaptive array configuration has many desirable features and permits signal acquisition and tracking in addition to interference rejection, on the other hand, but it has too many degrees of freedom in this case. Solutions to the latter problem presented in this section are the partially-adaptive array configuration, which uses an array of subarrays, and a fully-adaptive subarray configuration that controls the full phased array. These are discussed in Sections 5.5.2.2 and 5.5.2.3, respectively.

5.5.2.1 MSLC Configuration

The principal features of the MSLC configuration are depicted in Figure 5.5-1. The auxiliary elements are positioned around the periphery of the array so that the resolution of the auxiliary array will match the resolution of the main array. Experience has shown that this auxiliary configuration produces good cancellation performance over a wide variety of distributions of interference sources. There are no special requirements on the type of feed used for the main array. The main array is steered by commands from a beam-forming computer.

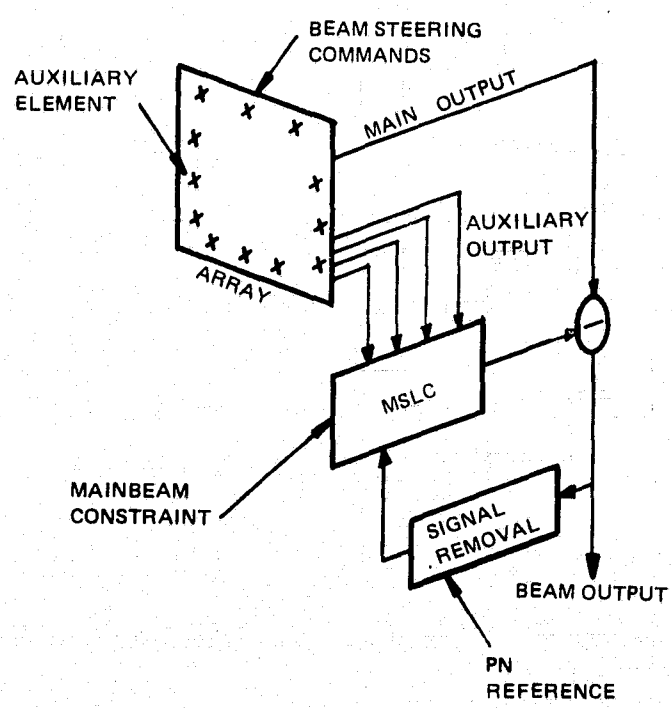

Figure 5.5-1. Multiple Sidelobe Canceller Configuration

With the MSLC configuration, the users must be acquired by searching with full gain multiple beams. In a severe interference environment it may be necessary to use the MSLC during this search. However, the processing gain achieved by the use of special acquisition waveforms should normally permit acquisition without the MSLC. The MSLC would of course be used after acquisition to improve interbeam isolation and reduce sidelobe interference.

C.2

Another disadvantage of the MSLC configuration is that monopulse "delta" beams are required for tracking, in addition to the sum beam. This would be particularly undesirable if, to obtain adequate tracking accuracy, independently optimized delta beam feeds were needed, or if additional MSLC capability was required for cancellation of sidelobe interference in the delta beams.

5.5.2.2 Partially-Adaptive Array Configuration

The problems discussed for the MSLC configuration may be avoided by using a fully-adaptive array configuration in which every element is independently weighted and then summed to form a beam. Independent sets of weights are required for each beam. Such a configuration would provide sidelobe interference rejection, spatial acquisition, and tracking - without spatial search for acquisition or monopulse for tracking. Unfortunately the large number of elements (576), precludes using the fully-adaptive array in the present application. Instead, a "partially"-adaptive array configuration is considered, in which the array is first organized into subarrays which are then treated as the "elements" of a smaller fully-adaptive array. This configuration is shown in Figure 5.5-2.

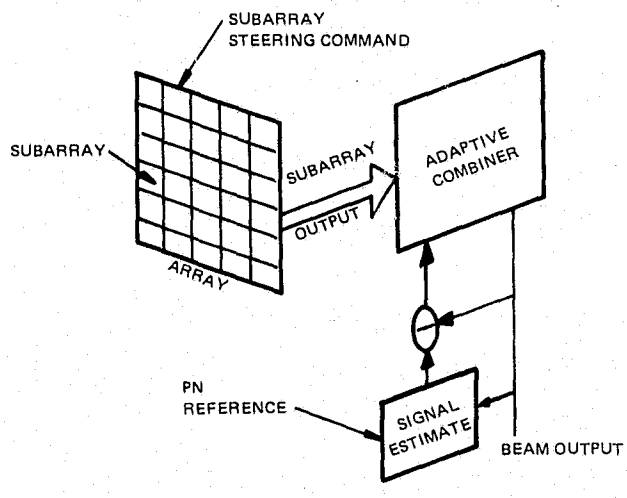

Figure 5.5-2. Partially-Adaptive Array Configuration

In the partially-adaptive array configuration, all the subarrays are steered in unison. A spatial search over subarray beam positions would be required for user acquisition. In this configuration, the signal code is first acquired and then the array adapts to maximize the reception of the signal code while simultaneously cancelling sidelobe interference.

This process keeps the array beam focused on the desired signal source. The subarrays can be made to track the signal by deriving steering commands from the combining weights determined by the adaptive processor. A disadvantage of this approach results from the grating lobes of the array pattern (the pattern that would be formed if the subarrays had

omni-patterns). Interference sources located at the grating lobe positions cannot be cancelled. If 16 subarrays are used in the partially-adaptive configuration, 16 well-separated interfering sources in the sidelobes can be cancelled but there would be approximately 25 grating lobe positions at which no cancellation could be obtained. Interfering sources at those locations would be rejected only by the sidelobes of the subarray pattern. The number of grating lobe positions decreases as the number of subarrays is increased. If possible, the number of subarrays should therefore be increased beyond 16 with the partially-adaptive array configuration.

5.5.2.3 Adaptive Subarray Control of Full Phased Array

A new adaptive technique was conceived during the Phase A Study which overcomes the limitations and disadvantages discussed above for the MSLC and partially-adaptive array configurations. This new technique adaptively controls a full phased array with a much smaller fully-adaptive subarray of the main array to provide adaptive signal acquisition, beamforming, tracking, and interference rejection. One configuration for implementing this technique is through processing of the signals from a 16-element subarray of pseudo-randomly-spaced, main-array radiating elements, as shown in Figure 5.5-3. Other subarray configurations and sizes could also be used for this technique, such as a filled subarray or a row and column subarray. The pseudo-randomly-spaced subarray is preferred, however, because it provides the same resolution as the main array without producing grating lobes.

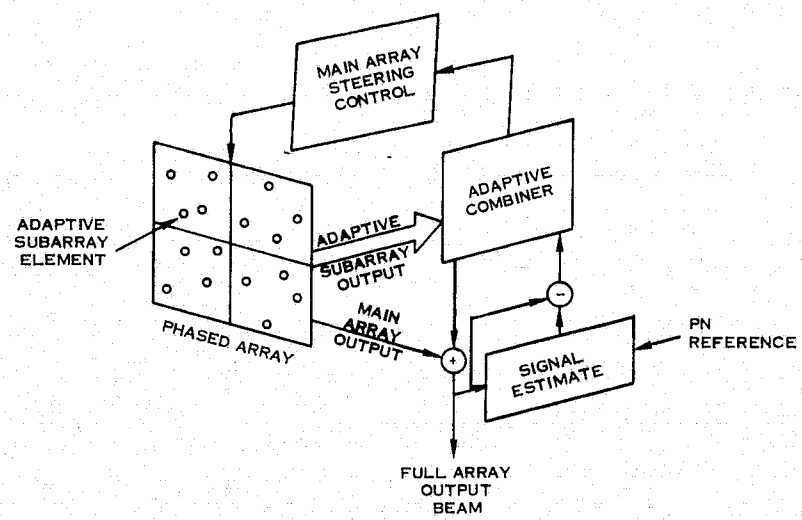

Figure 5.5-3. Configuration for Adaptive Subarray Control of Full Phased Array

No spatial search is required for user acquisition with this technique. The adaptive pseudo-randomly-spaced subarray covers the same field of view as the full phased array and has the same resolution. Users are acquired adaptively by first acquiring the user signal code, and then the fully-adaptive subarray adapts to maximize reception of the coded signal while simultaneously rejecting sidelobe interference.

The main beam of the full phased array is controlled by steering commands derived from the combining weights of the adaptive processor for the fully-adaptive subarray. These steering commands form a main beam on properly coded users and track the users. Combining weights of the fully-adaptive subarray processor also provide equivalent MSLC operation to reject uncoded interference.

5.5.3 RECOMMENDATIONS FOR MSLC AND ADAPTIVE ARRAY IMPLEMENTATION

Adaptive processing may be implemented in analog, digital, or hybrid forms. Analog implementation is usually less costly and is especially appropriate in wideband systems and where high convergence rates are required. The digital implementation is the most reliable, requires the least maintenance, and is versatile - particularly when a programmable controller is used in the processor. The hybrid implementation is used to obtain the advantages of a digital processor in a wideband system while avoiding the need for a wideband A/D converter. In the hybrid implementation the correlator multiplier and integrator are analog devices. These are followed by slow A/D converters whose outputs are then fed to a digital controller. The hybrid implementation is preferred for the Spacelab AMBA.

5.5.3.1 Multiple Sidelobe Canceller Implementation

In recommending the number of degrees of freedom for the MSLC, it was assumed that one degree of freedom was sufficient for each source to be cancelled. The validity of this assumption depends upon the bandwidth, antenna size, and the locations of the interfering sources. The antennas selected in Subsections 5.1 and 5.4 for the Spacelab AMPA consist of a 3m x 3m phased array at L-band and two 0.4 m x 0.4 m phased arrays at Ku-band. Each antenna will have 24 x 24 (576) elements in a filled array, or somewhat less in a thinned array aperture. The antenna beamwidth will be about 5^{o} in both bands. While the antenna RF bandwidth was given in Section 3 as 20 MHz and 500 MHz at L-band and Ku-band respectively, the information bandwidth of a desired or interfering signal will generally be much less.

For instance, if the information bandwidth at L-band is 7.5 MHz, the product of bandwidth times aperture transit time, B_T, will be 0.075 for a signal on the horizon. For user signals within 40 degrees of the antenna normal, the corresponding B_T is less than 0.05. The significance of the B_T product is shown in Figure 5.5-4. This figure is a plot of the cancellation ratio attainable with a single degree of freedom as a function of B_T and the signal spectrum. Note that a B_T of 0.05 will permit approximately 20 dB of cancellation with a single degree of freedom. The cancellation ratio will also be limited by channel matching errors. For 20 dB cancellation ratio, the main and auxiliary channels should track to within 0.83 dB in amplitude and 5.7 degrees phase.

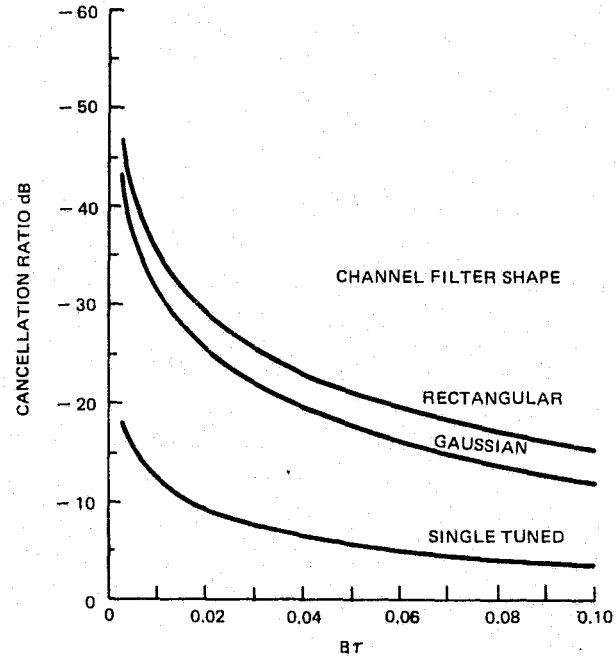

Figure 5.5-4. Cancellation Ratio vs Bandwidth X Transit Time

An MSLC configuration suitable for the Spacelab AMPA application is similar to the radar MSLC configuration shown in Figure 5.5-5. For the communications applications, however, some means must be incorporated to present or remove effects of the desired user's signal. Two methods are available for this purpose. The first is to incorporate one or more mainbeam angle constraints in the MSLC control algorithm. The other is to make use of the temporal characteristics of the user's signal to remove the signal before the correlators. The signal code of all users must be known at the satellite. The particular code being received and synchronization is established during acquisition. For example, if spread spectrum PN coding is used, the signal can be despread (compressed in bandwidth by multiplying the received signal with a synchronized locally generated reference PN sequence), removed by a narrow band rejection filter, and then the residue respread by remodulating with the reference PN sequence. This is shown in the communications MSLC block diagram of Figure 5.5-6.

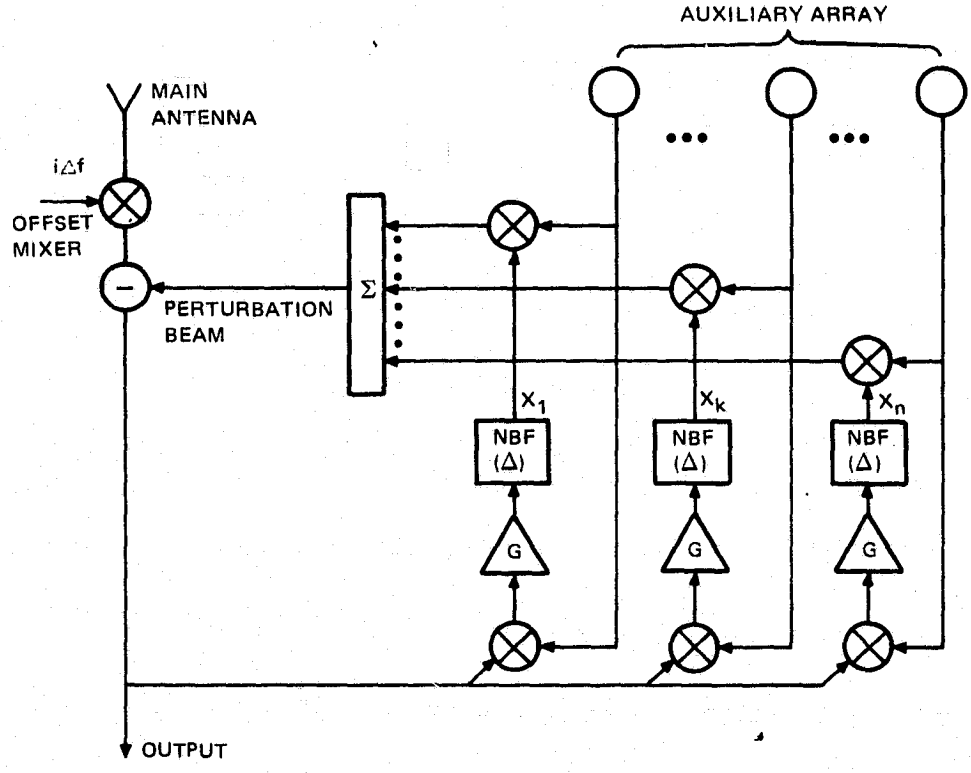

Figure 5.5-5. Block Diagram of Radar Multiple-Sidelobe Canceller

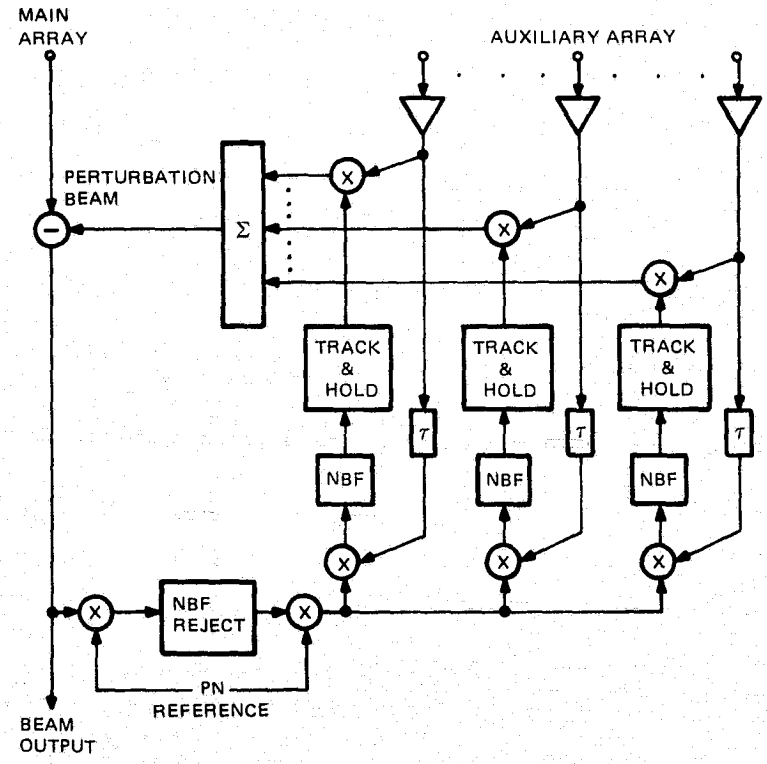

Figure 5.5-6. Block Diagram of Communications Multiple-Sidelobe Canceller

For mainbeam constraints, pilot signals are introduced into each element channel as shown. The pilot signals are phased to appear as if they originated from the same direction as the user in the mainbeam of the main antenna. The presence of the pilot signals forces the MSLC to place a null in the pattern of the perturbation beam in the direction of the desired user. The pilot signals are inserted out-of-band so that they can be removed from the output by filtering. Pilot signals are only one of many methods for implementing mainbeam constraints.

The MSLC is particularly advantageous for interference rejection. It can be applied to any type of antenna - optical or array. It is compatible with any form of beam steering since it works only on the output beam ports. Failures in the MSLC only affect its interference rejection capability and will not shut down the main antenna.

The block diagram shown in Figure 5.5-6 may be implemented in a number of ways - analog, digital, or hybrid. The hybrid implementation, as remarked earlier, is preferred. Since the electromagnetic environment seen by the antenna changes very slowly compared to the convergence rate of the MSLC, most of the MSLC equipment can be time-shared between beams or between elements of the same beam. There are many possible variations of the MSLC shown in Figure 5.5-6, which is shown to illustrate the concept and indicate the order of complexity involved.

5.5.3.2 Partially-Adaptive Array Implementation

One possible method for implementing the partially-adaptive array discussed earlier is shown in Figure 5.5-7. This method uses a Widrow Least Mean Square Configuration (see reference 10). The reference signal is obtained by a technique due to R. T. Compton of Ohio State. As in the MSLC, it assumes a synchronized reference PN sequence has been acquired. This reference sequence is used to generate a noise-free estimate of the desired user signal. The array output is despread by the reference sequence, smoothed by the narrowband filter, and then the user signal is regenerated by remodulating with the reference PN sequence. Note that time delay must be inserted to match the time delay of the narrowband filter. As in the case of the MSLC, most of the equipment can be time-shared between beams or between partially-adaptive subarrays of the same beam.

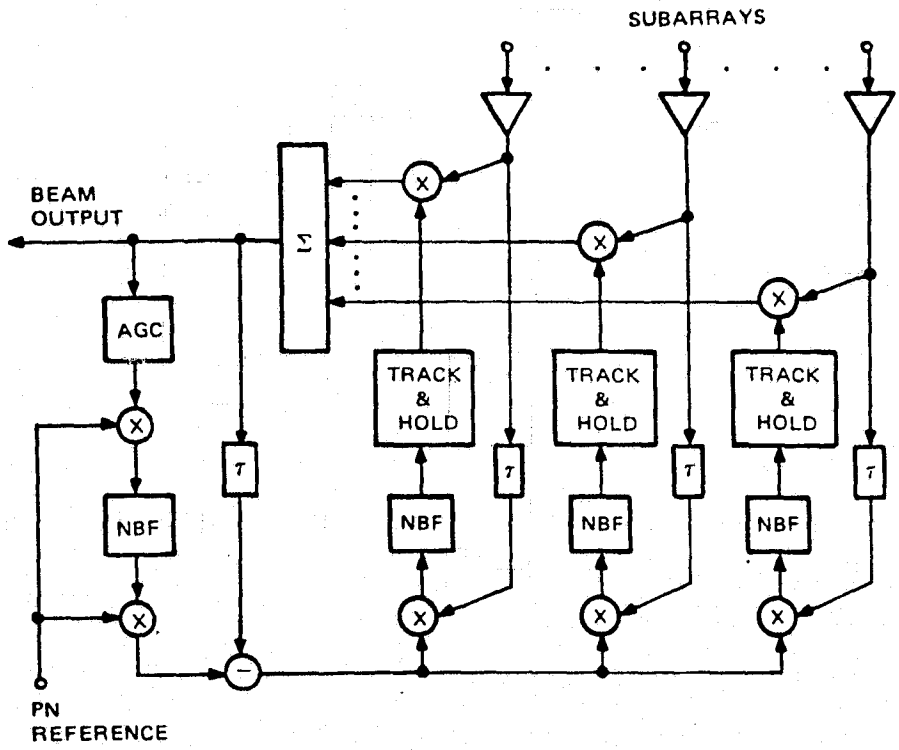

Figure 5.5-7. Block Diagram of Partially-Adaptive Array Processor

5.5.3.3 Fully-Adaptive Subarray Control Implementation

As shown in Figure 5.5-8, the method just described in Section 5.5.3.2 could be used for

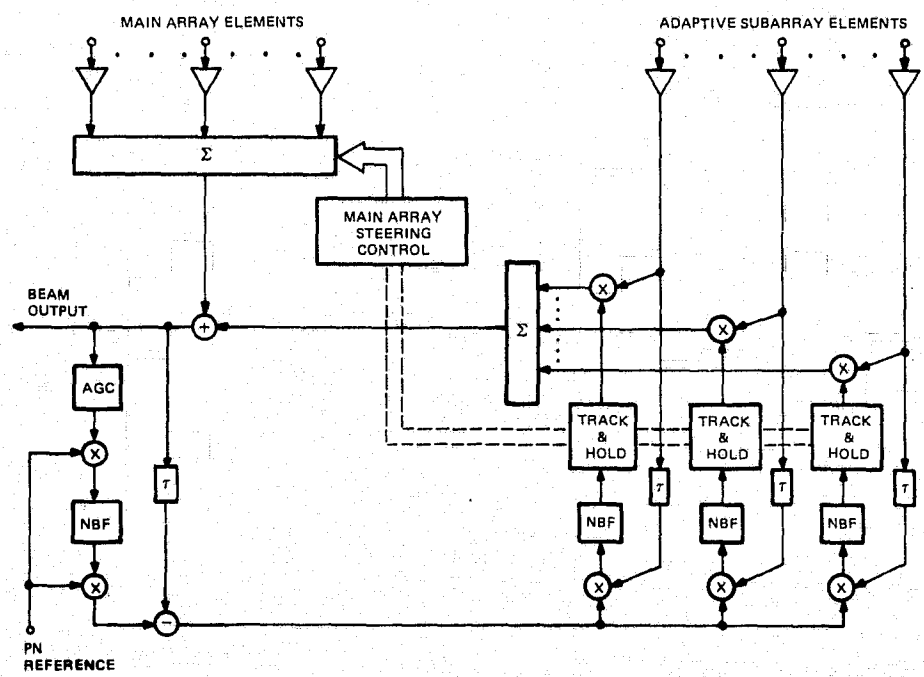

Figure 5.5-8. Block Diagram of Adaptive Subarray Processor and Control

implementing the fully-adaptive subarray portion of the technique discussed in Section 5.5.2.3 for adaptive subarray control of the full phased array. For that technique, however, the input signals to the adaptive processor would be from the adaptive subarray elements of the full array, rather than from subarrays of the array. The full array output beam is used for correlation in both cases. The main array steering control signals for this technique are generated by an algorithm from the adaptive processor weight signals, as indicated in Figure 5.5-8.

5.5.4 ADAPTIVE POLARIZATION CONTROL

In addition to the adaptive processing techniques required for signal acquisition, beamforming, and tracking of a valid transmitting source or user, and for interference rejection of undesired signals, the Ku-band Communications Experiment requires an adaptive processing technique for adaptive polarization control. This technique is required to isolate two signals on the same frequency that are nominally orthogonally polarized, so as to achieve frequency re-use within the same antenna beam. The application of adaptive polarization control and configurations for its implementation are discussed in this section.

Both the MSLC and the fully-or partially-adaptive array configurations may be combined with adaptive polarization control. The adaptive processing required for adaptive polarization is relatively simple, involving only two degrees of freedom. The most difficult aspect of adaptive polarization is the antenna. Adaptive polarization requires simultaneous cross-polarized inputs, which is difficult to obtain in a single aperture with phased arrays. Adaptive polarization for frequency re-use may be approached in two ways. The optimum processor would adjust the polarization to maximize the ratio of signal-to-noise plus cross-talk from the other "polarization" channel. A sub-optimal processor that may be used if the amount of depolarization is small, sets the polarization for the desired channel orthogonal to the polarization of the other channel. This approach leads to a relatively simple analog implementation.

5.5.4.1 Application of Adaptive Polarization Control

Dual-polarized antennas with adaptive polarization control can make an important contribution to satellite communication systems by providing frequency re-use. In this application, two independent channels, transmitted on orthogonal polarizations within the same beam, are provided on each communications link. Adaptive polarization control is required to separate the signal polarizations on receive and thus remove any cross-talk between the two channels that is introduced by the transmit and receive antennas or by propagation effects such as rain depolarization. Each of the two channels are also provided with adaptive spatial (angle) processing for sidelobe interference rejection and signal acquisition and tracking.

Dual polarization with adaptive polarization control can also be used advantageously with a singly polarized user for mainlobe interference rejection and to isolate legitimate users who are not resolved by the antenna beamwidth. The two emitters must be received with different polarizations, however, in order that an improvement in performance be obtained in that case.

5.5.4.2 Adaptive Polarization Configuration

A simplified block diagram of a dual-polarized antenna incorporating both adaptive sidelobe interference rejection and adaptive polarization isolation is shown in Figure 5.5-9. It is assumed that two almost cross-polarized signals are being received from the desired user. The two channels use different PN code sequences and it is assumed that both sequences have been acquired and that synchronized references are available. Adaptive processors are used to form two cross-polarized beams with the aid of the reference PN sequences. The LMS algorithm may be employed using an estimate of the stronger of the two signals in each beam as the reference. The weaker signal in each beam is rejected in the feedback path to prevent adverse effects of mainbeam interference on the operation of the adaptive array processors.

Signal estimation and signal rejection is accomplished by using the reference PN sequences to despread the signal followed by narrow-band filtering and then respreading, as discussed in Section 5.5.3.1. The two cross-polarized beams will acquire and track the same user while rejecting sidelobe interference. The outputs of the two beams are then fed to two adaptive polarization combiners to restore the separation between the channel A and channel

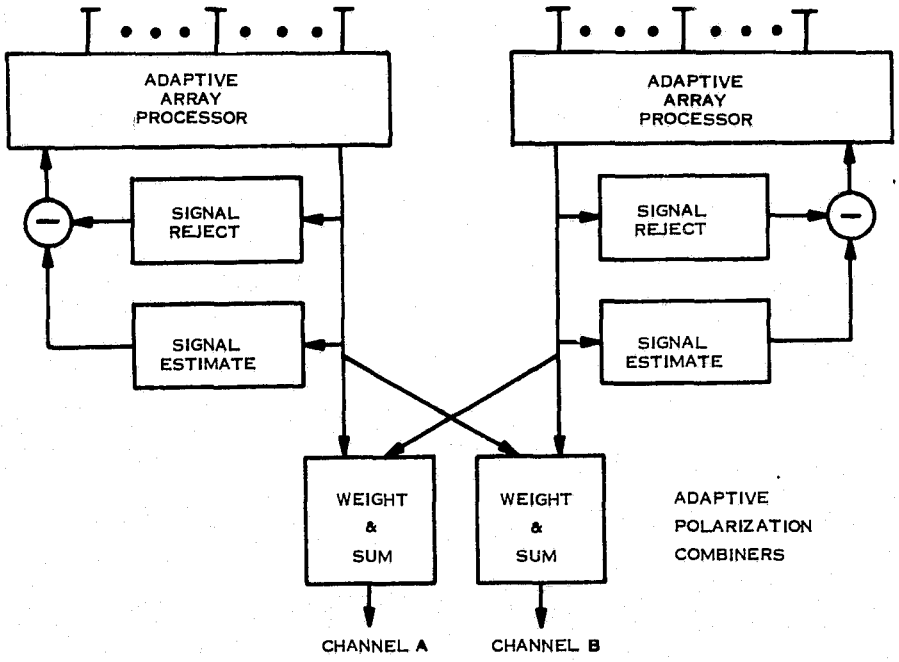

Figure 5.5-9. Adaptive Dual-Polarized System

B signals. In each of these combiners, the two beam outputs are weighted by complex weights and summed. The weights are adaptively derived to minimize the cross-coupling between the two channels or to maximize the ratio of signal-to-noise plus interference.

An adaptive polarization combiner for minimizing the cross-coupling between channels A and B is shown in Figure 5.5-10. In this configuration, the polarization is transformed by a sequence of unitary transformations so that the undesired signal appears in one output port and is cancelled in the other. This is accomplished with two phase shifters and two 3 dB couplers. The phase shifters are controlled by the in-phase and quadrature components of the cross-correlation of the two outputs. The cross-correlator is only allowed to respond to the undesired signal of the originally cross-polarized pair by using the reference PN sequence and a narrow band filter as shown. The phaser diagrams on the right hand side of Figure 5.5-10 are intended to illustrate the effect of the processor on the carrier of the undesired signal at various stages.

In this example, the adaptive polarization combiner (APC) on the channel A output in Figure 5.5-9 is used to null out the undesired channel B signal. At the input to the APC, the two phasers represent channel B signal components that have unequal amplitudes and are ϕ radians apart. The first phase shifter brings the two carriers in-phase with each other. After the first coupler, the two phasers will have equal amplitudes and a phase separation of θ radians. Once again the phasers are brought into phase by the second phase shifter. Finally by adding and subtracting the two phasers, a null of the channel B signal is obtained in the channel A output port, while a co-phasal addition is obtained in the isolation port.

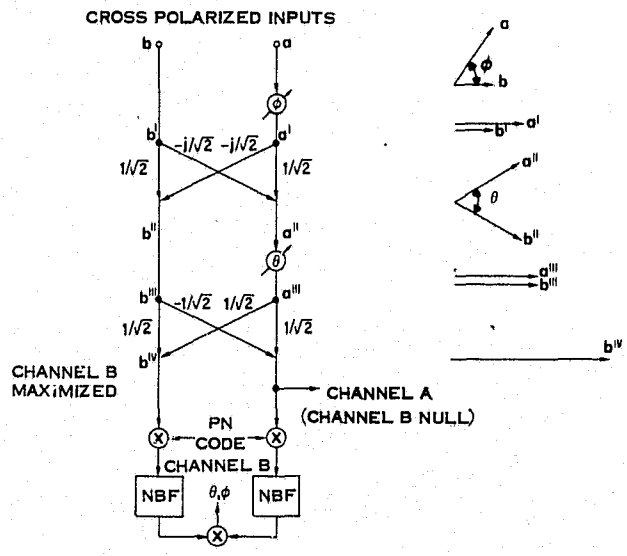

Figure 5.5-10. Adaptive Polarization Combiner

Similarly, the adaptive polarization combiner on the channel B output in Figure 5.5-9 is used to null out the undesired channel A signal. The channel A and B signals, which were orthogonal when transmitted, are thus restored to their respective channels A and B by the adaptive polarization control circuits.

Note that the undesired signal was nulled out in channels A and B, rather than the desired signal being maximized. This results in only a small loss in the desired signal in each channel, for a moderate amount of depolarization of the channel A and B received signals from their original orthogonal state.

SECTION 6

AMPA EXPERIMENT CONFIGURATION

The complete Adaptive Multibeam Phased Array (AMPA) experiment configuration and design requirements for that configuration are described in this section. The individual experiment configurations are described first, followed by the overall AMPA experiment configuration. The AMPA antenna system is described next using an overall system block diagram, and the AMPA design configuration is discussed using layout drawings of the AMPA antenna system in the Shuttle/Spacelab bay. Thinning of the L-band and Ku-band arrays to reduce the numbers of radiating elements is also discussed. Alternative ways of integrating the AMPA antenna system apertures are shown. Detailed experiment configuration design requirements for the AMPA experiment conclude this section.

6.1 SELECTED AMBA EXPERIMENT CONFIGURATIONS

The selected L-Band Communications, L-Band Radiometer, and Ku-Band Communications Experiments that were described in Section 3 are here presented as complete experiment configurations. A block diagram of the L-Band Communications experiment configuration is shown in Figure 6.1-1. Block diagrams for the L-Band Radiometer and the Ku-Band Communications experiments configurations are shown in Figures 6.1-2 and 6.1-3. In all cases, a data link from Shuttle/Spacelab to the TDRSS Ground Station via the Tracking and Data Relay Satellite (TDRS) for purposes of experiment coordination is shown. Equivalent experiment control links could be provided, or autonomous AMPA experiments could be planned without such a link.

For the L-band Communications Experiment low power cooperating shipboard terminals are assumed with an EIRP of 1 watt and near hemispheric overhead coverage. Operation at the maritime L-band communications frequencies of nominally 1.64 GHz for the up-link and 1.54 GHz for the down-link is also assumed. Buoys specially instrumented for an adaptive multibeam data collection experiment at L-band could be used as alternative experiment ground terminals that would give a greater amount of experiment operating time and data.

For the Ku-band Communications Experiment, medium size cooperating ground terminals are assumed that will track the Shuttle/Spacelab. An antenna gain of 40 to 50 dB and 10 to 100 watts of transmitter power are assumed.

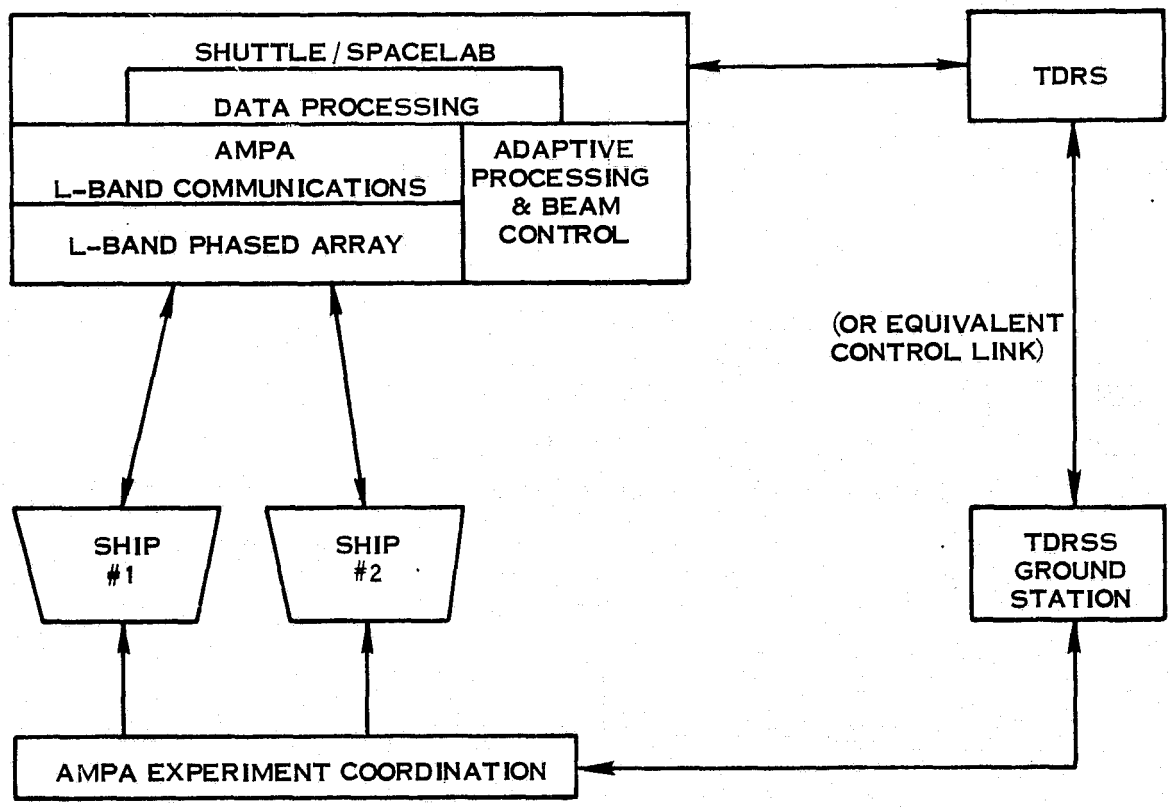

Figure 6.1-1. L-band Communications Experiment Configuration Block Diagram

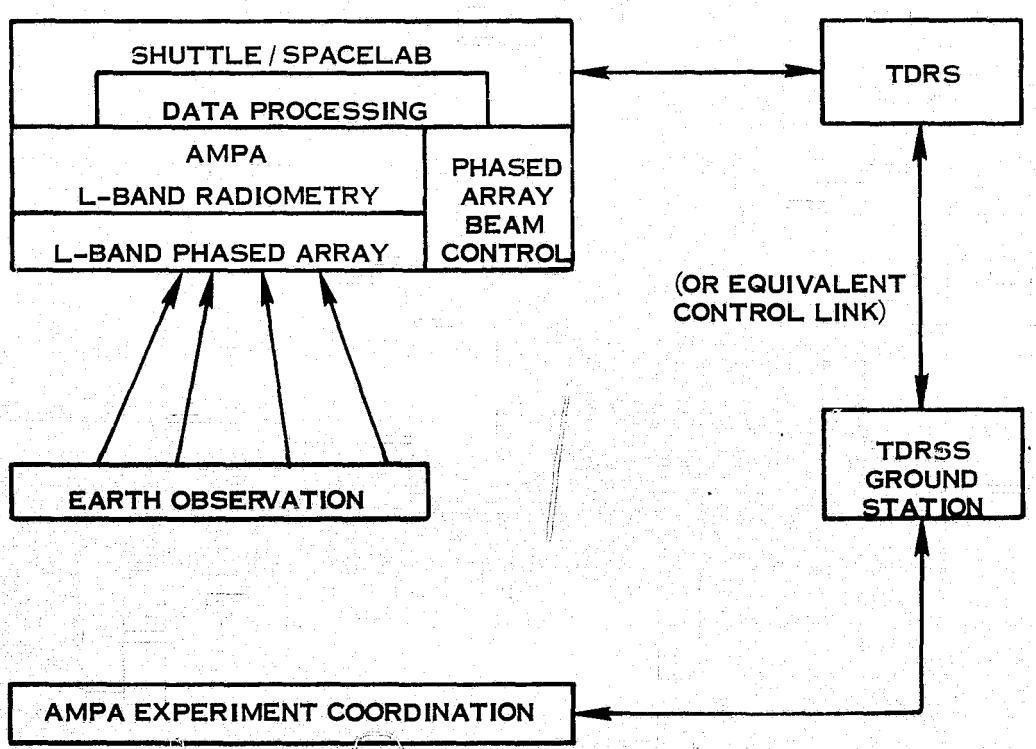

Figure 6.1-2. L-band Radiometer Experiment Configuration Block Diagram

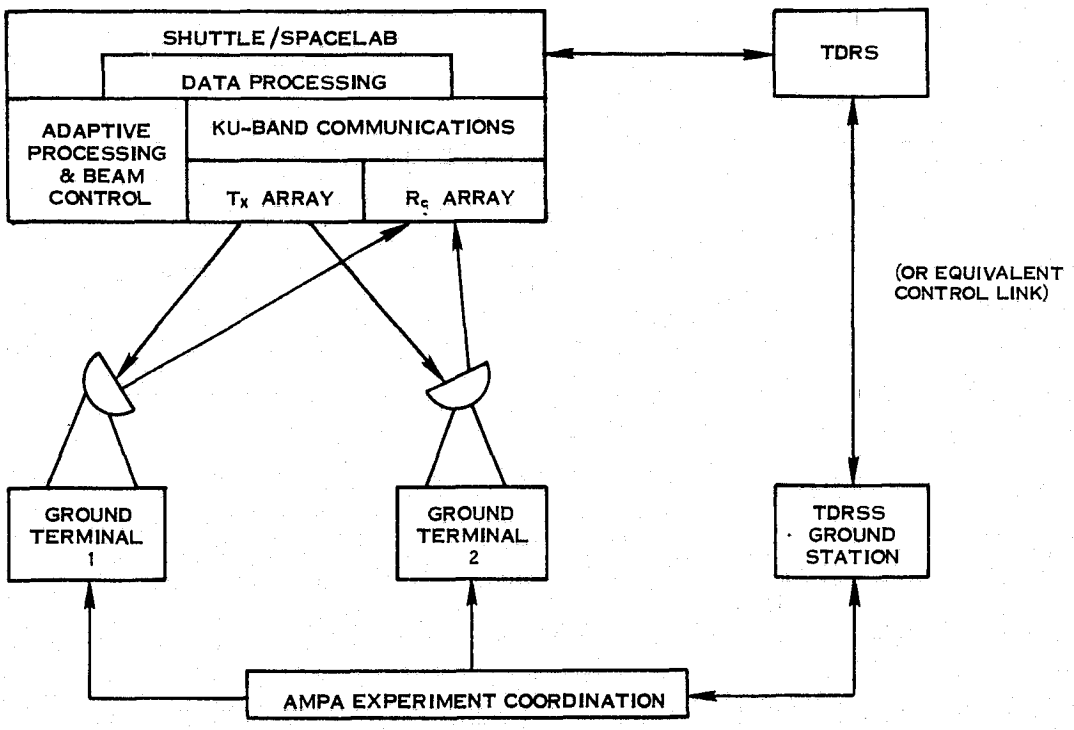

Figure 6.1-3. Ku-band Communications Experiment Configuration Block Diagram

For the L-band Radiometer Experiment, gross water sheds would be observed in mountainous regions and general distribution of soil moisture content in valleys and plains. A radiometer temperature resolution of better than 0.5^{o} can be obtained within a nominal 35 kilometer spot size resolution.

A block diagram of the overall AMPA experiment configuration is shown in Figure 6.1-4. The AMPA antenna system on Spacelab is integrated for the greatest commonality of equipment consistent with the objectives of the three selected experiments. A single L-band phased array is used for both the L-Band Communications Experiment at 1.5/1.6 GHz and the L-Band Radiometer Experiment at 1.4 GHz, with much of the RF circuitry shared by both experiments. Separate phased arrays are used on transmit and receive for the Ku-band Communications Experiment at 12/14 GHz because of the greater frequency separation and bandwidth. The adaptive processing and beam control equipment is shared by all three experiments, as is the on-board data processing equipment.

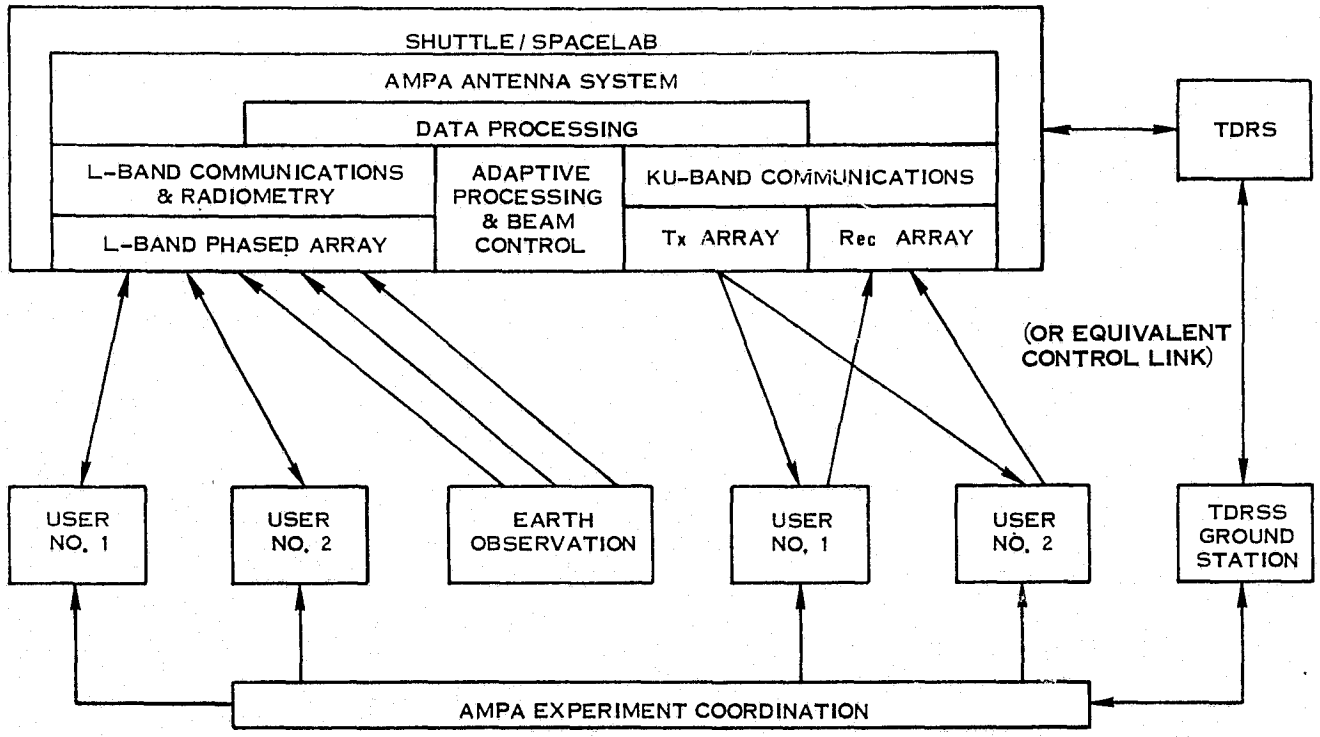

Figure 6.1-4. Block Diagram of Overall AMPA Experiment Configuration

6.2 AMPA DESIGN CONFIGURATION

This subsection is concerned with the design configuration of the AMPA antenna system in more detail and its installation aboard Shuttle/Spacelab. The block diagram of the selected design concept for the AMPA antenna system is repeated in Figure 6.2-1. The single L-band phased array with switchable RF circuitry is used for both the L-Band Communications Experiment and the L-Band Radiometer Experiment. As discussed in Section 5, a reference phased-array configuration was selected having 576 crossed-dipole radiating elements in a 24 x 24-element array with a 3-bit phase shifter per element.

For the L-band Communications Experiment, the selected reference array uses a 4-dB noise figure amplifier per radiating element on receive to achieve an overall 5-dB noise figure. A single transmit amplifier per beam is used, and the transmit power is divided with strip transmission line circuits. Diplexing is achieved with 5-pole interdigital filters. Thinning of the L-band array would be both acceptable and highly desirable for the communications experiment, but would seriously degrade beam efficiency for the radiometer experiment. Since little saving in hardware would result for communications with a filled array for radiometry, thinning probably would not be used at L-Band.

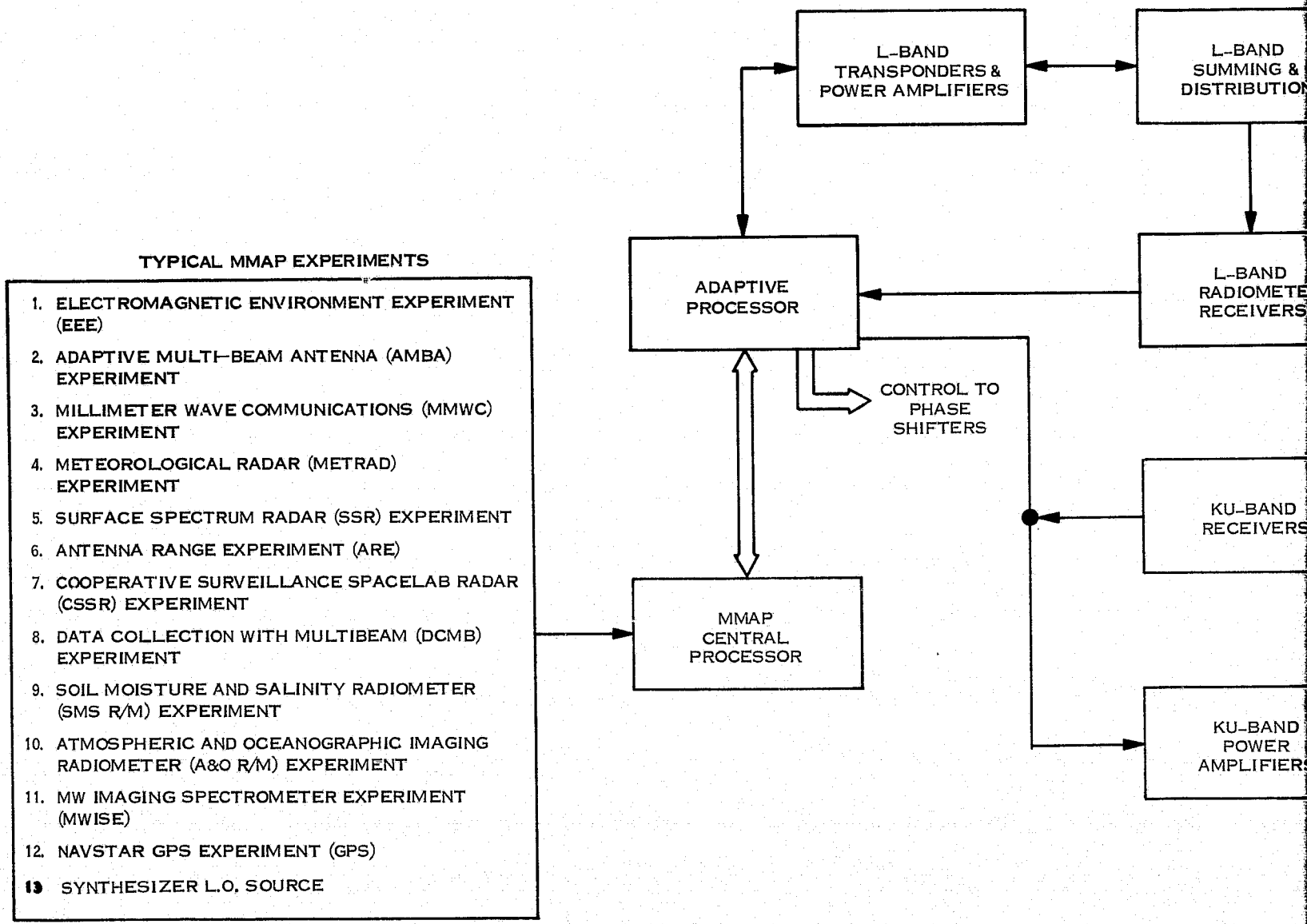

FOLDOUT FRAME 1

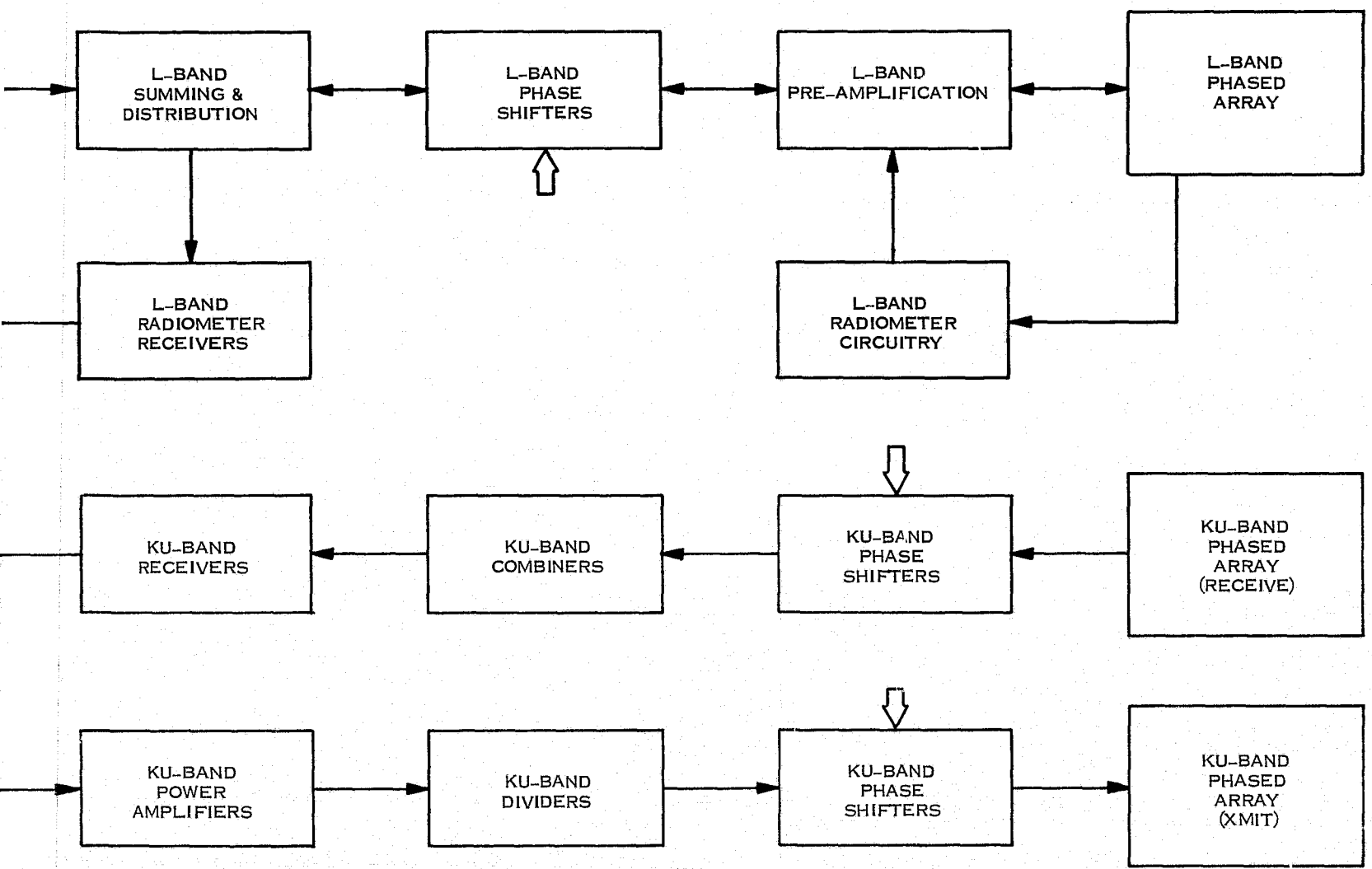

Figure 6.2-1. AMPA Antenna System Block Diagram (Integrated with MMAP)

FOLDOUT FRAME 2 6-5/6

For the L-band Radiometer Experiment, much of the equipment is shared in common with the L-band Communications Array. This is accomplished by switching the connections to the dipoles used in the L-band Communications Experiment so that the wideband, elemental, low-noise amplifiers can be used for either linear or horizontal polarization. This reconfiguration of the RF circuitry permits utilization of the low-noise amplifiers, phase shifters, and strip transmission line combiner/divider networks in both the L-Band Communications and the L-Band Radiometer Experiments at the expense of only about 2 dB of system noise figure.

For the Ku-band Communications Experiment, the two-array Ku-band antenna system configuration shown in the AMPA antenna system block diagram of Figure 6.2-1 was selected during the Phase A Feasibility Study. Using separate arrays for transmit and receive eliminates the requirement for broadband beam steering and eases the physical size constraints on the arrays, thus it presents the most attractive alternative in spite of some increase in the hardware requirement. The two-array approach has the added advantage that a proven GE developed Ku-band phase shifter is directly applicable without development. Each array would have 576 orthogonal dipole elements, if filled, with each element hybrid-connected to achieve both right-hand and left-hand circularly polarized operation on transmit and receive. If thinned arrays are used at Ku-band with the same aperture size, a considerable saving in hardware results as well as easier packaging, with some loss in gain. With 75% thinning for instance, only 144 radiating elements are needed in each array with only about 6 dB less gain. Thinning is thus very attractive for the Ku-band arrays.

Adaptive acquisition, beamforming, signal tracking, and interference rejection are accomplished in both the L-band and Ku-band phased arrays through processing of the signals from a 16-element subarray of pseudo-randomly-spaced, main-array radiating elements. In addition, frequency re-use for orthogonally-polarized dual-channel communications is accomplished at Ku-band through adaptive polarization isolation/separation.

The adaptive processor shown in Figure 6.2-1 would be shared by all arrays in the AMPA antenna system. This processor also provides phase shifter control signals derived from

the adaptively processed signals for forming and steering the multiple beams of the main arrays.

The block diagram of Figure 6.2-1 shows the AMPA antenna system integrated with other MMAP experiments and connected to an MMAP central processor. The AMPA antenna system can also be used alone effectively for conducting multiple Adaptive Multibeam Antenna (AMBA) experiments.

Layout drawings of the selected AMPA antenna system design concept stowed in the Shuttle/Spacelab bay are shown in Figure 6.2-2. Outline dimensions for the arrays are given on the layouts. The AMPA antenna system is shown deployed on two types of support masts in Figure 6.2-3. In both cases, the AMPA antenna system is merely extended straight out of the bay above its pallet. An alternative deployment to a position above the Spacelab Module is shown in the photograph of Figure 2-5. The actual deployment method used will depend to a great extent on the AMPA location with respect to other experiments that are flown on the same Shuttle/Spacelab flight.

Alternative AMPA antenna system configurations are shown in Figure 6.2-4. By eliminating a few radiating elements in the corners of the L-band array, the Ku-band arrays can be integrated into the same aperture outline. The cruciform and the octagonal methods of integrating the array apertures result in more compact system packaging with little effect on the L-band phased array performance, thus they should be seriously considered. The cruciform arrangement is attractive because of its simplicity, but the octagonal arrangement would produce better antenna patterns. In either case, the pair of Ku-band arrays could be located on a diagonal if center of gravity is a prime consideration, but the locations shown are preferable from a consideration of system interconnections.

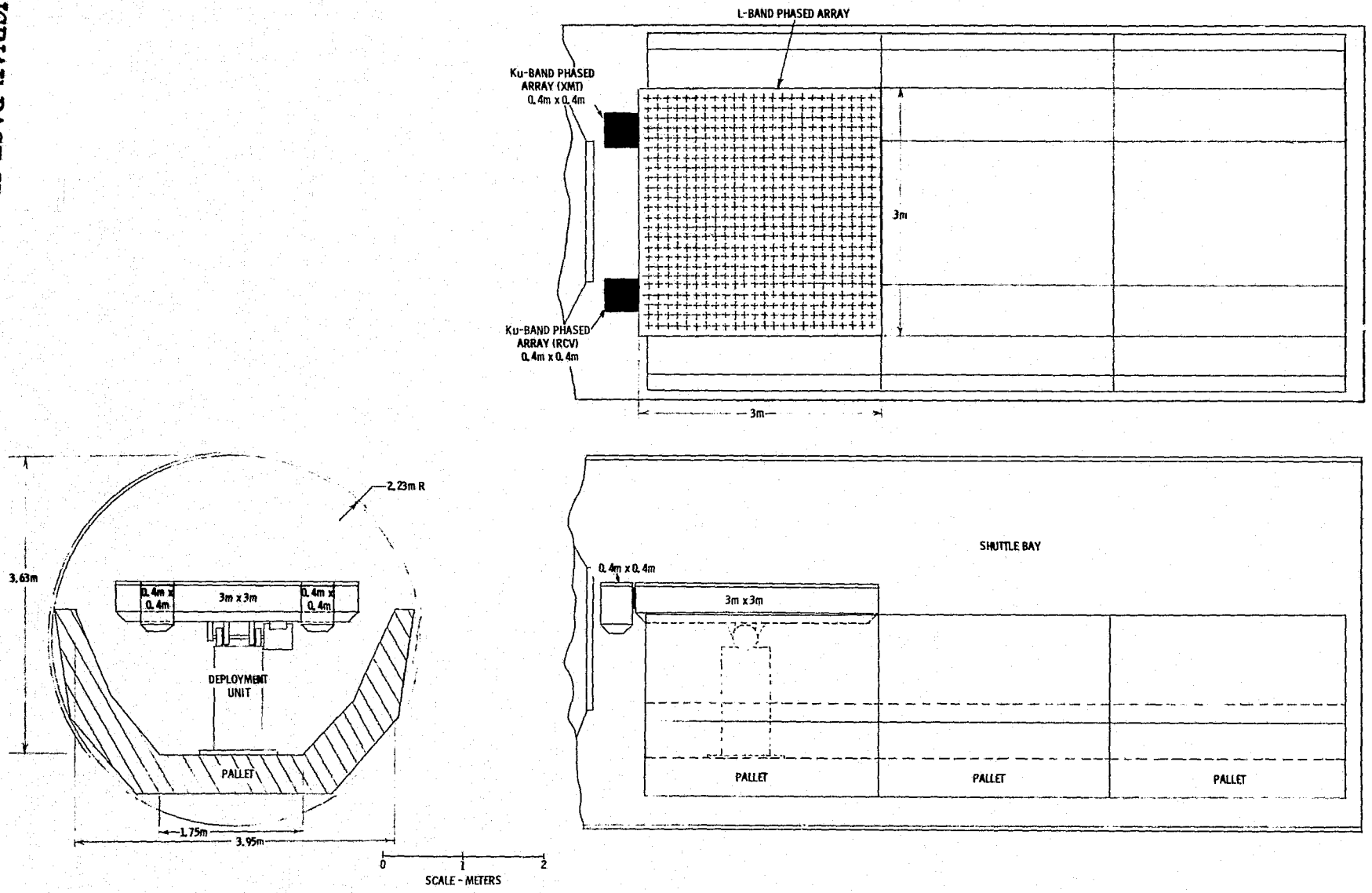

Figure 6.2-2. AMPA Antenna System in Shuttle Bay

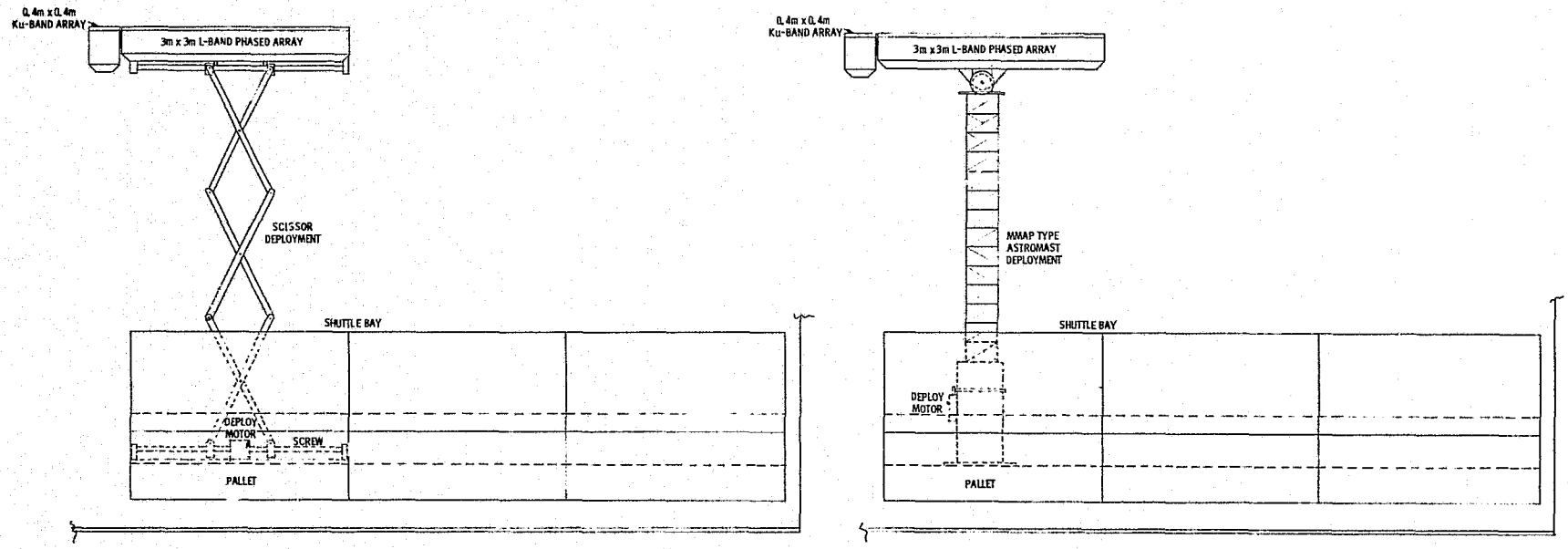

Figure 6.2-3. AMPA Antenna System/Typical Deployers

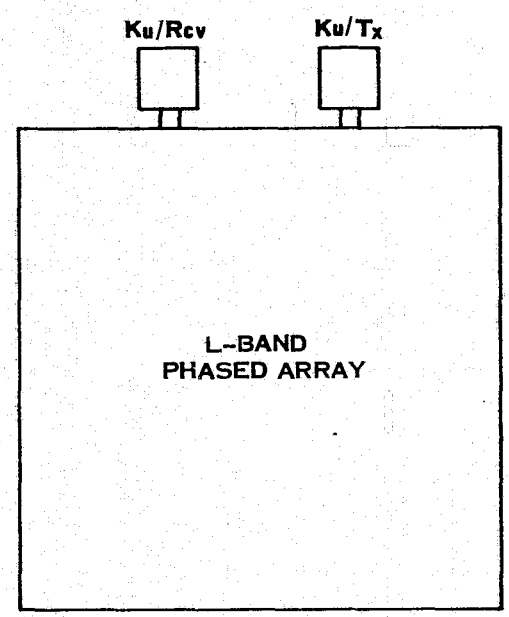

(a) Square Array Apertures

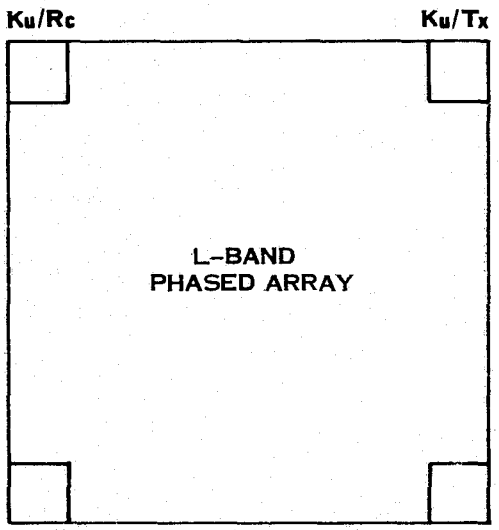

(b) Cruciform Integration of Array Apertures

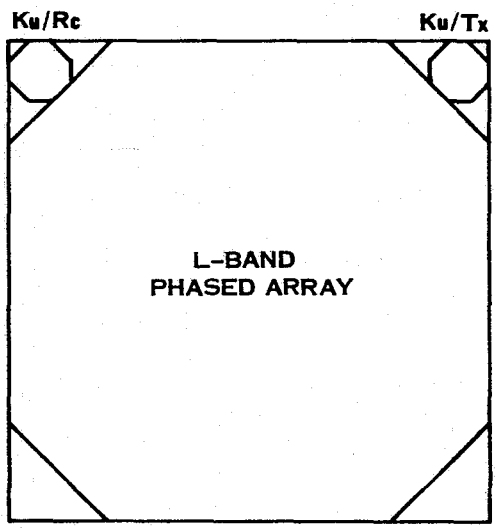

(c) Octagonal Integration of Array Apertures

Figure 6.2-4. Alternative AMPA Antenna System Configuration Outlines

6.3 EXPERIMENT CONFIGURATION DESIGN REQUIREMENTS

The first step in configuring a Spacelab experiment is to establish an integrated set of design requirements which provide for physical, functional and operational capabilities needed to perform its intended mission. These requirements are based on the scientific objectives of the experiment and the accommodation capability of Spacelab and Shuttle. In this section we develop the AMPA experiment design requirements, beginning with basic mission requirements and constraints, and continuing to a conceptual definition of the experiment configuration.

The tables which follow contain information compiled for the AMPA Sortie Payload Data Sheets, plus additional data useful in the logical development of the AMPA experiment configuration. Use of the tabular data is as illustrated below:

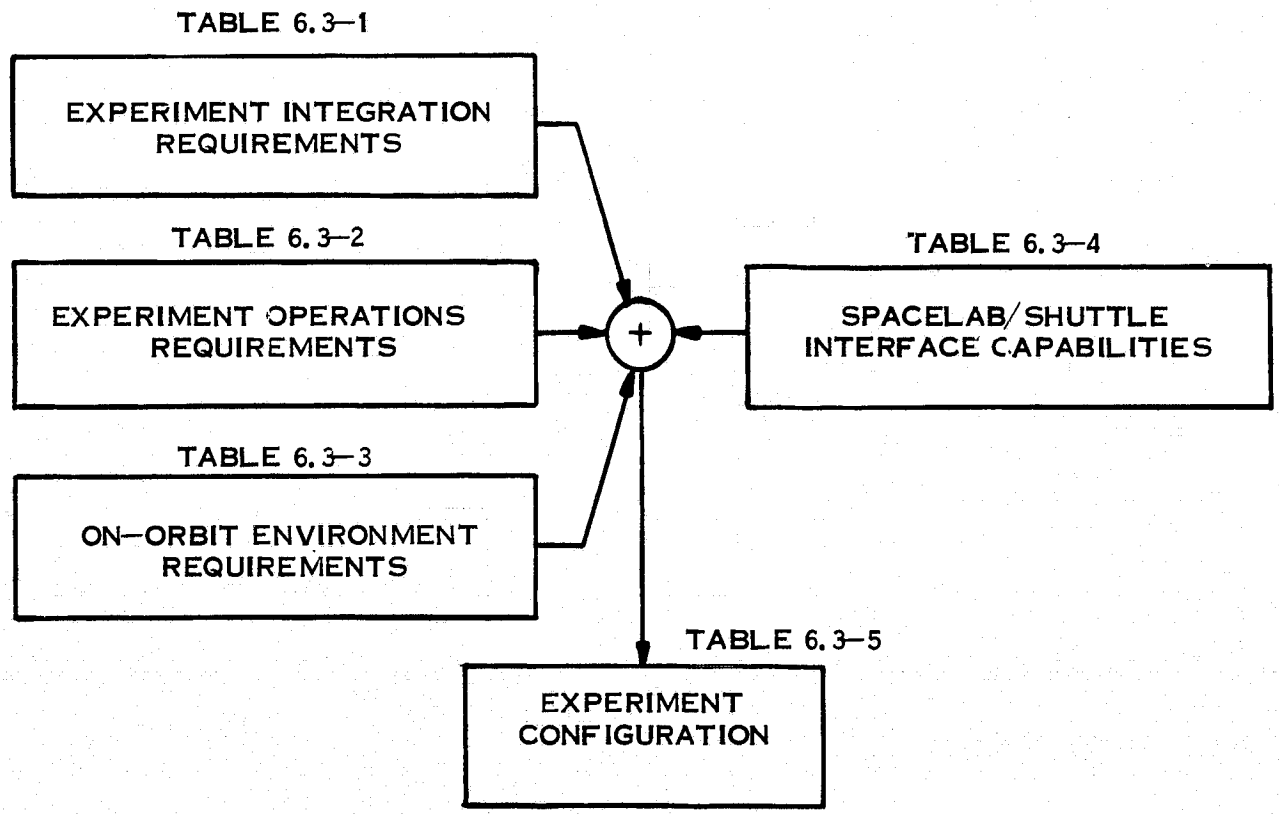

Table 6.3-1 presents experiment physical and functional integration requirements. Requirements derived by the AMPA are established using the general understanding of Spacelab experiments gained through our continuing involvement in Shuttle payload studies (including STSPDA).

Table 6.3-2 lists normal and contingency experiment operations. Normal operations are based on requirements of the three baseline experiments, supplemented by our general experience as was the case for experiment physical and functional requirements. Contingency operations consider experiment failure modes and logical responses to each situation.

Table 6.3-3 shows on-orbit operating and non-operating environment requirements for the baseline experiments augmented by our knowledge of Spacelab/Shuttle conditions and constraints. Our basic pholosophy is that experiments should be compatible with the Spacelab, Shuttle and near space environment, and that any special sensitivities should be handled by experiment design.

Table 6.3-4 summarizes interface capabilities of Spacelab and Shuttle. Physical interfaces consist of mounting, power, data, and Caution and Warning connections. Functional interfaces are highly variable depending on the extent to which resources are shared with other payloads. The most significant impacts are in the operational area, where crew involvement in experiment operations and Shuttle involvement in pointing and tracking can be significant. Contingency operations involving experiment jettison have a significant Shuttle impact.

A design concept for the AMPA experiment is outlined in Table 6.3-5. This concept builds upon the experiments and Spacelab/Shuttle requirements discussed above. Specific solutions and design goals are set forth to guide the conceptual design effort in the remainder of this task.

Table 6.3-1. Experiment Integration Requirements

Parameters	Requirement
(Physical)	
Antenna Dimensions	3m x 3m x 0.5m (L-band) 0.4m x 0.4m x 0.5m (Ku-band Xmit) 0.4m x 0.4m x 0.5m (Ku-band Receive)
Antenna Weight*	1500 kg (L-band) 100 kg (Ku-band Xmit) 100 kg (Ku-band Receive)
Electronics Volume*	0.5 m^3 (Internal)
Electronics Weight*	150 kg (Internal)
Antenna Alignment	$\sim 0.25^{o}$
Antenna Viewing	$\pm 40^{o}$ Scan Angle
Total FOV	Full Earth
Thermal Control	TBD
Consumables	None
Special Protection	None anticipated
(Functional)	
Electric Power	500 W (L-band Communication) 300 W (L-band Radiometer) 600 W (Ku-band Communication) 800 W (Standby)* dc
Data Rate	50 KBps (L-band Communication) 1 KBps (L-band Radiometer) 2 MBps (Ku-band Communication) TBD (Housekeeping) TBD (Commands)
Heat Rejection	600 W **
Caution and Warning	None
Fluids	None

*Estimates

** Does not include allowance for space heating or cooling.

Table 6.3-2. Experiment Operations Requirements

Parameter	L-band Communications	L-band Radiometer	Ku-band Communications
(Normal)			
Experiment Ops.	50 sec/pass	15 min/pass	50 sec/pass
Setup	TBD	TBD	TBD
Shutdown	TBD	TBD	TBD
Cycles/Day	2	8	2
Cycles/Mission	14	56	14
Deployment	15 min	Same	Same
Retraction	15 min	Same	Same
Targets	Two ships, 100 to 400 km apart	Selected land areas (CONUS)	Two earth stations, 100 to 400 km apart
Pointing	0.5^{o}	0.5^{o}	0.5^{o}
Stability	0.5^{o}	0.5^{o}	0.5^{o}
Stability Rate	0.1^{o}/sec	0.1^{o}/sec	0.1^{o}/sec
Crew	See Table 7-1	Same	Same
(Contingency)			
On Orbit Repair	Use EVA to repair simple malfunctions (mechanical problems, component replacement)	Same	Same
Retraction Malfunction	Jettison antenna, electronics, and deployment mechanism	Same	Same

Table 6.3-3. On-orbit Environment Requirements

Parameter	Requirements	Remarks
(Operating)		
Acceleration	N/A	Orbiter acceleration $\ll 1g$
Temperature	0-40°C	
Humidity	70% (+10, -20)	Internal Equipment Only
Pressure	50,662 N/M^2	Internal Equipment Only
Cleanliness	TBD	Spacelab imposes materials restrictions, venting restrictions. Orbiter emissions will be limited to 1 event/orbit for particles >5 microns in full view of instrument. Induced H_2O column density $< 10^{12}$ molecules/cm^2. Absorption of UV, visible, IR radiation < 1%.
Electrical	MIL-STD-461 (Must cope with the Orbiter/Spacelab environment and abide by its restrictions)	Orbiter/Spacelab environment < 1 V/m radiated RF, except ≈ 3.4 V/m in S-band.
Magnetic	MIL-STD-461 (Must cope with the Orbiter/Spacelab environment and abide by its restrictions)	Orbiter/Spacelab environment < 120 dB above pT at 30 Hz, < 20 dB above pT at 10 kHz
Radiation	8.2×10^{-6} J/KG-S (Must cope with the Orbiter/Spacelab environment)	Orbiter/Spacelab environment consists of galactic cosmic radiation, geomagnetically trapped radiation, solar flare particles per JSC 07700 Vol XIV paragraph 4.1.2.3
Materials	(Must cope with the Orbiter/Spacelab environment)	Orbiter/Spacelab environment consists of particles of cometary origin per SLP/2104 paragraph 5.2.11
(Non-Operating)	(Same as Operating Requirements)	

Table 6.3-4. Spacelab/Shuttle Interface Capabilities

Parameter	Capability	Remarks
(Physical)		
Experiment Dimensions	Max 14' W x 30'L (stowed)	For S/L module + 3 pallets
	Max 18' W x 60'L (deployed)	No radiation shielding
Experiment Weight	≤ 5000 kg	
Mounting Provisions	Racks and Pallets	
Power Hookups	28 VDC ± 4 VDC	Nominal
	28 VDC ± 2%	Mission Dependent
	115/200 VAC, 400 Hz	Mission Dependent
	220 VAC, 50 Hz	Mission Dependent
	115 VAC, 60 Hz	Mission Dependent
Data Hookups	Data Bus (RAU)	≤ 100 KBPS
	High Rate Digital Channel	Max 50 MBPS
	High Frequency Analog Channel	4.2 MHz
	CCTV System	Standard U.S.
C&W Hookups	Hardwires as required	Emergency, Caution, Warning Type 1 Advisory
	Data Bus (RAU)	Type 2 Advisory
Fluid Hookups	Experiment Heat Exchanger	
(Functional)		
Electric Power	≤ 3 KW	Allowing for other payload requirements
Electric Energy	≤ 250 KWH	Allowing for other payload requirements
Science Data	Up to 50 MBPS	Digital Channel
	Up to 102.4 KBPS	Data Bus (RAU)
	4.2 Hz	Analog Channel
	TV	CCTV
Housekeeping Data	Analog	8 Bit A/D conversion
	Discrete	TTL Standard
	Up to 102.4 KBPS	Serial Digital
Commands	Discrete	
	PCM	8 Bit Words
Heat Rejection	≤ 3 KW	
C & W	Signals as required	
(Operational)		
Experiment Operations	Continuous between ascent phase and descent phase, constant attitude or maneuvering (within practical limits), nominal 7 day mission extendable to 30 days.	
Navigation	≤ 740 m position error	Worst case
	≤ 1.4 m/sec velocity error	Worst case
Pointing	≤ 0.605° IMU error	Worst case
	≤ 2.5° payload pointing (open loop)	Misalignments, deformation, etc.
	≤ 0.5° payload pointing (closed loop)	Payload mounted sensor
Stability	± 0.1°/axis deadband	
	≤ 0.105°/hr/axis drift	Worst case
Stability Rate	± 0.1°/sec/axis (large thrusters)	
	± 0.01°/sec/axis (vernier thrusters)	
Target Tracking	Earth, orbit, deep space target tracking by Orbiter maneuvers, IPS, payload provided pointing provisions.	
Experiment Jettison	Release using RMS	Primary or back-up for experiment provided automatic jettison
	Release using EVA	

Table 6.3-5. Experiment Configuration

Parameters	Description	Remarks
(Physical)		
Dimensions-External	3m x 3.5m x 1m (Stowed) 3m x 3m x 0.5m (Deployed) with 15m mast	Antennas, electronics, mounts, mechanisms
Dimensions-Internal	0.5 m^3	Electronics
Weight-External*	2000 kg	Antenna System plus Cables and Support
Weight-Internal *	150 kg	
Location-External	Mounted on 3 m pallet segment. Deployed to position above pressurized module	
Location-Internal	Electronics mounted in standard 19-inch Spacelab rack	
Orientation	Normal to Orbiter + 20 axis when deployed	
Alignment	Misalignment $\leq 0.25^{o}$ to pallet reference	Total pointing error $\leq 0.5^{o}$
Power Hookups	28 VDC Reg, 115 VAC (Pallet) 28 VDC Reg, 115 VAC (Racks)	
Data Hookups	Data Bus, High Rate Digital (Pallets) Data Bus, High Rate Digital (Racks)	
C & W Hookups	N/A (Pallet) N/A (Racks)	
Fluid Hookups	N/A (Pallet) N/A (Racks)	
Special Protection	N/A	
(Functional)		
Electric Power	800 W Standby 1200 W Operating	
Electric Energy	140 kWh	
Science Data	2 MBPS (Ku-band Communication) 50 KBPS (L-band Communication)	
Housekeeping Data	TBD	
Commands	TBD	
Heat Rejection	TBD	
C & W Signals	None	

*Estimates

SECTION 7

ROLE OF MAN IN SPACELAB/AMPA EXPERIMENT

A top level analysis of the crew interaction with the Spacelab/AMPA experiment is depicted in Table 7-1. This analysis was conducted using the following assumptions:

- The experiment control console (crew station) will be located in the Spacelab module.
- The controls and displays will provide the capability for experiment control, antenna system deployment and retraction, data extraction and manipulation, and computer input criteria/program modification.
- Visual access to the antenna deployment/retraction mechanisms can be obtained through Spacelab viewing ports and/or the Shuttle CCTV*.
- The antenna system alignment can be fine tuned to the Shuttle axis or misalignment can be detected visually or by electronic means.
- No scheduled EVA activities will be planned.

The manned activities shown in Table 7-1 fall into the following three basic operational areas plus contingency operations:

Experiment Activation and Deactivation. A large percentage of crew participation is required in these two operational areas for reconfiguration from launch mode to orbital operations mode, equipment turn-on, checkout, and calibration, and preparations for reentry.

Experiment Operations. Crew involvement during experiment operations will be minimized and will consist of pre-pass configuration, experiment monitoring, and experiment data handling. This minimum involvement is governed by the experiment objectives of autonomous pointing/tracking, limited ground pointing opportunities, short duration tracking times, and complex time-limited scanning patterns.

Contingency Operations. Manned activity during contingencies will be governed by the mode/equipment selection provided at the experiment crew station and an analysis of resultant usable data made available through various levels of experiment degradation.

---

* CCTV = Closed Circuit TV

Man's role consists primarily, therefore, of configuring the AMPA experiments for the desired operation, monitoring their operation through the experiment pass, and coordinating ground requirements for optimum experiment utilization.

Although there is a minimum of manned involvement during the data acquisition portions of the AMPA experiments, some of the benefits resulting from man's presence are the following:

1. Continuous real time experiment monitoring regardless of orbital position and communication exclusion areas.

2. Cost reductions for:

   - Design of automated experiment mode selections
   - Antenna alignment analysis and alignment sensor development
   - Design of possible on-board experiment dedicated data recorders
   - Equipment design and implementation for contingency operations (due to manual mode selection)

3. Reduced data transmissions due to real time monitoring capability

4. Greater resolution of ambiguity during experiment operations through the integration of real time crew-sensed data (visual, audible, etc.)

5. Design improvements in antenna deployment mechanism through visual monitoring of zero "g" articulation

6. Greater experiment autonomy from orbiter support systems (data links, CDMS, etc.)

Table 7-1. Analysis of Man's Role in Spacelab/AMPA Experiment

Manned Activity / Experiment	Experiment Activation (Req'd Once Per Mission)	Experiment Operations	Experiment Deactivation and Preps for Reentry (Req'd Once Per Mission)	Contingency Operation	Remarks
L-band Communications Experiment	• Activate and checkout crew experiment station • Deploy adaptive multi beam phased array • Align antenna system to vehicle axis • Prepare data collection equipment • Initiate calibration sequences as required • Return experiment to standby until data pass(es)	• Update pre-experiment pass data from MCC • Select desired experiment and data collection equipment parameters/modes • Orient shuttle to predetermine attitude • Initiate calibrations • Monitor data pass(es) • Return experiment to standby until next data pass(es) • Communicate experiment operations to MCC (as required)	• Retract adaptive multi beam phased array system for reentry • Deactivate crew experiment station equipment • Collect and stow experiment data	• Alter experiment and data collection equipment to backup modes and/or degraded operations • Unscheduled EVA to deploy the antenna system • Unscheduled EVA to retract/jettison the antenna system • Deploy/retract antenna system with manipulator arm	• Max data pass duration of 50 sec • Requires interfacing - free and controlled interference environment • Automated acquisition, beam forming, and tracking
L-band Radiometer Experiment	(Same As Above)	(Same As Above)	(Same As Above)	(Same As Above)	• Max data pass duration of ~15 min • Collect landmass soil moisture data • Pre-Programmed scan, tracking, and stepping • Possibility of 3 or more modes of operation (pre-programmed)
Ku-band Communications Experiment	(Same As Above)	(Same As Above)	(Same As Above)	(Same As Above)	(Same As L-band Communications)

MCC = Mission Control Center

EVA = Extra-Vehicular Activity

SECTION 8

SPACELAB/AMPA EXPERIMENT PROGRAM PLAN

The overall experiment configuration for the Adaptive Multibeam Phased Array (AMPA) experiment and the estimated design requirements were presented in Section 6. The role of man in the experiment was discussed in Section 7.

In this section, an overall program plan is presented for implementation of the AMPA experiment, beginning with a Phase B System Definition Study and proceeding on through a Phase C & D Execution Phase for the development, manufacture, test, and integration of the Adaptive Multibeam Phased Array antenna system to the point where payload integration on Shuttle/Spacelab begins. An estimated master schedule developed for this program plan is shown in Figure 8-1 and is based upon the Level 4 Work Breakdown Structure elements shown in Figure 8-2. The schedule would be defined in greater detail and accuracy during Phase B and will serve as a baseline along with the WBS for estimating the costs of implementing the hardware phases of the program.

The emphasis during the AMPA Phase B Study would be on systems analysis and definition design to arrive at conceptual designs and specifications for AMPA, together with compatibility analysis and integration with other Spacelab experiments such as those of MMAP. Other related tasks concerned with mission profiles, cooperating platforms, potential users, and AMPA as a free flyer could also be done during Phase B. A description of these recommended Phase B tasks is given in Section 10 of this report.

Key features of the AMPA Phase C & D schedule include sufficient time for a comprehensive detailed analysis and design program prior to a commitment to purchase or manufacture flight hardware. A Preliminary Design Review (PDR) is scheduled 6 months after program go-ahead at which time a preliminary design and specification will be ready for review. Critical Design Review (CDR) is scheduled 12 months down the line after engineering model development tests are successfully completed and flight hardware is ready to be built. Qualification of the flight hardware consisting of environmental and performance testing is accomplished over a three-month period.

There should be no schedule problems with a Phase C/D go-ahead in Sept/Oct of 1977 following a Phase B System Definition Study. This start would provide an ample two years for detail design, development, fabrication, acceptance and qualification test of the flight hardware. Six months is then provided for total experiment system integration, test, and delivery of the flight system ready for payload integration by NASA. If launch is in January 1981, 9 months would be available to NASA for Payload Integration and Installation, and checkout into the Shuttle.

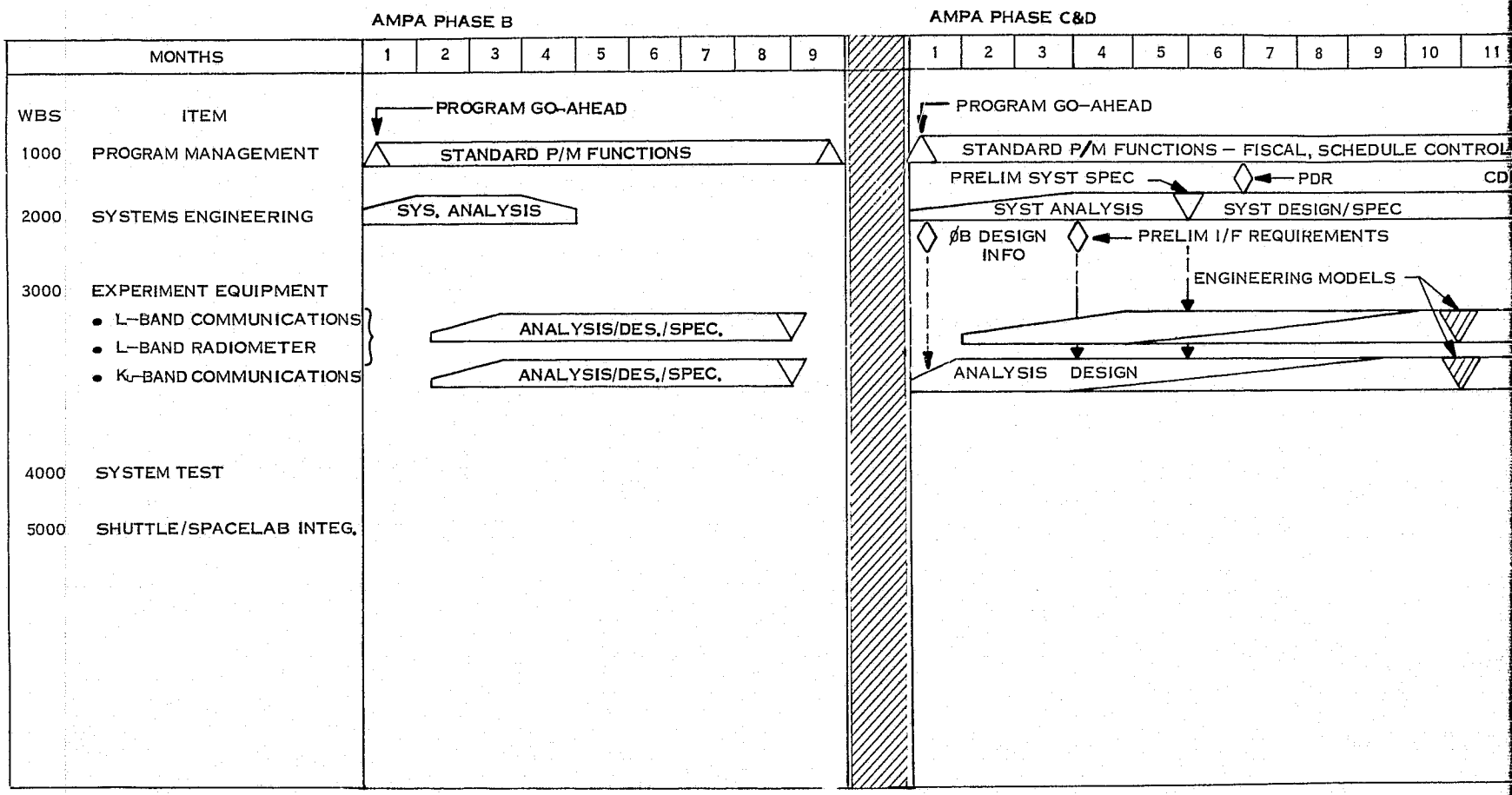

FOLDOUT FRAME 1

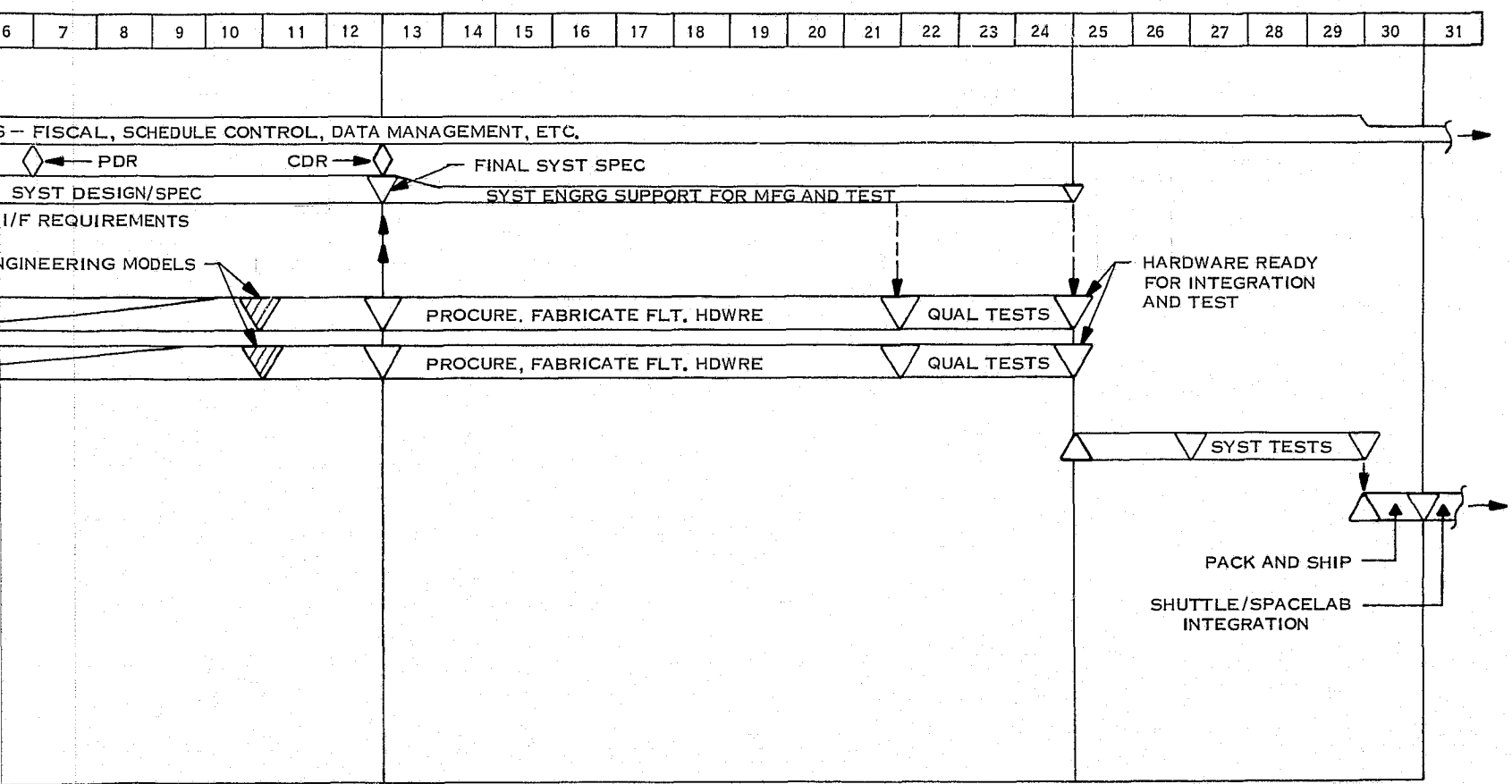

Figure 8-1. Estimated AMPA Phase B, C and D Schedule

FOLDOUT FRAME 2

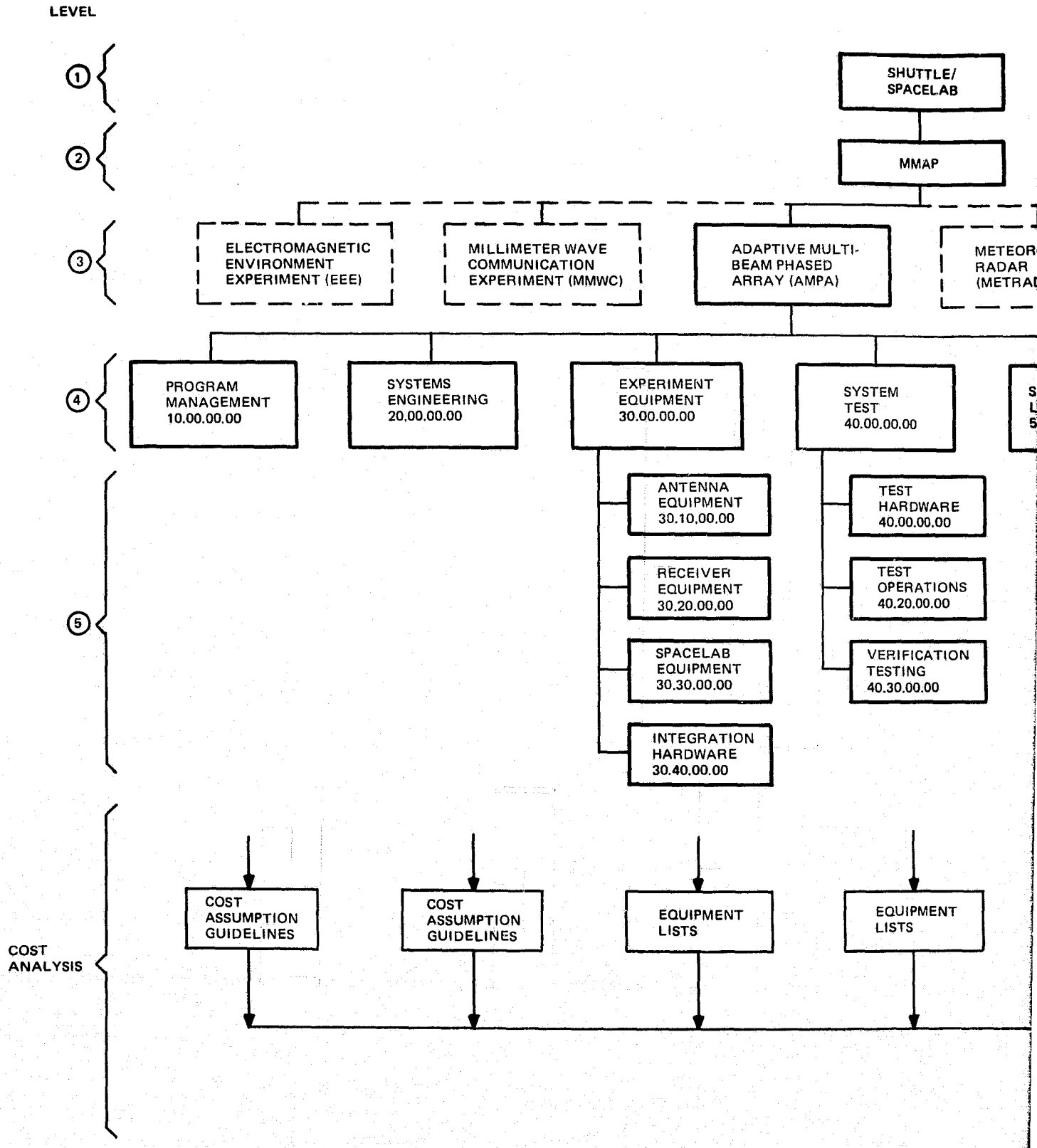

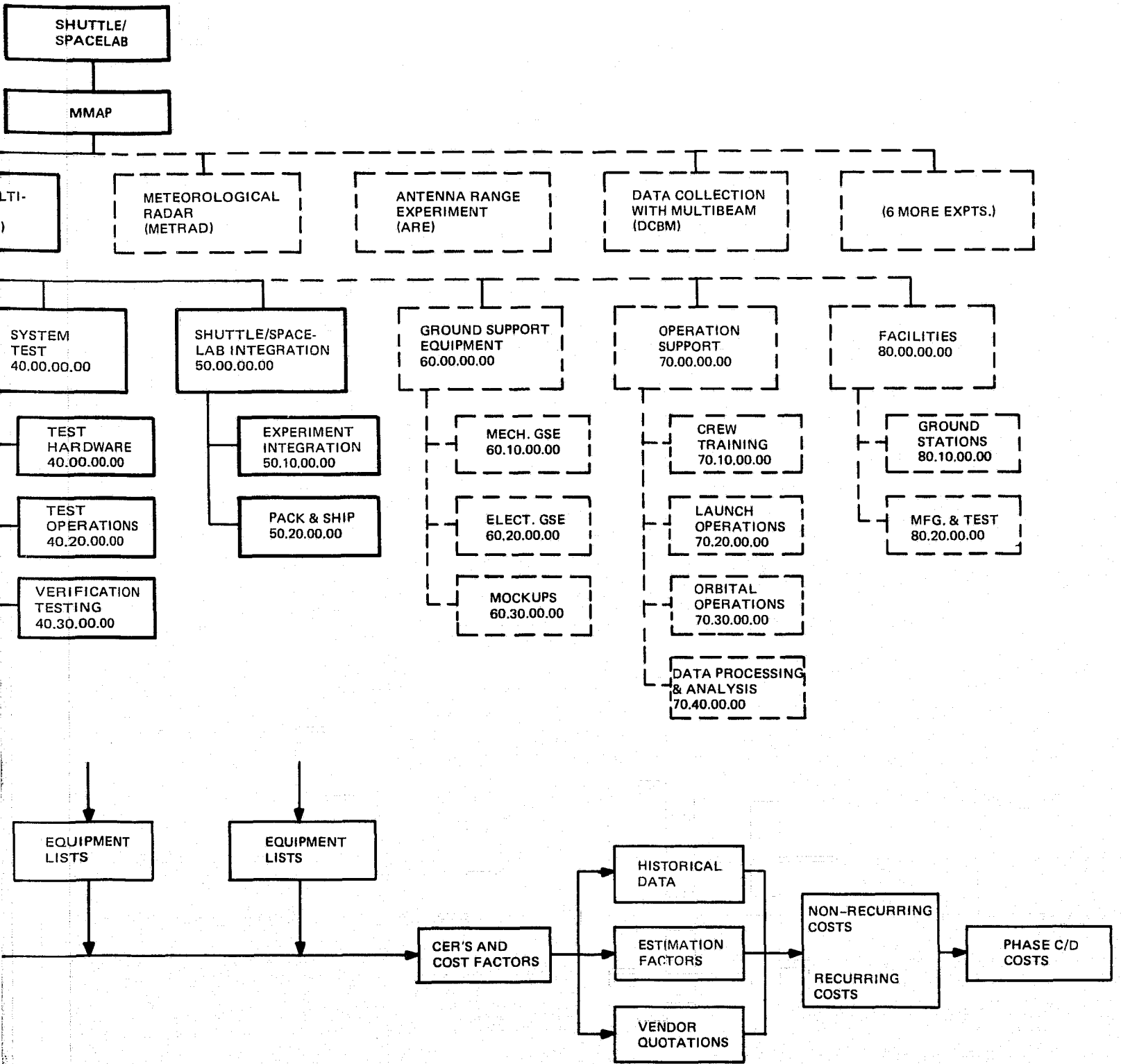

Figure 8-2. Work Breakdown Structure

FOLDOUT FRAME 2

SECTION 9

NEW TECHNOLOGY

During the Phase A Feasibility Study of Adaptive Multibeam Antennas for Spacelab, a new adaptive technique was conceived for adaptively controlling a full phased array with a much smaller fully-adaptive subarray of the main array. This technique provides adaptive signal acquisition, beamforming, tracking, and interference rejection. One configuration for implementing this technique is through processing of the signals from a 16-element subarray of pseudo-randomly-spaced, main-array radiating elements. Other subarray configurations and sizes could also be used for this technique, such as a filled subarray or a row and column subarray. The pseudo-randomly-spaced subarray is preferred, however, because it provides the same resolution as the main array without producing grating lobes.

A patent docket is being opened for this technique, which is described more fully in Sections 5.5.2.3 and 5.5.3.3. Basically, this technique provides the advantages of a fully-adaptive phased array for the acquisition and tracking of desired signals and the rejection of interference without the complexity and expense of making all radiating elements of the array adaptive.

SECTION 10

RECOMMENDATIONS

The output of the Phase A Adaptive Multibeam Antenna study provides experiment configurations defined as to their objectives, approach, equipment, observations, and data. Antenna characteristics and design concepts for an Adaptive Multibeam Phased Array (AMPA) are also defined, and a program plan has been developed.

A complementing Phase B system definition study should now follow to extend the Phase A results through engineering analyses to arrive at conceptual designs and specifications in sufficient detail to allow final hardware design and procurement to then proceed. The following tasks are recommended as part of Phase B and related additional studies:

1. AMPA System Design Analysis - This task provides the definition design studies necessary to advance from the selected candidate experiment configurations and AMPA design concepts to conceptual designs and specifications. Major AMPA elements to be analyzed include the antenna system itself as well as related support subsystems and interfaces. Design efforts and tradeoffs should focus on detailing characteristics and evaluating modifications to the experiment configurations emerging from the Phase A effort.

2. AMPA Shuttle/Spacelab Compatibility - Detailed analyses are required in this task to ensure experiment physical and operational compatibility with the carrier. Analyses should be performed to detail the mechanical and electrical interfaces with Shuttle/Spacelab as well as both stowed and deployed layouts. Integration of AMPA should be analyzed as a part of MMAP as well as with other experiments and as an antonomous AMPA experiment. Operationally data is required detailing manpower, electrical power, pointing, and data processing timelines. In addition, field of view, RF interference, and thermal interference must be analyzed.

3. Conceptual Designs and Specifications - This task provides the final conceptual description, performance specifications, interface specifications, and operation plans for the selected experiment configurations. Detailed drawings and layouts should supplement these specifications and provide the basis for final design and implementation in Phase C&D.

4. Mission Profiles for AMPA Utilization - These should be defined for the 1981-1991 decade beginning with shared missions as a part of MMAP and progressing through missions as an autonomous Shuttle payload to ultimate applications in free flying satellite modes.

5. Cooperating Platforms - Demonstration of AMPA feasibility is based on cooperating users. A task is required to define the type of users desired for demonstration purposes and to identify the requirements in terms of equipment, location, etc., which are to be placed on the cooperating users.

6. User Justification - This task is aimed at obtaining backing for the experimental objective in terms of both technical and societal benefits. Users are to be identified and confirmed where possible through written statements of support.

7. AMPA Free Flyer - As an off-shoot to task 1, a conceptual design of a free flying AMPA should be defined for an appropriate application such as TDMA/SDMA, search and rescue navigation, or multibeam data collection.

SECTION 11

REFERENCES

1. Durrani, S. H., "Multibeam Adaptive Antenna Experiment," 1975 IEEE Intercon Group/ Society Session E, New York, April 7, 1975.

2. Knittel, G. H., "Wide-Angle Impedance Matching of Phased-Array Antennas - A Survey of Theory and Practice," Phased Array Antennas, edited by Oliner and Knittel, Artech House, pp. 157-172, 1972

3. Lo, Y. T., Lee, S. W., and Lee, Q. H., "Optimization of Directivity and Signal to Noise Ratio of an Arbitrary Antenna Area," Proc. IEEE, Vol. 54, pp. 1033-1045, Aug., 1966

4. Butler, J. K., and Unz, H., "Beam Efficiency and Gain Optimization of Antenna Arrays with Nonuniform Spacings," Radio Sci., Vol. 2, No. 7, pp. 711-720, 1967

5. Kinesy, R. R., "Line Source Aperture Exitations," ASTIA No. AD671967, April 1967

6. Sanzgiri, S. M., Butler, J. K., "Constrained Optimization of the Performance Indices of Arbitrary Array Antennas," IEEE Trans. on Antennas and Propagation, Vol. 19, No. 4, pp. 493-498, July 1971

7. Taylor, T. T., "Design of Line Source Antennas for Narrow Beamwidth and Low Side-lobes," IRE Trans. on Antennas and Propagation, Jan. 1955

8. Irzinski, E., and Gillette, M., "High Gain Space/Ground Antennas," General Electric Co., TIS Report, No. 69SD330, Nov. 1, 1969.

9. Lockheed Missiles & Space Co., "Multibeam Antenna Study," Final Report under NASA contract NAS 5-21711, Phase I, Dec. 1972

10. B. Widrow, et al, "Adaptive Antenna Systems," Proc. IEEE, Vol. 55, No. 12, pp. 2143-2159, December 1967.

APPENDIX A

COMMUNICATIONS EXPERIMENT CONSTRAINTS

1. GEOMETRIC PARAMETERS

Shuttle Altitude = h = 400 km = 216.2 nm

Shuttle Period = P = $2.508 \times 10^{-2}\ a^{3/2}$ seconds; a = semi-major orbit axis in nm

= 92.6 minutes (circular orbit)

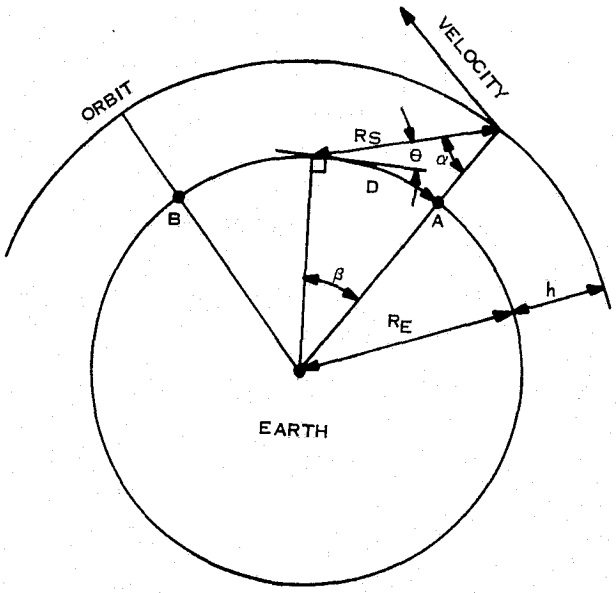

The following expressions relate the quantities shown in the figure at the left:

T_{AB} = Passage time from subsatellite points A to B

$= 2\,(\beta/360)\,P$

$\beta^{o} = 90 - (\theta + \alpha)$

$\theta = \cos^{-1}\left[\dfrac{R_e + h}{R_e}\ \sin\alpha\right]$

$R_s = \dfrac{\cos(\theta+\alpha)}{\cos\theta}\ (R_e + h)$

$D = \left(\dfrac{\pi}{180}\ \beta\right) R_e = (\pi/180)\ R_e \left[90-(\theta^{o} + \alpha^{o})\right]$

$f_{doppler}$ = maximum at α = max and for overhead pass

$\dfrac{v_R}{c}\ f_T = \dfrac{2\,\pi\,(R_e + h)\,\sin\alpha_{max}\ f_T}{c \quad P}$

Given: $\alpha_{max} = 40^{o}$

and $R_e = 6374$ km;

Then: $\theta = 46.9^{o}$

$\beta = 3.09^{o}$

$T_{AB} = 1.59$ minutes

$R_{s_{max}} = 534.2$ km

$f_{d_{max}} = \pm 26.9$ kHz

D = 344.9 km

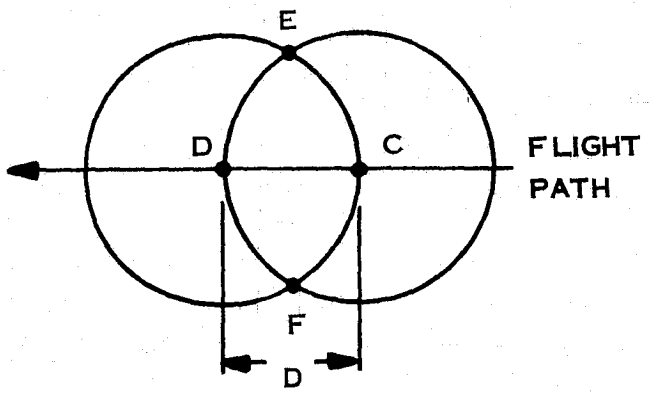

Signal Sources at Points E & F

Points E & F are simultaneously in view from subsatellite points C & D

$$T_{CD} = \frac{T_{AB}}{2} = \frac{1.59}{2} = 0.795 \text{ min} =$$

47.7 seconds

2. L-BAND LINK CALCULATIONS

2.1 UPLINK POWER

		Comment
Ground EIRP	EIRP dBw	
$L_s = 32.4 + 20 \log f_{MHz} + 20 \log d_{Km}$	-150.7 dB	
f = 1539 MHz		
d= 543.2 kM		
Atmosphere Loss	Negligible	
Polarization Loss (circular receive)	-0.5 dB	
Array Element Gain ($\alpha = 40^{o}$)	+2 dB	For single element acquisition
RF Circuit Loss	-5 dB	Estimate
Receive Power	EIRP-154.2 dBw	

Two specific modulation approaches are now considered: PCM/PSK - PM and FM. In the former, a PCM data stream phase shift key modulates a subcarrier which in turn phase modulates the carrier. In the latter, data directly frequency modulates the carrier.

The aim is to locate signal sources with the gain of only one element and transmit data using the gain of the entire steered array. As will be seen, PCM/PSK - PM is strongly preferred because narrow bandwidth carrier acquisition can be used for signal direction location which, at the single element gain level, requires far less uplink EIRP (or satellite antenna G/T) than does the FM approach.

2.2 CARRIER ACQUISITION FOR PCM/PSK-PM (i.e., for modulated subcarrier and uncluttered carrier)

Kt at 290°K	- 204 dBw/Hz	
PLL BW ($2B_{LO}$ = 600 Hz)	+ 27.8 dB-Hz	Large BW for rapid acquisition

Acquisition Time (T_{acq})

$$T_{acq} \approx \frac{9\ \Delta F}{B_n^{\ 2}}$$

ΔF = doppler uncertainty + signal bandwidth

ΔF = 2 x 27 + 25 = 79 KHz

B_n = 2 B_{LO} = 600 Hz

T_{acq} = 1.975 seconds

$\overline{NF}$	+ 5 dB	Assumed
$P_N = K\ T\ B_n\ \overline{NF}$	- 171.2 dBw	
Carrier Suppression (assume subcarrier M.I = 1.0 radian	- 2.4 dB	
Available C/N	= EIRP + 14.6 dB	
Required C/N for acquisition	6 dB	
Margin (carrier tracking)	EIRP + 8.6 dB	

For margin ≥ 0 dB, EIRP ≥ - 8.6 dBw.

2.3 ACQUISITION (AND DATA) FOR FM

Data Bandwidth

= Channel BW + 2 (doppler BW)

= 25 KHz + 2 (27 KHz) = 79 KHz

Noise power in 79 kHz - 150 dBw

NF = 5 dB

KT = -204 dBw/Hz

BW = 79 kHz = dB-Hz

C/N	(EIRP-154.2)- (-150) = EIRP - 4.2 dB
Required threshold C/N	13dB
Margin	EIRP-17.2 dB

For margin ≥ 0 dB, EIRP ≥ 17.2 dBw

This is 25.8 dB higher than PCM/PSK-PM and stands decisively against this approach, even though direct FM modulation would be "more" compatible to the Marisat transmission format.

Having just considered the link requirements for carrier acquisition -- which will be used for signal direction location -- we now consider the available data capacity of the selected PCM/PSK - PM approach, first on a single element gain basis and next on a full array basis. The full array is, of course, far more important of the two cases and is, in fact, the intended use, but the former may also be important. An example use of the single element gain for data transmission (as opposed to just for source direction location) might be for signalling (e.g., order-wire) usage.

2.4 DATA MARGINS IN THE PCM/PSK - PM SYSTEM

Case 1: Single Element Gain

Received Signal	EIRP-154.2 dBw
Data Modulation Loss (MI = 1.0 radian)	-4 dB
Available Data Power	EIRP-158.2 dBw
Data Bandwidth B	B dB-Hz
Noise Power in B	B-199 dBw
NF = 5 dB	
KT = -204 dBw/Hz	
B = B Hz	
S/N Available	(EIRP - 158.2) - (B-199) = EIRP-B + 40.8 dB

Required S/N for BER $\leq 10^{-5}$	12 dB	Allows 2.5 dB for non-perfect detector performance
Margin	(EIRP-B+40.8) -(12) dB =EIRP-B+28.8 dB	

For margin $\geq$ 0 dB, Bit Rate $\leq$ EIRP + 28.8 dB - BPS

Case 2: Full Array Gain

Reference to Section 2.1 (Uplink Power) shows a Received Power = EIRP - 154.2 dBw based upon a +2 dB element gain. Assume the full array gain (including RF losses) is +27 dB. The received power would thus be (EIRP - 154.2) -2 + 27 = EIRP -129.2 dBw at normal incidence to the array. 1.16 dB must be subtracted for the gain decrease at 40^{o} offset angle and another 3 dB subtracted to account for the beam splitting (2 equal beams needed for the communication link). The Net Received Power = EIRP - 133.4 dBw.

Net Receive Signal	EIRP - 133.4 dBw	
Data Modulation Loss (MI=1.0 radian)	-4 dB	
Available Data Power	EIRP-137.4 dBw	
Data Bandwidth B	B dB-Hz	
Noise Power in Data Bandwidth B NF = 5 dB KT = -204 dBw/Hz B = B dB-Hz	B-199 dBw	
S/N Available	(EIRP-137.4) -(B-199) =EIRP-B+61.6 dB	
Required S/N for BER $\leq 10^{-5}$	12 dB	Allows 2.5 dB for non-perfect detector performance
Margin	(EIRP-B+61.6) -(12) dB =EIRP-B+49.6 dB	

For margin $\geq$ 0dB, Bit Rate $\leq$ EIRP + 49.6 dB - BPS

In summary for 0dB margin

EIRP required for Carrier Acquisition ≥ -8.6 dBw

Single Element Bit Rate ≤ EIRP + 28.9 dB-BPS

Full Array (Two Channel Link) Bit Rate ≤ EIRP + 49.6 dB-BPS

If we assume a 3.0 dB margin requirement throughout, then

EIRP ≥ -8.6 + 3.0 = 5.6 dBw = 275 mw

Single Channel Bit Rate ≤ (EIRP + 28.8) - 3.0

= EIRP + 25.8 dB-BPS

= -5.6 + 25.8 = 20.2 dB-BPS

= 105 BPS

Full Array (Duplex Channel) Bit Rate Capability

≤ (EIRP + 49.6) - 3.0

= EIRP + 46.6 dB-BPS

= -5.6 + 46.6 = 41 dB-BPS

= 12.6 KBPS

For an assumed channel bandwidth of 25 kHz, the full 12.6 KBPS capacity cannot be used. The following spectrum illustrates this point:

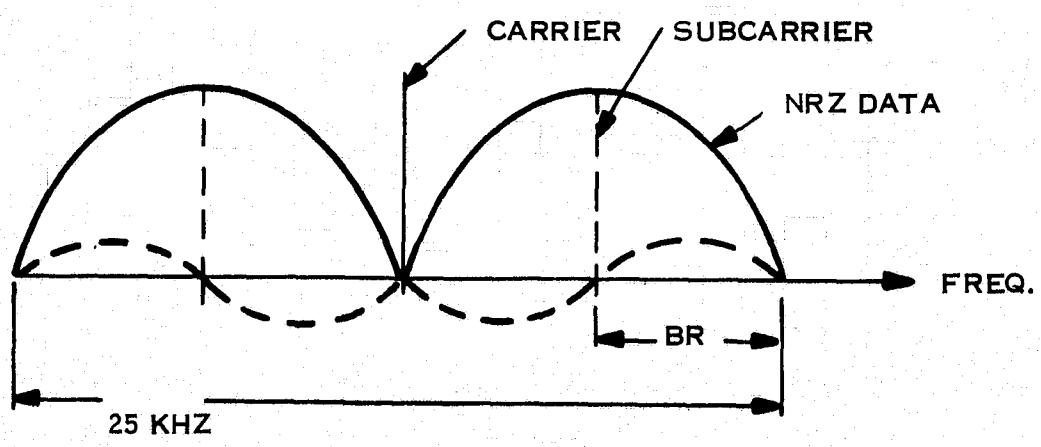

Therefore BR ≤ $\frac{25 \text{ kHz}}{4}$ = 6.25 KBPS

Furthermore, to (a) keep the carrier uncluttered, and (b) to prevent spectrum for upper and lower sidebands, the data bit rate must be further reduced by another factor of approximately two. Realistically the maximum bandwidth will be approximately 3000 BPS.

In this regard, the FM approach is superior. That is, more data can be transmitted within the fixed 25 KHz bandwidth allotment by the direct carrier modulation of the FM approach than by the modulated subcarrier approach of PCM/PSK - PM but at the expense of considerably more uplink EIRP. Overall, the PCM/PSK - PM approach is preferred.

3. SUMMARY OF SELECTED L-BAND APPROACH

Ground EIRP	275 mw
Modulation	PCM/PSK-PM
MI Assumed	1.0 radian (subcarrier on carrier)
PLL Bandwidth	$2\ B_{LO} = 600$ Hz
Acquisition Time	2 sec
Contact Time (Total)	47.7 sec
Data Rate -	
Single element	105 BPS
Full array in two beam mode	3000 BPS
Data and Carrier Margin	3 dB at worst distance

4. L-BAND GROUND ANTENNA CONSIDERATIONS

A 46.9^{o} half-cone angle is required for the ground antenna to match the satellites 40^{o} look angle. Assume the "ground" antenna is ship (or buoy) mounted and assume a maximum ocean-caused pitch of $\pm 23^{o}$, then the total cone angle becomes $\theta = \pm (46.9 + 23) = \pm 70^{o}$. The gain associated with $\pm 70^{o}$ solid angle is:

$$\text{Gain} = \frac{4\pi r^2}{2\pi r^2 (1-\cos\theta)} = 2/(1-\cos\theta) = 2/(1-\cos 70^{o}) = \pm 4.8 \text{ dB}.$$

Allowing 1.8 dB for circuit losses still leaves a +3.0 dB ground antenna gain (minimum). Therefore it will be assumed that the ground antenna will have a gain $\geq$ 3.0 dB.

(Without the requirement for ship motion the antenna gain can be $2/[1-\cos 46.9^{o}]$ = 8.0 dB or 6.2 dB after RF circuit losses.) The required ground transmitter power P_T is:

$$P_T = EIRP - G_T = -5.6 \text{ dBw} - 3.0 \text{ dB} = -8.6 \text{ dBw} \simeq 138 \text{ milliwatts}$$

(Without ship motion P_T = -5.6 dBw - 6.2 dB = 11.8 dBw = 66 mw.)

5. L-BAND DOWNLINK CONSIDERATIONS

The downlink is not the limiting link in the acquisition phase because, (a) the ground receive antenna gain essentially equals its transmit gain, (b) its system noise temperature will not differ significantly from the satellites noise temperature (because the wide beamwidth will give about 290^{o} antenna temperature and a relatively inexpensive pre-amp is anticipated), and (c) most importantly because the downlink transmission will make use of the AMPA gain instead of only an element gain. Thus, the uplink link acquisition requirements, once satisfied, will suffice.

For downlink data capacity via the full array, again the downlink is not the limiting link for the same reasons as above plus the following reason. It is shown in Section 4 that the uplink power required was only 138 milliwatts. If more than this much power is used for the spacecraft downlink, the downlink will not be limiting. At this power level, the realistic limit is the available channel bandwidth in the L-band Maritime frequency assignment.

6. WIDE-BAND DATA COMMUNICATIONS AT Ku-BAND

6.1 FULL Ku-BAND ARRAY GAIN

The applicability of the Ku-band link for wideband data is considered in this section. A summary of the up and down link calculations is shown below. This summary shows that a 50 MHz duplex link is reasonable for modest ground and spacecraft RF power and offers a 3 dB margin in the presence of a 7 dB rainfall attenuation. The example used is for an FM video application similar to the Landsat wideband data link which is characterized by the following parameters:

IF BW	20 MHz
Baseband video	3.5 MHz
S/N at IF	15 dB
Modulation	FM
Deviation	$\pm$ 6.5 MHz

The ground station performance is based on a 15 foot parabolic antenna, 5 dB receiver noise figure, and a transmitter power of 6.18 watts. Atmospheric rainfall attenuation data used shows that < 7 dB attenuation at an elevation of 10^{o} occurs less than 0.1% of the time (Ref. R. T. Wolfe "Modeling to Estimate the Effects of Site Diversity on Performance of Multiple Link Ku-band Communications Systems" MITRE Publication MTR-6916, May 1973).

The spacecraft performance is based on 24 dB array gain, since two simultaneous beams are formed, and have an effective receive noise figure of 15 dB. Transmitter power required is 10 dB below the ground station power (0.618 watts).

6.2 Ku-BAND UPLINK CALCULATION

Transmitter Power	P_T dBw
Antenna Gain (15.4 GHz, 15 ft. dish)	54.68 dB
(20 log f + 20 log D - 52.6)	
EIRP	P_T + 54.68 dBw
Space loss (534.2 Km)	-169.9 dB
Atmospheric Attenuation, rain (7 dB at 10^{o} elevation < 0.1% of the time)	- 7.0 dB
Polarization loss	- 0.5 dB
Pointing Loss (Autotrack)	- 0.2 dB
Receive Antenna Gain	24.0 dB
Receive Carrier Power	P_T - 98.92 dBw
KT dBw/Hz	-204.0 dBw/Hz
Array Noise Figure	15.0 dB
(Single Receive Amplifier)	

Signal Bandwidth (50 MHz)	76.99
Total Noise Power	-112.01 dBw
Carrier to Noise Ratio (C/N)	P_T + 13.09 dB
Required C/N for FM Video	15 dB
PT	1.91 dBw
RF Losses at Transmitter	3.0 dB
Link Margin	3.0 dB
Transmit Amplifier Power	7.91 dBw
	(6.18 watts)

Note: All parameters identical for the downlink except that the ground station noise figure is assumed to be 5 dB. Therefore, equivalent performance is obtained with 0.618 watts transmitter power.

6.3 Ku-BAND CARRIER ACQUISITION

The purpose during carrier acquisition is to locate signal sources with the gain of only one antenna radiating element. The preferred modulation technique is PCM/PSK-PM rather than FM, since narrow-bandwidth carrier acquisition can be used for signal direction location which, at the single radiating element gain level, requires far less uplink EIRP (or satellite antenna G/T) than does the FM approach. A summary of the significant acquisition link parameters is given below:

KT at 290°K	-204 dBw/Hz	
PLL BW ($2B_{LO}$ = 600 Hz)	+27.8 dB-Hz	Moderate BW for rapid acquisition

Acquisition Time (T_{acq})

$$T_{acq} \approx \frac{9 \Delta F}{B_n^2}$$

ΔF = doppler uncertainty + signal bandwidth

= 2 x 27 + 25

= 79 kHz

$B_n = 2 B_{LO} = 600$ Hz		
$T_{acq} = 1.975$ seconds		
$\overline{NF}$	+5 dB	Assume only for the radiating elements involved in adaptive acquisition
$P_N = KTB_n \overline{NF}$	-171.2 dBw	
Carrier Power for 2 dB Radiating Element		
Gain (P_T - 98.92 - 22)	P_T - 120.92 dBw	
Carrier Suppression (Assumes MI = 1.0 Radian)	-2.4 dB	
Available C/N	P_T + 47.88 dB	
Required C/N for Acquisition	10 dB	
Acquisition Link Margin	3 dB	
P_T	-34.88 dBw	
RF Transmit Losses	3.0 dB	
Transmitter Power	-31.88 dBw	

The requirements for Ku-band carrier acquisition, which will be used to obtain the signal direction adaptively, are thus met with a transmitter power of -31.88 dBw or 0.648 mw.

APPENDIX B

RADIOMETER ANALYSIS

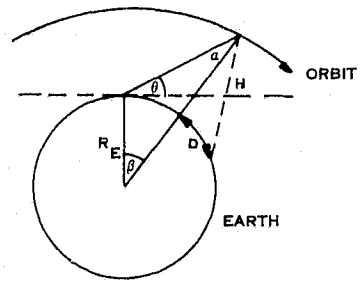

1. DWELL TIME FOR SPOT

Find the time to travel one 5^o spot size:

$\alpha = 2.5^o$ P = Orbit Period = 92.61 minutes

= 5555.6 seconds

$$\theta = \cos^{-1}\left[\frac{Re + h}{Re}\sin\alpha\right] = \cos^{-1}\left[\frac{6374 + 400}{6374}\sin 2.5^o\right] = 87.34^o$$

$$\beta = 90 - (\theta + \alpha) = 90 - (87.34 + 2.5) = 0.157^o$$

$$\text{Time to travel one spot size} = P\left[\frac{2\beta^o}{360^o}\right] = \underline{4.847 \text{ seconds}}$$

$$\text{Dwell time per spot} = \frac{\text{Time to travel one spot size}}{\text{No. of beam locations in above time}} = \frac{4.847}{4}$$

Dwell time = 1.212 seconds for 4 radiometer beams (4 locations each);

= 0.606 seconds for 2 radiometer beams (8 locations each)

(For case 3 of Section 4.1, the travel distance per scan line and the number of spots illuminated for each beam both double so that the dwell time per spot remains the same.)

2. TEMPERATURE RESOLUTION

For the Dicke Type Radiometer the one sigma temperature resolution (i.e., the rms temperature measurement error per measurement period), called ΔT, is given by:

$$\Delta T = \frac{(T_A + T_S) + (T_R + T_S)}{\sqrt{B\,\tau}} \qquad (1)$$

where

T_A = Antenna Temperature

T_S = System Noise Temperature exclusive of antenna temperature

T_R = Temperature of a calibrated reference load

B = Radiometer Processor Bandwidth

τ = Integration time

Note that $B\tau$ is the number of independent noise measurement samples from bandwidth B in time τ.

T_A is ideally the temperature of the spot on earth illuminated by the beam but differs from this ideal value because of the following factors:

1. The temperature of the "spot" viewed is the radiometric temperature, not the physical temperature. The difference is that the source has an emissivity less than unity.

2. The "spot" is not illuminated by the total receiving beam. This would only happen if the beam uniformly filled the "spot" and had zero intensity elsewhere, i.e., if its efficiency were 100%. If, however, the beam efficiency were 85%, and this requirement were exactly met, 85% of the beam would illuminate the "spot" but <u>not</u> uniformly, and 15% of the beam would illuminate the remainder of 4π steradians in an unspecified manner. The radiometric temperature viewed thus would be the integral of the beam relative intensity over the "spot" times the radiometric temperature function across the "spot" times 0.85 plus 0.15 times the product of beam intensity and radiometric temperature over the remainder of the 4π steradians.

   Thus it is obviously desirable to have as high a beam efficiency as possible and as much of the non-spot part of the beam viewing cold space as is feasible. In practice some sidelobes will intercept the relatively warm earth and cause measurement inaccuracies.

3. T_A is also directly affected by differential RF losses in two measurement paths. The two paths are from antenna input to the radiometer processor and from a reference temperature load to the radiometer processor. These losses are <u>not</u> removed by the differencing process accomplished by a Dicke (or Hach) Radiometer. The antenna and RF equipment losses prior to the common point in the following sketch are to be minimized and the common point should be made as far forward as possible.

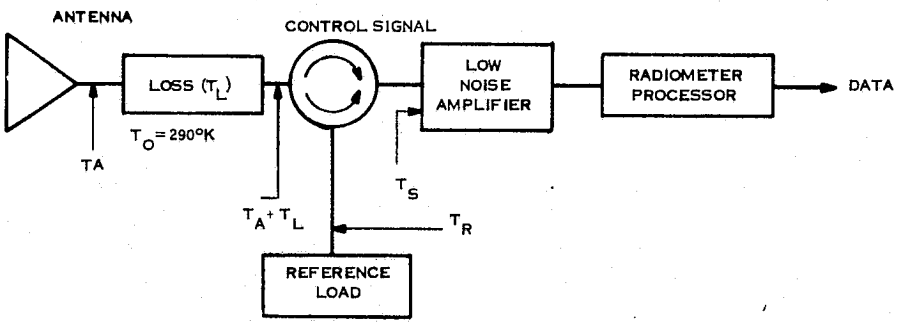

Equation 1 also shows that the lower the system temperature, T_S, the better (lower) ΔT will become. In fact, typical values for the functions involved are:

$T_A \approx 290^oK$ over land

$T_A \approx 100$ to 150^o over water

$T_L = \left(\frac{L-1}{L}\right) T_O = 31.5^oK$ for assumed values of $L = 0.5$ dB loss and $T_O = 290^oK$ (physical temp.)

$T_A + T_L = 322^oK$ (which is the value to be used in equation 1 in place of T_A)

$T_R \approx 290^oK$ (unless special effort is made to cool the reference below the typical spacecraft physical temperature)

$T_S \approx (\overline{NF} - 1)\ 290^oK = 627^oK$ for an assumed 5 dB noise figure for the receiving system from the common point onward.

Using B = 27 MHz (1.4 to 1.427 GHz) and $\tau = 1.200$ seconds (which allows 12 milliseconds of the total available dwell time for beam switching)

ΔT becomes

$$\Delta T = \frac{(322 + 627) + (290 + 627)}{\sqrt{(27 \times 10^6)\ (1.2)}}$$

$\Delta T = \underline{0.328^oK \text{ for 4 radiometer beams;}}$

$= \underline{0.464^oK \text{ for 2 radiometer beams}}$

From an equipment viewpoint, the design will be simpler if the system noise figure requirement can be eased. For that reason, ΔT is given as a function of noise figure ($\overline{NF}$) in the following figure.

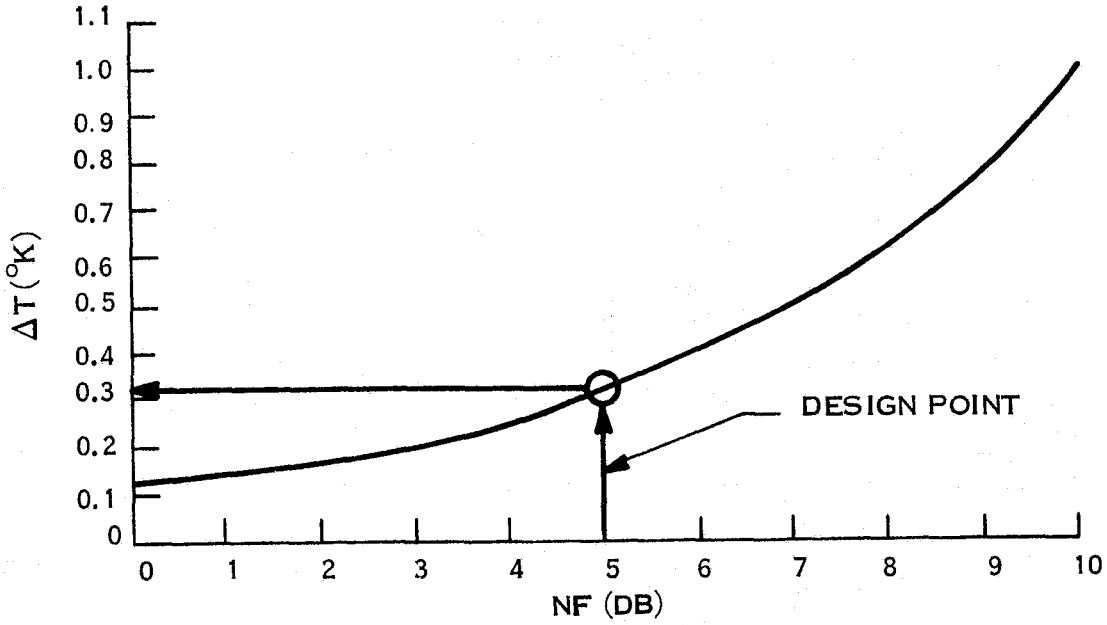

A ΔT value less than $0.5^{o}K$ is desirable. On the basis of NASA's - GE built - Skylab S-193 Microwave Radiometer/Scatterometer/Altimeter experience ($\Delta T = 1.0^{o}K$) and the NASA Langley - GE built - RadScat ($\Delta T = 3^{o}$), $\Delta T = 0.5^{o}K$ is a very reasonably derived specification. The current design point is $\overline{NF} = 5$ dB and $\Delta T = 0.33^{o}K$ for 4 radiometer beams, or $0.46^{o}K$ for 2 radiometer beams.

3. TIME SEQUENCE FLEXIBILITY

The timing will be set by the Shuttle velocity and the requirement of a contiguous scan pattern. Thus (ΔT) timing is not an independent variable, however, it may be used to an advantage. For example, in Case 1 of Section 4.1, beam A is not limited to being stepped sequentially to positions A1, A2, A3, A4 with A4 being 4.8 seconds later than A1. If time is subdivided as shown below, all four positions are measured essentially simultaneously.

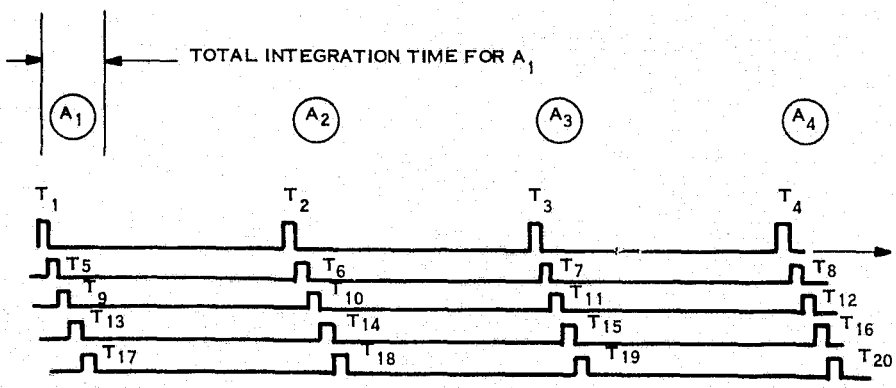

Each t_i is a small burst of successive integration time and where beam A steps back and forth between the four positions. The advantage of this approach is that spots 40 degrees to the right and to the left of the satellite track are inspected (1) essentially simultaneously instead of about 4 seconds apart, and (2) the rearward viewing angles to each spot are equal instead of about 5 degrees different.

(Note: The radiometric intensity of a source differs with different viewing angles.)